FCP Report No. 32

A MODEL FOR JOINING THE FATIGUE CRACK INITIATION AND PROPAGATION ANALYSES

by

W.-C. Chen
Department of Metallurgy and Mining Engineering

and

F. V. Lawrence
Professor of Civil Engineering and Metallurgy

A Report of the
FRACTURE CONTROL PROGRAM

College of Engineering, University of Illinois
Urbana, Illinois 61801
November, 1979

A MODEL FOR JOINING THE FATIGUE CRACK INITIATION AND PROPAGATION ANALYSES

ABSTRACT

An analytical model for nonarbitrarily defining the crack initiation length (a_I) of a notched member on the basis of the minimum total life estimate (Life-calculation method) is proposed. The crack initiation length (a_I) is not a fixed value, as usually assumed, but varies with stress level (or life), notch size, notch geometry, and material. The partitioning of crack initiation life (N_I) and crack propagation life (N_p) can be achieved using this model. This model provides an interpretation of fatigue notch size effect and a powerful means for numerically determining Neuber and Peterson parameters "$\sqrt{\rho}$" and "a".

On the basis of crack initiation life, K_f is determined from the stress-strain parameter $(\Delta S_I \Delta e_I E)^{1/2}$ at the crack initiation length (a_I). The longstanding problem as to how to join the N_I estimate using the local stress-strain approach and the N_p estimate using fracture mechanics concepts appears to be solved through the use of a_I defined by the proposed model.

ACKNOWLEDGMENTS

The results of this study are based upon the Doctor's Thesis of Mr. W.-C. Chen, the funds for which were provided by the Fracture Control Program at the University of Illinois at Urbana-Champaign. The Fracture Control Program is supported by a consortium of midwest ground vehicle industries. The authors wish to thank Professor JoDean Morrow, Department of Theoretical and Applied Mechanics and Professor D. F. Socie, Department of Mechanical Engineering for allowing the authors to use the basic concepts which they developed. Further, the authors wish to thank Mr. Peter Kurath for the use of experimental test results which he has generated as a part of his doctoral work.

TABLE OF CONTENTS

Page

APPENDICES

LIST OF TABLES

LIST OF FIGURES

LIST OF FIGURES (Cont'd)

LIST OF FIGURES (Cont'd)

LIST OF FIGURES (Cont'd)

LIST OF SYMBOLS

a	Peterson's Parameter relating K_f to K_t and r; also, crack length
a_f	Final crack length
a_I	Nonarbitrarily defined crack initiation length using the proposed analytical model
a_{th}	Crack length resulting in a stress intensity factor range equal to ΔK_{th}
b	Fatigue strength exponent; also, half minor-axis of an elliptical notch
c	Fatigue ductility exponent; also, half major-axis of an elliptical notch
C	Paris' crack growth coefficient
C'	Forman's crack growth coefficient
δ	Peterson's postulated constant distance beneath the notch surface
E	Elastic modulus
F	Stress intensity correction factor
e, Δe	Nominal strain, range
Δe_I	Strain range experienced by the micro-element at a distance equal to a_I from the notch root
Δe_x	Strain range experienced by the micro-element at a distance x from the notch root
ε, $\Delta\varepsilon$	Notch root strain, range; also true strain, range
ε'_f	Fatigue ductility coefficient
$\Delta\varepsilon_p$	Plastic strain range
$\Delta\varepsilon_s$	Strain range experienced by a smooth specimen
ε_{tr}	Strain amplitude resulting in a fatigue life equal to the transition fatigue life $2N_t$

k	Mean stress relaxation exponent
K_c	Fracture toughness
K_{max}	Maximum stress intensity factor
K_{min}	Minimum stress intensity factor
ΔK	Stress intensity factor range
ΔK_{th}	Threshold stress intensity factor
K'	Cyclic strength coefficient
K_f	Fatigue notch factor
K_f^N	Fatigue notch factor calculated from Neuber's formula and $\sqrt{\rho}$ reported in the literature
K_f^P	Fatigue notch factor calculated from Peterson's formula and "a" reported in the literature
K_ε	Strain concentration factor
K_σ	Stress concentration factor
K_t	Theoretical stress concentration factor
m	Paris' crack growth exponent
m'	Forman's crack growth exponent
n'	Cyclic strain hardening exponent
$2N_f$	Number of reversals to failure of a smooth specimen
N_I	Fatigue crack initiation life
N_P	Fatigue crack propagation life
N_T	Total fatigue life
$2N_t$	Transition fatigue life

q	Fatigue notch sensitivity index
r	Notch root radius
R	Stress ratio (min./max.)
$\sqrt{\rho}$	Neuber's parameter relating K_f to K_t and r
S, ΔS	Nominal stress, range
ΔS_I	Stress range experienced by the micro-element at a distance equal to a_I from the notch root
ΔS_x	Stress range experienced by the micro-element at a distance x from the notch root
S_u	Ultimate tensile strength
S_y	0.2% offset yield strength
σ, $\Delta\sigma$	Notch root stress, range; also true stress, range
σ_f'	Fatigue strength coefficient
σ_o	Mean stress
$\sigma_{o,i}$	Initial mean stress
$\sigma_{o,\,2N}$	Mean stress at 2N reversals
$\Delta\sigma_s$	Stress range experienced by a smooth specimen
x	Distance from the notch root; also, assumed crack initiation length
W	Specimen half width
da/dN	Crack propagation rate
dx/dN	Crack initiation rate
$(\Delta S \Delta e E)^{1/2}$	Nominal stress-strain parameter
$(\Delta S_I \Delta e_I E)^{1/2}$	Stress-strain parameter experienced by the micro-element at a distance equal to a_I from the notch root

$(\Delta S_x \Delta e_x E)^{1/2}$	Stress-strain parameter experienced by the micro-element at a distance x from the notch root
$(\Delta\sigma\Delta\varepsilon E)^{1/2}$	Notch root stress-strain parameter
$(\Delta\sigma_s \Delta\varepsilon_s E)^{1/2}$	Stress-strain parameter experienced by a smooth specimen

I. INTRODUCTION

1.1 General

The control of fatigue through structural design, material selection, surface treatment and/or in-service maintenance requires a precise knowledge of the fatigue phenomenon. The optimization of a notched member's resistance to fatigue failure is heavily dependent on the relative amount of life spent in crack initiation and crack propagation. Since the crack initiation mechanisms are quite different from crack propagation mechanisms [1], the mechanical properties controlling crack initiation may be different from those controlling the crack propagation. The mechanical properties good for crack initiation resistance may not be good (or even harmful) for crack propagation resistance.

The fatigue process can be divided into three periods [1]: (1) crack nucleation through the persistent slip bands mechanism; (2) Stage I crack growth, a shear-mode, slip-plane cracking which may be considered an extension of (1); and (3) Stage II crack growth, tensile-mode crack propagation resulting from crack tip deformation and often characterized by striations on the fracture surface. The total fatigue life should be the sum of the cycles spent in these three periods. The different mechanisms and methods of life calculation for these three periods have made the estimation of total fatigue life impossible to date.

From an engineering point of view, it is more convenient to separate the total fatigue life (N_T) into two portions: the crack

initiation life (N_I), which is spent in developing an active stage II crack, and the crack propagation life (N_p), which is spent in propagating that initiated crack to final failure. Low cycle fatigue concepts [2-5] are usually used for the estimation of crack initiation life (N_I), while fracture mechanics concepts are used for the estimation of crack propagation life (N_p).

1.2 Low Cycle Fatigue Concepts

The fatigue resistance of a smooth specimen subjected to completely reversed cyclic loading can be characterized by Eqs. (1) and (2) and four material parameters which relate the stress amplitude ($\Delta\sigma/2$) and the strain amplitude ($\Delta\varepsilon/2$) to the fatigue life ($2N_f$)[2],

$$\Delta\sigma/2 = \sigma_f' (2N_f)^b \tag{1}$$

and

$$\Delta\varepsilon/2 = \frac{\sigma_f'}{E} (2N_f)^b + \varepsilon_f' (2N_f)^c \tag{2}$$

where: E = the elastic modulus

σ_f' and b = the fatigue strength coefficient and exponent

ε_f' and c = the fatigue ductility coefficient and exponent

$2N_f$ = the fatigue life of the smooth specimen

In the presence of a mean stress (σ_o), Eq. (1) and (2) can be modified by introducing a mean stress term to account for the mean stress effect on the stress/strain-life relationships[3];

$$\Delta\sigma/2 = (\sigma_f' - \sigma_o) (2N_f)^b \tag{3}$$

and

$$\Delta\varepsilon/2 = \frac{(\sigma_f' - \sigma_o)}{E} (2N_f)^b + \varepsilon_f' (2N_f)^c \tag{4}$$

The mean stress relaxation in constant strain amplitude tests has been found to obey a power function [6]:

$$\sigma_{o,2N} - \sigma_{o,i} (2N - 1)^k$$

$$k = -4625 (\Delta c_p/2E\, c_{tr}) (ksi^{-1}) \qquad (5)$$

where $\sigma_{o,2N}$ = the mean stress at any reversal 2N

$\sigma_{o,i}$ = the initial mean stress

k = the relaxation exponent

$\Delta\varepsilon_p/2$ = the plastic strain amplitude

ε_{tr} = the strain amplitude resulting in a fatigue life equal to the transition fatigue life $2N_t^*$

To account for the actual mean stress effect on the fatigue life estimation, Eq. (5) in combination with Eqs. (3) and (4) may be employed.

The fatigue crack initiation life of a notched specimen (N_I) depends upon a stress-strain parameter $K_f(\Delta S \Delta e E)^{1/2}$ and those material parameters characteristic of the fatigue resistance of a smooth specimen[5]:

$$K_f(\Delta S \Delta e E)^{1/2} = (\Delta\sigma \Delta\varepsilon E)^{1/2} \qquad (6)$$

where ΔS and Δe = nominal stress and strain ranges

$\Delta\sigma$ and $\Delta\varepsilon$ = notch root stress and strain ranges

K_f = the fatigue notch factor of the notched specimen

---

* The transition fatigue life $2N_t$ is the fatigue life of a smooth specimen subjected to equal components of elastic strain and plastic strain.

A notched specimen subjected a notch root stress-strain $K_f(\Delta S \Delta e E)^{1/2}$ will have the same life to initiate a crack as does an unnotched specimen subjected to a stress-strain $(\Delta\sigma\Delta\varepsilon E)^{1/2}$: this concept is known as the local stress-strain approach for N_I estimation.

1.3 Fracture Mechanics Concepts

The successful application of fracture mechanics concepts to fatigue crack propagation rate problems enables the estimation of the remaining crack propagation life of a cracked member with a known initial crack size. Many theories and empirical equations relating fatigue crack propagation rate (da/dN) to stress intensity factor range (ΔK) have been proposed[7-10]; the most commonly used is the Paris power law[7]:

$$\frac{da}{dN} = C\,(\Delta K)^m \qquad (7)$$

where

$$C \text{ and } m = \text{material constants}$$

Fatigue crack propagation life (N_p) can be calculated by integrating Eq. (7) from the initial crack length (a_I) to the final crack length (a_f)

$$N_p = \int_{a_I}^{a_f} \frac{1}{C(\Delta K)^m}\, da \qquad (8)$$

The influence of mean stress on the crack propagation rate can be accounted for in terms of stress ratio ($R = S_{min}/S_{max}$)[9] (Eq. 9) or effective stress intensity factor range (ΔK_{eff})[10] (Eq. 10):

$$\frac{da}{dN} = \frac{C' (\Delta K)^{m'}}{(1-R) K_c - \Delta K} \tag{9}$$

$$\frac{da}{dN} = C (\Delta K_{eff})^{m} \tag{10}$$

where

C' and m' = Forman's crack growth coefficient and exponent,

K_c = the fracture toughness

C and m = Paris' crack growth coefficient and exponent

As the stress intensity factor range (ΔK) is decreased below a certain value, called the threshold stress intensity factor range (ΔK_{th}), the crack propagation rate diminishes rapidly to vanishingly small levels[11-12]. This implies that a crack may not propagate unless the stress intensity factor range (ΔK) exceeds the threshold value (ΔK_{th}).

1.4 When is a Crack a Crack?

Although the local stress-strain approach for estimating crack initiation life of a notched member has been developed to a practical state and although the crack growth power law enables (in many circumstances) a precise estimate of crack propagation life for a cracked member with a known initial crack size, the estimation of the total fatigue life is still problematic, because the proper means

of joining of these two analyses remains unclear. An arbitrary crack initiation length must be assumed to proceed with the estimation of N_T.

Recently, many investigators have been studying the problem, known as, "when is a crack a crack?" Nelson and Fuchs[13] postulated that the fatigue damage due to crack initiation at an arbitrary element located along the potential crack path decreased with increasing distance from the notch root, while the fatigue damage due to crack propagation increased with increasing distance from the notch root. The intersection of the two damage curves was proposed as the demarcation between crack initiation and propagation. Methods for calculating the damage due to crack initiation and propagation were not described.

The growth of fatigue cracks emanating from holes have been studied by Broek[14], Smith and Miller[15], and Hammouda and Miller[16]. Cracks emanating from holes initially grow somewhat faster than would be expected on the basis of ΔK but at a decreasing rate, reaching a minimum, and then at an increasing rate as might be expected on the basis of ΔK. Smith and Miller[15] proposed that these observed crack growth rates result from the superposition of the rate controlled by notch root plasticity and the rate controlled by the crack tip plasticity. The former decreases, while the latter increases, as the distance from the notch root increases. The two rates become equal at some distance from the notch root. Notch root plasticity controls both crack initiation and the early stage of crack growth, while crack tip plasticity controls the later crack growth stage. The above arguments imply a competition between the damage rate due to crack initiation mechanisms and that due

to crack propagation mechanisms, but Smith and Miller made no attempt to define a boundary between crack initiation and propagation using this idea.

Meanwhile, Socie, Morrow, and Chen[17] proposed a model for calculating the damage rate due to crack initiation mechanisms from low cycle fatigue concepts and the damage rate due to crack propagation mechanisms from fracture mechanics concepts. The onset of the crack propagation phase was thought to occur when the damage rate due to the crack propagation mechanism exceeds that due to crack initiation mechanism. This model will be discussed in detail in the next chapter and in Appendix I.

1.5 Scope

The purposes of this work are to search for physical and analytical evidence which confirms or refutes the proposed nonarbitrary definition of the crack initiation length and to further understand the joining of the fatigue crack initiation and propagation analyses. An alternative but numerically equivalent method for defining the nonarbitrary crack initiation length and the total fatigue life of a notched member is proposed. An interpretation of the fatigue notch size effect employing the developed analytical model is given. A numerical method for determining $\sqrt{\rho}$ and "a" of Neuber's and Peterson's formulae relating K_f to K_t and r employing this analytical model is proposed. The sensitivity of total fatigue life estimates (N_T) to the precise value of crack initiation length (a_I) is examined by comparing the N_T estimates

resulting from the nonarbitrarily defined crack initiation length (a_I) to values less or greater than a_I.

II. MODEL FOR THE NONARBITRARY DEFINITION OF CRACK INITIATION LENGTH

2.1 General

The zone ahead of a notch root is simulated by an infinite number of micro-elements, see Fig. 1(a). The transition from crack initiation to propagation is determined by the competition of the damage rate due to crack initiation (low cycle fatigue mechanisms) with the damage rate due to crack propagation. Socie, et al. [17] proposed that the damage rate due to crack initiation could be calculated using low cycle fatigue concepts, and that the damage rate due to crack propagation can be calculated using fracture mechanics concepts: see Appendix I. The fatigue crack propagation phase is considered to begin when the damage rate due to crack propagation mechanisms exceeds that due to crack initiation mechanisms.

Subsequently, Chen and Lawrence[18] have analysed the total fatigue life (N_T) as a function of the assumed crack initiation length and have proposed an alternative but numerically equivalent method for defining the crack initiation length (a_I) and the total fatigue life (N_T) of a notched member: see Appendix II. The determination of a_I on the basis of damage rate calculation[17] is termed the rate-calculation method and the determination of a_I on the basis of total life calculation[18] will be termed the life-calculation method.

Although the rate-calculation method and the life-calculation method are numerically equivalent, the latter has two advantages: (1) it is easier and simpler to apply, and (2) it provides predictions for the crack

initiation length and total fatigue life of a notched member as well as a simple model for understanding the effect of the arbitrarily assumed crack initiation length on the fatigue life predictions.

2.2 Life-calculation Method[18]

Using concepts originally proposed by Morrow, the material ahead of a notch root is considered to be a series of micro-elements, see Fig. 1(a). From an elasto-plastic finite element analysis[19] of the stresses and strains experienced by each element and from the stress-life and strain-life relationships [2,3] (Eqs. (1) through (4)), the fatigue life (N_f) of any element a distance (x) from the notch root may be determined. Equation (5) is used in combination with Eqs. (3) and (4) to account for the time variation of mean stress on the fatigue life of the micro-element. This calculated life (N_f) is regarded as the fatigue crack initiation life (N_I) corresponding to the choice of *that* element as the arbitrarily assumed boundary between crack initiation and propagation. The crack propagation life (N_p) is calculated assuming an initial crack length (x) equal to the distance of *that particular* element from the notch root and assuming an appropriate final crack length (a_f).

Newman's results[20] of stress intensity correction factor (F) are used for the calculation of stress intensity factor. Paris' crack-propagation-rate law[7] for a specific stress ratio (R) (Eq. (7)) or Forman's crack-propagation-rate law[9] (Eq. (9)) is used in crack propagation life calculation to account for the mean stress effect. The calculated N_I and N_p for a given element (x) are summed to give a total fatigue life (N_T) associated

with *that choice* of element (x). A brief summary of this calculation is illustrated in Fig. A-3. A sample calculation is given in Appendix III.

Because the calculated N_I increases and the calculated N_p decreases with increasing x, the values of N_T at first decrease, pass through a minimum and then increase as the choice of element (x) increases: see Figs. 1(b) or A-3(f). This minimum value of N_T is taken as the predicted or true total fatigue life (N_T) of the notched member, and the distance from the notch root of the element at which this minimum occurs is defined as the nonarbitrary crack initiation length (a_I). The fatigue life of the micro-element at a_I is the predicted crack initiation life (N_I). The predicted crack propagation life (N_p) is calculated from the crack initiation length (a_I) to the appropriate final size (a_f).

The application of this method to a circularly notched specimen of HY-130 steel is shown in Figs. 2 and 3. As seen in Fig. 2, the calculated N_p (and hence N_T) becomes infinite for very small x, since the crack propagation rate becomes vanishingly small as x approaches a_{th} (ΔK approaches ΔK_{th})[11,12]. The solid arrows indicate a_I defined by the proposed model, and the open arrow denotes the crack size (a_{th}) determined by the threshold stress intensity ΔK_{th}. At high stress levels, the minimum of N_T estimates occur at a_I larger than a_{th}. At low stresses, the minimum of N_T estimates occur when x approaches a_{th}, see Fig. 2(c). Since it may take an enormous number of cycles to propagate a crack of a size less than a_{th} to a_{th} and since it takes far fewer cycles to break the micro-elements from the notch root to a distance equal to a_{th} through the low cycle fatigue mechanisms, the crack should initiate through the crack intiation

mechanism to a distance a_{th}, and then extend to failure through the crack propagation mechanism. Therefore, at low stresses, ΔK_{th} determines a_I.

2.3 Propagating Crack Shape Correction

Scanning electron microscope fractography of notched specimens showed that the cracks either (i) nucleated in the mid-thickness of the notch root and propagated as semi-circular cracks, or (ii) nucleated at one of the corners of the notch root and propagated as a quarter-circular corner crack, or (iii) nucleated somewhere in between and propagated as a semi-circular crack at first, then, after propagating to one edge, as a quarter-circular corner crack. Thus, the actual crack shape had to be considered in the crack propagation calculations since the assumption of a through-thickness crack would be incorrect during the early stage of crack propagation.

In addition to Newman's results of stress intensity correction factor for the cracks emanating from the circular or elliptical hole in a finite plate, a penny shape crack correction factor $(2/\pi)$, was introduced for the semi-circular crack correction; and the multiplication of the penny shape crack correction factor $(2/\pi)$ and the surface crack correction factor (1.12) was introduced for the quarter-circular corner crack correction. Because the fatigue crack propagation life resulting from case (iii) is between those found for cases (i) and (ii), only the corrections for cases (i) and (ii) need be considered.

Figure 4 shows the improvement in total life predictions, a factor of 1.5 to 2, caused by the inclusion of the shape factor corrections in the

calculation of N_p. Since the predictions for a_I and N_T on the basis of a semi-circular crack and those on the basis of a quarter-circular corner crack do not differ much, only the semi-circular crack shape is used unless otherwise specified.

2.4 Mean Stress Effect

For any loading cycle having a non-zero mean stress, cyclic mean-stress relaxation may occur. Due to the large plastic strain amplitudes experienced by micro-elements near the notch root it is expected the mean stress relaxation could be very rapid for the elements and that mean stress relaxation must be considered in the estimation of N_I through the application of Eq. (5). Mean stress relaxation is expected to be particularly rapid for materials having small E and ε_{tr}.

Figure 5 shows the N_T vs. x curves for both the mean stress relaxation (solid curve) and invariant mean stress (dashed curve) cases. Although the difference between the predicted N_T considering mean stress relaxation (solid arrow) and invariant mean stress (open arrow) is small, the predicted a_I are markedly different. Since the fatigue notch factor (K_f) is determined by the stress-strain parameter $(\Delta S_I \Delta e_I E)^{1/2}$ at the crack initiation length a_I (discussed in the next chapter) and since the partitioning of crack initiation life (N_I) and crack propagation life (N_p) depends on the crack initiation length a_I (discussed in Chapter IV), modelling mean stress relaxation is very important. The details of the method are given in Appendix III.

2.5 Experimental Verification

A comparison of the fatigue lives predicted using this analytical model with experimental results[21-23] is given for circularly notched specimens of 4340 steel (Fig. 6), 7075-T6 aluminum alloy (Fig. 7) and AISI 1020 steel (Fig. 8), and for various notched specimens of 7075-T651 aluminum alloy (Figs. 9-12). The life-predictions follow the procedures of the Life-calculation method described in Section 2.2 and Appendix III. The necessary material properties for the life-predictions were taken from the literature[21-25]: see Tables 1-4. Agreement between the experimental results and the analytical predictions is good, within a factor of 3.

2.6 Scanning Electron Microscope Fractography

In addition to comparing the predicted fatigue lives with the experimental results, the model was verified by comparing the predicted crack initiation lengths with the observed ones.

A JSM-25 scanning electron microscope was employed to locate the boundary between the fatigue crack initiation and propagation on fatigue fracture surfaces. The fatigue striation is one of the features on aluminum alloy fatigue fracture surface which may be readily observed. The absence of the fatigue striations on the fatigue fracture surface in the vicinity of a notch root may not be evidence of the fatigue crack initiation process, but their presence is evidence of fatigue crack propagation. Tracing along the crack path from the notch root using a scanning electron microscope, the first appearance of fatigue striations may be regarded as the onset of fatigue crack propagation.

Figure 13 shows a portion of the crack initiation site (marked by a solid arrow). The top edge of the figure is the notch root. In this figure, striations do not appear until the crack had advanced to 0.178 mm (0.007 in.) from the notch root. A magnification of 1000X is not high enough to reveal the finely spaced fatigue striations, however. The higher magnification (3000X and 10000X) fractographs of Fig. 14 reveal finely spaced striations within the areas marked by squares in Fig. 13, which are less than 0.178 mm (0.007 in.) from the notch root-edge. The fractographs in Fig. 14 show that the fatigue striations first appear at a distance 0.102 mm (0.004 in.) from the notch root. This distance was defined as the upper bound of crack initiation.

It would be desirable to define a lower bound of the crack initiation length. Since the fatigue fracture surface morphology of the fatigue crack initiation and the early stage of crack propagation (Stage I crack propagation) are not well established at this time, it is difficult to accomplish this.

The predicted crack initiation length of the specimen corresponding to the electron fractographs in Figs. 13 and 14 is 0.102 mm (0.004 in.) agrees favorably with the observed upper bound, 0.102 mm (0.004 in.). The results of electron fractography for several 7075-T651 aluminum alloy notched specimens are summarized in Fig. 15, in which the predicted crack initiation length is plotted against the observed upper bound of crack initiation length.

III. INTERPRETATION OF THE FATIGUE NOTCH SIZE EFFECT

3.1 General

The effect of a notch on a material's strength is generally found to be less in fatigue than in the monotonic loading. Thus, the fatigue notch factor (K_f), which is defined as the ratio of the fatigue endurance limit of smooth specimens to the fatigue endurance limit of notched specimens at a given life, is equal to or less than the theoretical stress concentration factor (K_t). Unlike the theoretical stress concentration factor (K_t) which is constant for geometrically similar notched specimens, the fatigue notch factor (K_f) is size dependent: it decreases with decreasing specimen size.

3.2 Fatigue Notch Size Effect

The fatigue notch size effect has been studied for more than a half century[26-37]; yet, the phenomenon remains poorly understood. The notch sensitivity index (q):

$$q = \frac{K_f - 1}{K_t - 1} \tag{11}$$

where: K_f = fatigue notch factor

K_t = theoretical stress concentration factor

is often used to quantify the fatigue notch sensitivity of a notched specimen. The fatigue notch sensitivity index (q) decreases with decreasing notch root radius (r).

Many theories of the fatigue notch size effect have been proposed which relate q and r and, hence, K_f to K_t and r[26-37]. Neuber[26]

interpreted the fatigue notch size effect in terms of the stress gradient at the notch tip and considered the material ahead of the notch root to be composed of an aggregate of small "blocks" each of which was incapable of sustaining a stress gradient. The maximum stress, K_f S, occurred in the "block" at the notch root which is always less than theoretical value K_t S because of the finite size of the block. Neuber proposed a relationship between K_f and K_t:

$$K_f = 1 + \frac{K_t - 1}{1 + \sqrt{\frac{\rho}{r}}} \tag{12}$$

where, ρ is the size of material "block" at the notch root, a material constant which must be determined by experiment.

Peterson[29,30] interpreted the fatigue notch size effect in terms of the stress gradient ahead of the notch and a distance (δ) characteristic for a particular material. Peterson assumed that fatigue failure would occur when the stress at a distance (δ) ahead of the notch (K_f S) equalled the endurance limit of an unnotched specimen. This assumption lead to the result commonly called Peterson's equation:

$$K_f = 1 + \frac{K_t - 1}{1 + \frac{a}{r}} \tag{13}$$

where a is an experimentally determined material constant. For design purposes in steel $a \approx 0.001\ [300/S_u(\text{ksi})]^{1.8}$ inches[3].

Other theories such as the statistical approaches[31-34] and the highly stressed volume approaches[35-37] have suggested other empirical relationships between K_f and K_t, but none predicts the fatigue

notch effect more successfully than Neuber's and Peterson's formulae which are widely used in design because of their simplicity.

3.3 Influence of Notch Root Plasticity

Most of the above developments are restricted to the case of purely elastic notch root deformations, and it is for that reason that the fatigue notch factor has been studied at or near the endurance limit. Neuber[38] studied the nonlinear stress-strain behavior at the notch root and concluded:

$$K_t = (K_\sigma K_\varepsilon)^{1/2} = \left(\frac{\sigma\varepsilon}{Se}\right)^{1/2} \tag{14}$$

where $K_\sigma = \sigma/S$

$K_\varepsilon = \varepsilon/e$

Topper, et al.[5] modified Eq. (14), known as Neuber's rule, for fatigue by substituting K_f for K_t and defining the stresses and strains in terms of their ranges:

$$K_f = \left(\frac{\Delta\sigma\Delta\varepsilon E}{\Delta S\Delta e E}\right)^{1/2} \tag{15}$$

where ΔS, $\Delta\sigma$ = nominal, notch root stress ranges

Δe, $\Delta\varepsilon$ = nominal, notch root strain ranges

E = Young's Modulus

rewriting Eq. (15):

$$K_f (\Delta S\Delta e E)^{1/2} = (\Delta\sigma\Delta\varepsilon E)^{1/2} \tag{6}$$

which implies that a notched specimen subjected to a stress-strain $K_f(\Delta S\Delta e F)^{1/2}$ at its notch root should have the same crack initiation life as an unnotched specimen subjected to a stress-strain equal to $(\Delta\sigma\Delta\varepsilon E)^{1/2}$.

This assumption is known as the local stress-strain approach for N_I estimation.

The failure criterion used to define K_f may be a source of its reported variability[39-41]. While K_f is often defined on the basis of total life, it should be defined solely on the basis of crack initiation. The lack of agreement as to what constitutes crack initiation makes this approach difficult. In this connection, the recent model for the non-arbitrary definition of the crack initiation length[17,18], as described in Chapter 2, provides a basis for defining the initiation life and, hence, of circumventing this problem.

3.4 Estimations of K_t and K_f

From the elasto-plastic finite element analyses of the notch geometries shown in Fig. 9, K_t can be derived from Eq. (14) as the ratio of the notch root stresses and strains $(\Delta\sigma\Delta\epsilon E)^{1/2}$ to the nominal stresses and strains $(\Delta S\Delta e E)^{1/2}$ (see Fig. 1):

$$K_t = \frac{(\Delta\sigma\Delta\epsilon E)^{1/2}}{(\Delta S\Delta e E)^{1/2}} \tag{16}$$

As shown in Figs. 17 and 18, K_t defined in this manner varies slightly with applied stress and, hence, with fatigue life.

Likewise, K_f can be estimated as the ratio of an unnotched (smooth) specimen stresses and strains $(\Delta\sigma_s\Delta\epsilon_s E)^{1/2}$ to the notched specimen (nominal) stresses and strains $(\Delta S\Delta e E)^{1/2}$ at some given life, as shown in Fig. 16.

$$K_f = \frac{(\Delta\sigma_s \Delta\varepsilon_s E)^{1/2} \text{ at } N_f}{(\Delta S \Delta e E)^{1/2} \text{ at } N_T = N_f} \quad \text{(Total life basis)} \tag{17}$$

or

$$K_f = \frac{(\Delta\sigma_s \Delta\varepsilon_s E)^{1/2} \text{ at } N_f}{(\Delta S \Delta e E)^{1/2} \text{ at } N_I = N_f} \quad \text{(Initiation life basis)} \tag{18}$$

The K_f (and to a lesser extent K_t) defined in this traditional manner varies with applied stress level and, hence, fatigue life as shown in Figs. 17 and 18.

As implied by Eqs. 17 and 18, the situation is complicated by the possibility of defining K_f on the basis of total fatigue life (N_T) or initiation life (N_I) (as defined herein). Using the initiation life basis, K_f can be defined alternatively as the ratio of $(\Delta S_I \Delta e_I E)^{1/2}$ (the stress-strain parameter for a hypothetical micro-element at a distance a_I from the notch root) to the nominal stress-strain parameter $(\Delta S \Delta e E)^{1/2}$,

$$K_f = \frac{(\Delta S_I \Delta e_I E)^{1/2}}{(\Delta S \Delta e E)^{1/2}} \tag{19}$$

This definition results from the fact that the N_I of the notched specimen (subjected to a nominal stress-strain $(\Delta S \Delta e E)^{1/2}$) is equal to the N_f of the micro-element at a_I which is subjected to a stress-strain parameter $(\Delta S_I \Delta e_I E)^{1/2}$ (see Fig. 1). The micro-element at a_I experiences an N_f identical to that of the *unnotched* specimen subjected to a stress-strain parameter equal to $K_f(\Delta S \Delta e E)^{1/2}$ (because of Eq. 18) and therefore, the

micro-element stress-strain parameter $(\Delta S_I \Delta e_I E)^{1/2}$ must be the same as that of the *unnotched* specimen $(\Delta\sigma_s \Delta\varepsilon_s E)^{1/2}$ which is equal to $K_f(\Delta S \Delta e E)^{1/2}$: see Eq. (19).

3.5 Variation of K_f and q

For HY-130 steel, both total and initiation life bases produce the same estimates of K_t and K_f at lives greater than 10^6; but for shorter lives, the values of K_f, particularly, vary greatly: see Figs. 19 and 20. Using the total life basis (Fig. 19), the model predicts the variation in K_f with life observed by Raske[39]. Less variation in K_f at short lives is observed if K_f is defined on the basis of initiation life: see Fig. 20. Figures 19 and 20 also show the variation of the notch sensitivity index (q) (defined by Eq. (11)) with life. The variation in q is similar to K_f, since K_t, although inconstant, does not vary much.

Figures 19 and 20 also show the variations in K_f and q with the notch size at various life levels. On the initiation life basis, the variation of K_f and q with notch size is only pronounced at long life levels (low stresses): see Fig. 20(a) and (c). This phenomenon can be explained by Fig. 21, where the normalized crack initiation lengths with half specimen width (a_I/W) of four geometrically similar notched specimens are plotted as a function of stress level.

At high stress levels, the a_I/W of the four notched specimens are almost the same; while at low stress levels, a large specimen (with a large notch) has a small a_I/W. The stress-strain distribution ahead of

the notch exhibits geometric similitude: it is independent of scale. Thus, at high stress levels, one obtains the same K_f for the four similar notched specimens: only at low stress levels is the notch size effect pronounced.

3.6 Estimation of Neuber and Peterson Parameters, $\sqrt{\rho}$ and a

Using either the initiation or total life bases of defining q produces consistent estimates of that quantity at long lives. Estimates of q at 10^7 cycles as a function of notch root radius have been made for the three notch geometries shown in Fig. 9 and for three different materials: HY-130, a high strength quenched and tempered steel (Fig. 22); a 7075-T651 aluminum alloy (Fig. 23); and, A-36 mild steel (Fig. 24). The estimated values of q are more or less independent of notch geometry in all cases. Best fit Neuber ($\sqrt{\rho}$) and Peterson (a) parameters have been fitted to the calculated points (solid curve and dashed curve). The values of $\sqrt{\rho}$ and "a" producing the best fit to the calculated points agree well with reported experimental values[3, 27-30]:

Material	$\sqrt{\rho}$ (in.$^{1/2}$)		a (in.)	
	calc.	exp.	calc.	exp.
HY-130	.042	.0313 [27]	.0055	.0031 [3]
7075-T651	.1	.125 [28]	.017	.02 [30]
A-36	.17	.106 [27]	.035	.018 [3]

3.7 Variation of $\sqrt{\rho}$ and "a" with Life

Figures 22-24 show that the fatigue notch size effect of a given material may be characterized by Neuber ($\sqrt{\rho}$) or Peterson (a) parameters. However, Figs. 19 and 20 show that the fatigue notch size effect varies with life. Thus, a variation of Neuber ($\sqrt{\rho}$) and Peterson "a" parameters with life may be expected. Estimates of q at various life levels as a function of notch root radius (r) are plotted in Figs. 25-27 (q on basis of N_T) and Figs. 28-30 (q on basis of N_I) for the three materials in Figs. 22-24. The q-r curves in Figs. 25-30 are the best fit curves to the calculated data points (not shown in the figures). Best fit Neuber ($\sqrt{\rho}$) and Peterson (a) parameters to the calculated data points are also given in the same figures.

Defining q on the basis of N_T, the notch size effect decreases with increasing life, reaching a minimum, and then increasing. However, defining q on the basis of N_I produces a more orderly variation of that quantity with life: the notch size effect increases with increasing the crack initiation life. The notch size effect of HY-130 steel and 7075-T651 aluminum alloy is only pronounced at lives greater than 10^6 cycles (in this region, q varies with r) and vanishes at a life of 10^3 cycles (q reaches a limiting value), as shown in Figs. 28 and 29. This result also leads to the surprising conclusion that small radius notches should be more effective (have higher value of q) at short lives than at long lives: see Figs. 28 and 29.

The best fit Neuber ($\sqrt{\rho}$) and Peterson (a) parameters on the basis of both N_I and N_T in Figs. 25-30 are plotted against N_I and N_T in Figs. 31-33. On the total fatigue life basis, $\sqrt{\rho}$ and "a" decrease, reach a minimum, and then increase with increasing life. On the crack initiation life basis, $\sqrt{\rho}$ and "a" always increase with increasing the life. The experimental values of $\sqrt{\rho}$ and "a" reported in the literature[3,27-30] are also plotted in the figures (solid symbols) for comparison.

IV. PARTITIONING OF FATIGUE CRACK INITIATION AND PROPAGATION LIVES

4.1 Factors Influencing a_I

The crack initiation length (a_I) is not a fixed value as usually assumed, but varies with load level, notch size, notch geometry, and material. As seen in Figure 3, the value of a_I defined by the model decreases with decreasing stress level until a_I approaches a_{th}, after which both a_I and a_{th} increase with further decreases in stress level.

In addition to the load dependence, the dependence of a_I on notch-geometry, notch-size and material has been studied (Figs. 34-36). Predictions of a_I as a function of N_T have been made for three notch geometries shown in Fig. 9 and three different materials: HY-130 steel, 7075-T651 aluminum alloy and A-36 mild steel. Although a_I varies with the notch geometries (Fig. 34), no consistent variation has been found for the three different materials. A-36 mild steel exhibits longer crack initiation lengths than HY-130 steel and 7075-T651 aluminum alloy: see Fig. 35.

The notch size effect on a_I was studied (Fig. 36) by plotting a_I against N_T for four geometrically similar notches differing only in size. The larger the notch size, the longer is the crack initiation length. As seen in Figs. 34-36, the variation in a_I with the notch size and material is more significant than the variation with notch geometry.

For the three materials studied, a_I ranges from 2.54 mm to 0.011 mm (0.1 in. to 0.00045 in.) for HY-130 steel; from 1.78 mm to 0.010 mm (0.07 in. to 0.0004 in.) for 7075-T651 aluminum alloy; and from 6.60 mm to

0.10 mm (0.26 in. to 0.004 in.) for A-36 mild steel depending on stress level (or life level), notch size and notch geometry.

The influence of R ratio was not studied.

4.2 Partitioning of N_I and N_P

Using the definition of the crack initiation length (a_I) provided by the model, the N_I and N_P of a notched member can be partitioned. Calculations of N_I and N_T are illustrated in Section 2.2 and Fig. 1. Plots of $N_I\%$ as a function of N_T are given in Figs. 37-42 for three notch geometries of Fig. 9 and for three materials: HY-130 steel, 7075-T651 aluminum alloy and A-36 mild steel. For a given material, a blunt notch is more crack-initiation dominant than the sharp notch, as seen in Figs. 37-39. For a given notch geometry, mild steel is more crack propagation dominant than high strength steel or high strength aluminum alloy in the intermediate and high cycle regimes, see Figs. 40-42.

The notch size effect on $N_I\%$ is shown in Figs. 43-45, where the $N_I\%$ is plotted as a function of N_T for four geometrically similar notched specimens of HY-130 steel. A large specimen (with a large notch size) is more crack initiation dominant than the small specimen (with a small notch size) in the low and intermediate life regimes.

As seen in Figs. 37-45 at lives greater than 10^7 or 10^8 cycles, the total fatigue life is almost entirely crack initiation regardless of notch size, notch geometry and material. Also, all these figures are characterized by the S-shape of the $N_I\%$ vs. N_T curves which indicates a transition from crack propagation dominance to crack initiation dominance with increasing the total life.

4.3 Effect of Arbitrary Assumed Crack Initiation Length on N_T Estimation

The Life-calculation method allows the effect of an arbitrarily assumed crack initiation length (x) on the fatigue life predictions to be studied: see Figs. 1(b) and 2. An assumed crack initiation length (x) larger/smaller than a_I results in a longer/shorter N_I estimate and a shorter/longer N_P estimate. The decrease/increase in N_I partially compensates for the increase/decrease in N_P resulting in little variation in N_T with x about a_I. In other words, the N_T estimation may not be too sensitive to the exact value of the assumed crack initiation length (x).

At high stress levels, the N_T estimation is relatively insensitive to the assumed crack initiation length over a range of x, as seen in Figs. 46-48; but, the sensitivity of N_T estimate to x increases with decreasing stress level. Since a small decrease in $(\Delta\sigma_s\Delta\varepsilon_s E)^{1/2}$ results in a greater increase in $2N_f$ at low $(\Delta\sigma_s\Delta\varepsilon_s E)^{1/2}$ than at high, as seen in Fig. A-3(c), a small increase in x (which results in a small decrease in $(\Delta S_x\Delta e_x E)^{1/2}$) leads to a greater increase in N_I estimate at low stress levels than that at high: see Fig. A-4(a)-(d). Also, with increasing x the estimated N_I becomes dominant over the estimated N_P and determines the estimated N_T. The estimated N_T is, thus, more sensitive to the assumed x at low stress levels than at high.

The sensitivity of the total fatigue life estimation to the assumed x also increases with decreasing notch size, as seen in Figs. 46-48. Since the $(\Delta S_x\Delta e_x E)^{1/2}$ gradient ahead of a notch root increases with decreasing notch size (same notch geometry), a small change in x may result

in a greater change in N_I estimate for a small notch than for a large notch. Thus, the estimated N_T for a small notch is more sensitive to the assumed crack initiation length (x) than for a large notch.

4.4 Effect of Calculated K_f on N_T Estimation

As described in Section 3.4, the hypothetical micro-element at a_I experiences a stress-strain parameter $(\Delta S_I \Delta e_I E)^{1/2}$ equal to $K_f(\Delta S \Delta e E)^{1/2}$, Eq. (19). Knowing K_f and the $(\Delta S_x \Delta e_x E)^{1/2}$ distribution ahead of a notch root, a_I can be determined (see Fig. (1)); and the N_T of the notched specimen can be obtained by summing up the N_I estimated from $K_f(\Delta S \Delta e E)^{1/2}$ or $(\Delta S_I \Delta e_I E)^{1/2}$ and the N_p estimated from a_I to a_f. Thus, the long standing problem as to how to join the N_I estimate using the local stress-strain approach and the N_p estimate using fracture mechanics concepts appears to be solved.

Usually, for design purposes K_f is calculated from Neuber's formula, Eq. (12), or Peterson's formula, Eq. (13), with a Neuber parameter $\sqrt{\rho}$ or Peterson parameter "a" reported in the literature[3, 27-30]. Since $\sqrt{\rho}$ and "a" are not fixed values but vary with life (as argued in Sec. 3.7 and Figs. 31-33) and since those reported $\sqrt{\rho}$ and "a" are restricted to lives at or near the endurance limit, the application of K_f calculated at the endurance limit to the N_T estimation at high stress levels (or short lives) may not be appropriate. In this connection, it would be nice to know the effect of the use of calculated K_f on the N_T estimation.

As defined herein, the K_f^N refers to the fatigue notch factor K_f calculated from the theoretical notch factor K_t and notch root radius r

using Neuber's formula, Eq. (12), with $\sqrt{\rho}$ reported in the literature. The K_f^P refers to that calculated using Peterson's formula, Eq. (13), and value of "a" reported in literature.

The crack initiation lengths (x) and the estimated total fatigue lives (N_T) determined from the calculated K_f^N and K_f^P are given on the N_T vs. x curves at various stress levels in Figs. 46-48. In these figures the arrows indicate the minima of the N_T vs. x curves, which give the predicted a_I and N_T on the basis of the proposed model. Although the crack initiation length x determined from the calculated K_f^N or K_f^P may deviate a great deal from a_I, the N_T estimates do not differ greatly. The reason is similar to that given in the previous section. At high stress levels, N_T estimation is rather insensitive to the assumed crack initiation length (x) and, hence, the value of K_f derived from an inappropriate $\sqrt{\rho}$ or a. The sensitivity of N_T to x increases with decreasing stress level. However, since the differences between K_f^N, K_f^P and K_f are least in this low-stress, long-life region (as discussed in Section 3.7), N_T estimates using K_f^N or K_f^P in this regime deviate little from the N_T estimate using the model.

Figs. 49 and 50 give the comparisons of the N_T estimates using Neuber's K_f^N (Fig. 49) and Peterson's K_f^P (Fig. 50) with the N_T estimates using the model for specimens of HY-130 steel. At low stress levels, the K_f^N or K_f^P may result in a crack initiation length less than a_{th}. Since a crack will not propagate unless the stress intensity range (ΔK) exceeds the threshold (ΔK_{th}), a_{th} is chosen as the crack initiation length when K_f^N or K_f^P determines a crack initiation length less than a_{th}. The solid symbols in Figs. 49 and 50 denote these cases.

A scatter band with a factor of 2 is plotted in each figure. The total fatigue lives estimated from Neuber's K_f^N (Fig. 49) and from Peterson's K_f^P (Fig. 50) agree well with the N_T estimates made using the model.

V. SUMMARY AND CONCLUSIONS

1. It was shown that the life-calculation and rate-calculation methods for nonarbitrarily defining the crack initiation length (a_I) are numerically equivalent. The life-calculation method enjoys two advantages: (1) it is easier and simpler to use; (2) it provides not only predictions for the crack initiation length (a_I) and the fatigue life (N_T) of a notched member but also a simple model for understanding the effect of the crack initiation length on the fatigue life estimation.

2. The crack initiation length (a_I) is not a fixed value, as usually assumed, but varies with stress level (or life), notch size, notch geometry, and material.

3. The partitioning of crack initiation life (N_I) and crack propagation life (N_P) can be achieved using the model.

4. The model provides an interpretation of fatigue notch size effect and a powerful means for numerically determining Neuber and Peterson parameters $\sqrt{\rho}$ and "a".

5. On the basis of crack initiation life, K_f is determined from the stress-strain parameter ($\Delta S_I \Delta e_I E$) at the crack initiation length (a_I).

6. The longstanding problem as to how to join the N_I estimate using the local stress-strain approach and the N_P estimate using fracture mechanics concepts appears to be solved by the use of a_I defined by the proposed model.

7. N_T estimates are relatively insensitive to the assumed crack initiation length at high stress levels; but, the sensitivity of N_T

estimation to the assumed crack initiation length (x) increases with decreasing stress level and with decreasing notch size.

REFERENCES

1. Forsyth, P. J. E., The Physical Basis of Metal Fatigue, American Elsevier Publishing Co., Inc., New York, 1969.

2. Morrow, JoDean, "Cyclic Plastic Strain Energy and Fatigue of Materials," ASTM STP 378, American Society for Testing and Materials, 1965, pp. 45-87.

3. Morrow, JoDean, "Fatigue Properties of Metals," SAE Fatigue Design Handbook, Section 3.2, Graham, J. A., Editor, Society of Automotive Engineers, 1968, pp. 21-30.

4. Raske, D. T. and Morrow, JoDean, "Mechanics of Materials in Low Cycle Fatigue Testing," ASTM STP 465, American Society for Testing and Materials, 1969, pp. 1-25.

5. Topper, T. H., Wetzel, R. M. and Morrow, JoDean, "Neuber's Rule Applied to Fatigue of Notched Specimens," Journal of Materials, Vol. 4, No. 1, March 1969, pp. 200-209.

6. Burke, J. D. and Lawrence, F. V., Jr., "The Effect of Residual Stresses on Weld Fatigue Life," FCP Report No. 29, University of Illinois at Urbana-Champaign, Urbana, Illinois, 1977.

7. Paris, P. C., and Erdogan, F., "A Critical Analysis of Crack Propagation Laws," Transactions of the ASME, J. of Basic Engineering, Series D, Vol. 85, No. 3, 1963, pp. 528-534.

8. Pelloux, R. M., "Review of Theories and Laws of Fatigue Crack Propagation," Proceedings of the Air Force Conference on Fatigue and Fracture of Aircraft Structures and Materials, AFFDL TR 70-144, 1970, pp. 409-416.

9. Forman, R. G., Kearney, V. E., and Engle, R. M., "Numerical Analysis of Crack Propagation in Cyclic-Load Structures," Trans. of ASME, J. of Basic Engineering, Series D, Vol. 89, September, 1967, pp. 459-464.

10. Elber, W., "The Significance of Fatigue Crack Closure," ASTM STP 486, American Society for Testing and Materials, 1971, pp. 230-242.

11. Pook, L. P., "Fatigue Crack Growth Data for Various Materials Deduced from the Fatigue Lives of Precracked Plates," ASTM STP 513, American Society for Testing and Materials, 1972, pp. 106-124.

12. Bucci, R. J., Paris, P. C., Hertzberg, R. W., Schmidt, R. A. and Anderson, A. F., "Fatigue Threshold Crack Propagation in Air and Dry Argon for a Ti-6Al-4V Alloy," ASTM STP 513, American Society for Testing and Materials, 1972, pp. 125-140.

13. Nelson, D. V. and Fuchs, H. O., "Prediction of Fatigue Crack Growth Under Irregular Loading," ASTM STP 595, 1976, pp. 267-291.

14. Broek, D., "The Propagation of Fatigue Crack Emanating from Holes," NLR TR 72134 U, National Aerospace Laboratory NLR, The Netherlands, 1972.

15. Smith, R. A. and Miller, K. J., "Fatigue Cracks at Notches," International Journal of Mechanical Science, Vol. 19, No. 1, 1977, pp. 11-22.

16. Hammouda, M. N. and Miller, K. J., "Elastic-Plastic Fracture Mechanics of Notches," Presented at Symposium on Elastic-Plastic Fracture ASTM, Atlanta, Georgia, November, 1977.

17. Socie, D. F., Morrow, J. and Chen, W. C., "A Procedure for Estimating the Total Fatigue Life of Notched and Cracked Members," Journal of Engineering Fracture Mechanics, Vol. 11, No. 4, 1979, pp. 851-860.

18. Chen, W. C. and Lawrence, F. V., Jr., "Fatigue Life Prediction Based on Arbitrary and Nonarbitrary Crack Initiation Length," Progress Report in Advisory Committee Meeting of Fracture Control Program, College of Engineering, University of Illinois at Urbana-Champaign, November, 1977.

19. Socie, D. F., "Prediction of Fatigue Crack Growth in Notched Members under Variable Amplitude Loading History," Engineering Fracture Mechanics, Vol. 9, No. 4, 1977, pp. 849-865.

20. Newman, J. C., Jr., "An Improved Method of Collocation for the Stress Analysis of Cracked Plates with Various Shaped Boundaries," NASA TN D-6376, 1971.

21. Raske, D. T., "Section and Notch Size Effects in Fatigue," T.& A.M. Report No. 360, Dept. of Theoretical and Applied Mechanics, University of Illinois, Urbana, IL., August, 1972.

22. Herman, P. M., "Initiation and Propagation of Fatigue Cracks in Notched Steel Plates," Term paper for CE 497, Department of Civil Engineering, University of Illinois, Urbana, IL., 1974.

23. Kurath, P., "Investigation into a Nonarbitrary Fatigue Crack Size Concept," T.& A.M. Report No. 429, Department of Theoretical and Applied Mechanics, University of Illinois, Urbana, IL., October 1978.

24. Hadley, J. C., "Corrosion Fatigue Cracking Behavior of 190 ksi Yield Strength 4340 Steel in 3.5% Sodium Chloride Solutions," M. S. Thesis, Dept. of Theoretical and Applied Mechanics, University of Illinois, Urbana, IL., 1971.

25. Wilhem, D. P., "Investigation of Cyclic Crack Growth Transitional Behavior," ASTM 415, American Society for Testing and Materials, 1967, pp. 363-380.

26. Neuber, H., Theory of Notch Stresses: Principle for Exact Stress Calculations, J. W. Edwards, Ann Arbor, Michigan, 1946.

27. Kuhn, P. and Hardrath, H. F., "An Engineering Method for Estimating Notch-Size Effect in Fatigue Tests on Steels," National Advisory Committee for Aeronautics, Technical Note 2805, Oct. 1952.

28. Kuhn, P. and Figge, I. E., "Unified Notch-Strength Analysis for Wrought Aluminum Alloys," National Aeronautics and Space Administration, Technical Note D-1259, May 1962.

29. Peterson, R. E., "Notch-Sensitivity," Metal Fatigue, Chap. 13, Sines and Waisman, Editors, McGraw-Hill Book Co., Inc., 1959.

30. Peterson, R. E., "Analytical Approach to Stress Concentration Effect in Fatigue of Aircraft Materials," Proceedings on Fatigue of Aircraft Structures, WADC Technical Report No. 59-507, August 1959, pp. 273-299.

31. Aphanasiev, N. N., "The Effect of Shape and Size Factors on the Fatigue Strength," The Engineers' Digest, Vol. 5, No. 3, March-April 1948, pp. 132-136.

32. Heywood, R. B., Design by Photoelasticity, Chapman and Hall Ltd., London, 1952, p. 348.

33. Harris, W. J., "Size Effects and their Possible Significance for Non-Propagating Cracks in Metal," Metallurgia, Vol. 57, No. 342, April 1958, pp. 193-197.

34. Endo, K. and Uede, T., "Studies on the Size Effect of Bending and Twisting Fatigue Strength," Bulletin, Japanese Society of Mechanical Engineers, Vol. 8, No. 31, August 1965, pp. 314-321.

35. Kuguel, R., "A Relation Between Theoretical Stress Concentration Factors and Fatigue Notch Factor Deducted from the Concept of Highly Stressed Volume," Proceedings, American Society for Testing and Materials, Vol. 61, 1961, pp. 732-748.

36. Switek, W. and Buch, A., "The Problem of Maximum Notch Effect in Case of Flat Elements with Transverse Holes," Proceedings of the third Conference on Dimensioning and Strength Calculations, Hungarian Academy of Science, Budapest, Nov. 1968, pp. 275-286.

37. Raske, D. T., "Fatigue Failure Predictions for Plates with Holes and Edge Notches," Journal of Testing and Evaluation, Vol. 1, No. 5, Sept. 1973, pp. 394-404.

38. Neuber, H., "Theory of Stress Concentration for Shear-Strained Prismatical Bodies with Arbitrary Non Linear Stress-Strain Law," Journal of Applied Mechanics, Vol. 28, Dec. 1961, pp. 544-550.

39. Raske, D. T., "The Variation of the Fatigue Notch Factor with Life," M. S. Thesis, University of Illinois at Urbana-Champaign, Illinois, 1971.

40. Leis, B. N. and Topper, T. H., "Assessing Notch Strength Reduction in Cyclically Loaded Notched Components," the second International Conference on Structural Mechanics in Reactor Technology, Vol. 5, Part L, 1973.

41. Gowda, C. V. B., Leis, B. N. and Smith, K. N., "Dependence of Fatigue Notch Factor on Plasticity and Duration of Crack Growth," Journal of Testing and Evaluation, Vol. 2, No. 1, January, 1974, pp. 57-61.

42. Majumdar, S., "Low Cycle Fatigue Behavior and Crack Propagation in Some Steels," T.& A.M. Report No. 387, Department of Theoretical and Applied Mechanics, University of Illinois, Urbana, IL., April 1974.

43. Rolfe, S. T. and Barsom, J. M., Fracture and Fatigue Control in Structures - Applications of Fracture Mechanics, Chaps. 7 and 8, Prentice-Hall, Inc., Englewood Cliffs, New Nersey, 1977.

44. Mattos, R. J. and Lawrence, F. V., Jr., "Estimation of the Fatigue Crack Initiation Life in Welds Using Low Cycle Fatigue Concepts," FCP Report No. 19, College of Engineering, University of Illinois, Urbana, IL., October 1975.

TABLE 1. MECHANICAL PROPERTIES OF 4340 STEEL[21,24]

Monotonic Properties:			
Elastic Modulus,	E	208,911 MPa	(30,300 ksi)
Yield Strength (0.2%),	S_y	1,103.2 MPa	(160.0 ksi)
Tensile Strength,	S_u	1,172.1 MPa	(170.0 ksi)
Reduction in Area,	% RA	56.0%	
True Fracture Strength,	σ_f	1,634.0 MPa	(237.0 ksi)
True Fracture Ductility,	ϵ_f	0.83	
Cyclic Properties:			
Cyclic Yield Strength,	S'_y*	723.9/414.8 MPa	(105.0/60.2 ksi)
Cyclic Strength Coefficient,	K'	1,760.9 MPa	(255.4 ksi)
Cyclic Strain Hardening Exponent,	n'	0.146	
Fatigue Strength Coefficient,	σ'_f	1,713.3 MPa	(248.5 ksi)
Fatigue Strength Exponent,	b	-0.095	
Fatigue Ductility Coefficient,	ϵ'_f	0.83	
Fatigue Ductility Exponent,	c	-0.65	
Transition Fatigue Life,	$2N_t$	4100	
Propagation Properties:			
Crack Growth Coefficient (R = 0),	C	5.68×10^{-11}	
Crack Growth Exponent (R = 0),	m	3.3	
Threshold Stress Intensity (R = 0),	ΔK_{th}	6.6 MPa $\sqrt{m}$	(6.0 ksi $\sqrt{in}$)
Fracture Toughness,	K_C	87.9 MPa $\sqrt{m}$	(80 ksi $\sqrt{in}$)

*The first value is the 0.2% offset value. The second value is the elastic limit.

TABLE 2. MECHANICAL PROPERTIES OF 7075-T6 ALUMINUM ALLOY [21,25]

Monotonic Properties:			
Elastic Modulus,	E	71,016 MPa	(10,300 ksi)
Yield Strength (0.2%),	S_y	468.8 MPa	(68.0 ksi)
Tensile Strength,	S_u	579.2 MPa	(84.0 ksi)
Reduction in Area,	% RA	33.0%	
True Fracture Strength,	σ_f	744.6 MPa	(108.0 ksi)
True Fracture Ductility,	ε_f	0.41	
Cyclic Properties:			
Cyclic Yield Strength,	S'_y*	517/331 MPa	(75.0/48.0 ksi)
Cyclic Strength Coefficient,	K'	2,514.0 MPa	(185.8 ksi)
Cyclic Strain Hardening Exponent,	n'	0.146	
Fatigue Strength Coefficient,	σ'_f	1,917 MPa	(278.1 ksi)
Fatigue Strength Exponent,	b	-0.176	
Fatigue Ductility Coefficient,	ε'_f**	0.156/0.8	
Fatigue Ductility Exponent,	c**	0.526/0.839	
Transition Fatigue Life,	$2N_t$	140 reversals	
Propagation Properties:			
Crack Growth Coefficient (R = 0),	C	1.12×10^{-8}	
Crack Growth Exponent (R = 0),	m	3.23	
Threshold Stress Intensity (R = 0),	ΔK_{th}	2.75 MPa $\sqrt{m}$	(2.5 ksi $\sqrt{in}$)
Fracture Toughness,	K_C	36.3 MPa $\sqrt{m}$	(33.0 ksi $\sqrt{in}$)

*The first value is the 0.2% offset value. The second value is the elastic limit.

**The arched curve of $\Delta\varepsilon_p/2$ vs. $2N_f$ is approximated by two linear lines of $\Delta\varepsilon_p/2 = \varepsilon'_f (2N_f)^c$. The first value is for the one in the short life region, and the second one is for the one in the long life region. These two lines intersect at a life of 150 reversals.

TABLE 3. MECHANICAL PROPERTIES OF AISI 1020 STEEL [22]

Monotonic Properties:			
Elastic Modulus,	E	206,843 MPa	(30,000 ksi)
Yield Strength (0.2%),	S_y	289.6 MPa	(42.0 ksi)
Tensile Strength,	S_u	455.1 MPa	(66.0 ksi)
Reduction in Area,	% RA	59.0%	
True Fracture Strength,	σ_f	765.3 MPa	(111.0 ksi)
True Fracture Ductility,	ϵ_f	0.90	
Cyclic Properties:			
Cyclic Yield Strength,	S'_y*	248.2/95.8 MPa	(36.0/13.9 ksi)
Cyclic Strength Coefficient,	K'	1,441 MPa	(209.0 ksi)
Cyclic Strain Hardening Exponent,	n'	0.283	
Fatigue Strength Coefficient,	σ'_f	882.5 MPa	(128.0 ksi)
Fatigue Strength Exponent,	b	-0.118	
Fatigue Ductility Coefficient,	ϵ'_f	0.160	
Fatigue Ductility Exponent,	c	-0.412	
Transition Fatigue Life,	$2N_t$	226,000 reversals	
Propagation Properties:			
Crack Growth Coefficient (R = 0),	C	1.018×10^{-8}	
Crack Growth Exponent (R = 0),	m	3.3	
Threshold Stress Intensity (R = 0),	ΔK_{th}	6.6 MPa $\sqrt{m}$	(6.0 ksi $\sqrt{in}$)
Fracture Toughness,	K_C	49.5 MPa $\sqrt{m}$	(45 ksi $\sqrt{in}$)

*The first value is the 0.2% offset value. The second value is the elastic limit.

TABLE 4. MECHANICAL PROPERTIES OF 7075-T651 ALUMINUM ALLOY[23]

Monotonic Properties:			
Elastic Modulus,	E	69,640 MPa	(10,100 ksi)
Yield Strength (0.2%),	S_y	537 MPa	(77.9 ksi)
Tensile Strength,	S_u	589 MPa	(85.4 ksi)
Reduction in Area,	% RA	13.5%	
True Fracture Strength,	σ_f	656 MPa	(95.1 ksi)
True Fracture Ductility,	ε_f	0.1451	
Cyclic Properties:			
Cyclic Yield Strength,	S'_y*	541/487 MPa	(78.5/70.6 ksi)
Cyclic Strength Coefficient,	K'	694 MPa	(100.7 ksi)
Cyclic Strain Hardening Exponent,	n'	0.040	
Fatigue Strength Coefficient,	σ'_f**	791.5/166.4 MPa	(114.8/241.4 ksi)
Fatigue Strength Exponent,	b**	-0.04/-0.149	
Fatigue Ductility Coefficient,	ε'_f	0.158	
Fatigue Ductility Exponent,	c	-0.83	
Transition Fatigue Life,	$2N_t$	30 reversals	
Propagation Properties:			
Crack Growth Coefficient (R = 0.1),	C	1.18×10^{-8}	
Crack Growth Exponent (R = 0.1),	m	2.94	
Threshold Stress Intensity (R = 0.1),	ΔK_{th}	2.75 MPa $\sqrt{m}$	(2.5 ksi $\sqrt{in}$)
Fracture Toughness,	K_C	44 MPa $\sqrt{m}$	(40 ksi $\sqrt{in}$)

*The first value is the 0.2% offset value. The second value is the elastic limit.

**The arched curve of $\Delta\varepsilon_e/2$ vs. $2N_f$ is approximated by two linear lines of $\Delta\varepsilon_e/2 = (\sigma'_f/E)\ (2N_f)^b$. The first value is for the one in the short life region, and the second value is for the one in the long life region. These two lines intersect at a life of 10^3 reversals.

TABLE 5. MECHANICAL PROPERTIES OF HY-130 STEEL[42,43]

Monotonic Properties:			
Elastic Modulus,	E	193,100 MPa	(28,000 ksi)
Yield Strength (0.2%),	S_y	1,014 MPa	(147 ksi)
Tensile Strength,	S_u	1,103 MPa	(160 ksi)
Reduction in Area,	% RA	67%	
True Fracture Strength,	σ_f	1,544 MPa	(224 ksi)
True Fracture Ductility,	ε_f	0.92	
Cyclic Properties:			
Cyclic Yield Strength,	S'_y*	814/538 MPa	(118/78 ksi)
Cyclic Strength Coefficient,	K'	1,517 MPa	(220 ksi)
Cyclic Strain Hardening Exponent,	n'	0.100	
Fatigue Strength Coefficient,	σ'_f	1,489 MPa	(216 ksi)
Fatigue Strength Exponent,	b	-0.060	
Fatigue Ductility Coefficient,	ε'_f	0.90	
Fatigue Ductility Exponent,	c	-0.64	
Transition Fatigue Life,	$2N_t$	3,660 reversals	
Propagation Properties:			
Crack Growth Coefficient (R = 0.1),	C	7.74×10^{-9}	
Crack Growth Exponent (R = 0.1),	m	2.16	
Threshold Stress Intensity (R = 0.1),	ΔK_{th}	6.04 MPa $\sqrt{m}$	(5.5 ksi $\sqrt{in}$)
Fracture Toughness,	K_C	91.2 MPa $\sqrt{m}$	(83 ksi $\sqrt{in}$)

*The first value is the 0.2% offset value. The second value is the elastic limit.

TABLE 6. MECHANICAL PROPERTIES OF A-36 MILD STEEL[43,44]

Monotonic Properties:			
Elastic Modulus	E	189,600 MPa	(27,500 ksi)
Yield Strength (0.2%),	S_y	224 MPa	(32.5 ksi)
Tensile Strength,	S_u	414 MPa	(60.0 ksi)
Reduction in Area,	% RA	69.7%	
True Fracture Strength,	σ_f	951 MPa	(138 ksi)
True Fracture Ductility,	ϵ_f	1.19	
Cyclic Properties:			
Cyclic Yield Strength,	S'_y*	232/93 MPa	(33.6/13.5 ksi)
Cyclic Strength Coefficient,	K'	1,489 MPa	(216 ksi)
Cyclic Strain Hardening Exponent,	n'	0.293	
Fatigue Strength Coefficient,	σ'_f	1,016 MPa	(147.4 ksi)
Fatigue Strength Exponent,	b	-0.132	
Fatigue Ductility Coefficient,	ϵ'_f	0.27	
Fatigue Ductility Exponent,	c	-0.451	
Transition Fatigue Life,	$2N_t$	217,000 reversals	
Propagation Properties:			
Crack Growth Coefficient (R = 0.1),	C	1.018×10^{-10}	
Crack Growth Exponent (R = 0.1),	m	3.3	
Threshold Stress Intensity (R = 0.1),	ΔK_{th}	6.6 MPa $\sqrt{m}$	(6.0 ksi $\sqrt{in}$)
Fracture Toughness,	K_C	49.5 MPa $\sqrt{m}$	(45 ksi $\sqrt{in}$)

*The first value is the 0.2% offset value. The second value is the elastic limit.

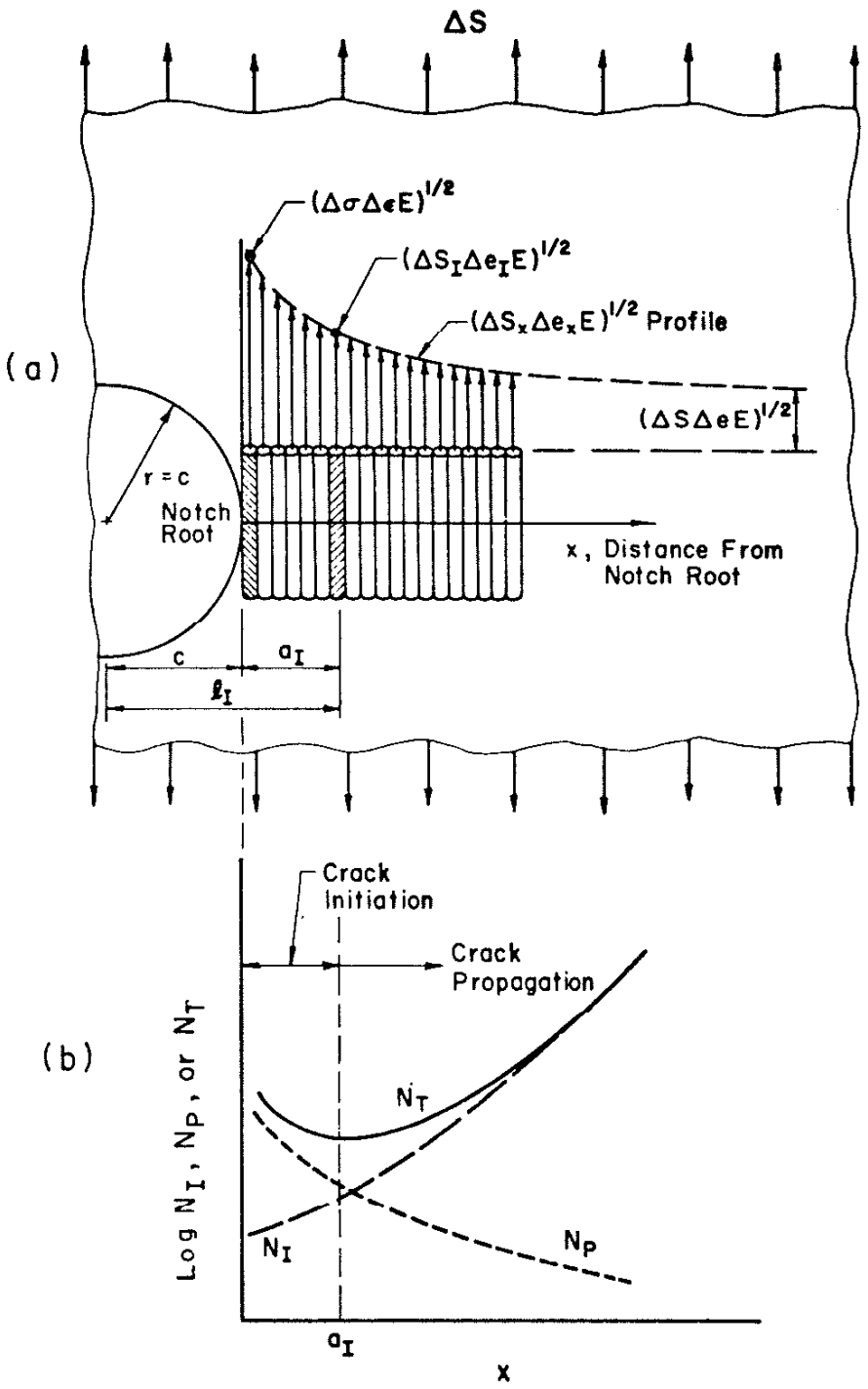

FIGURE 1. CONCEPT OF THE LIFE CALCULATION METHOD AND a_I

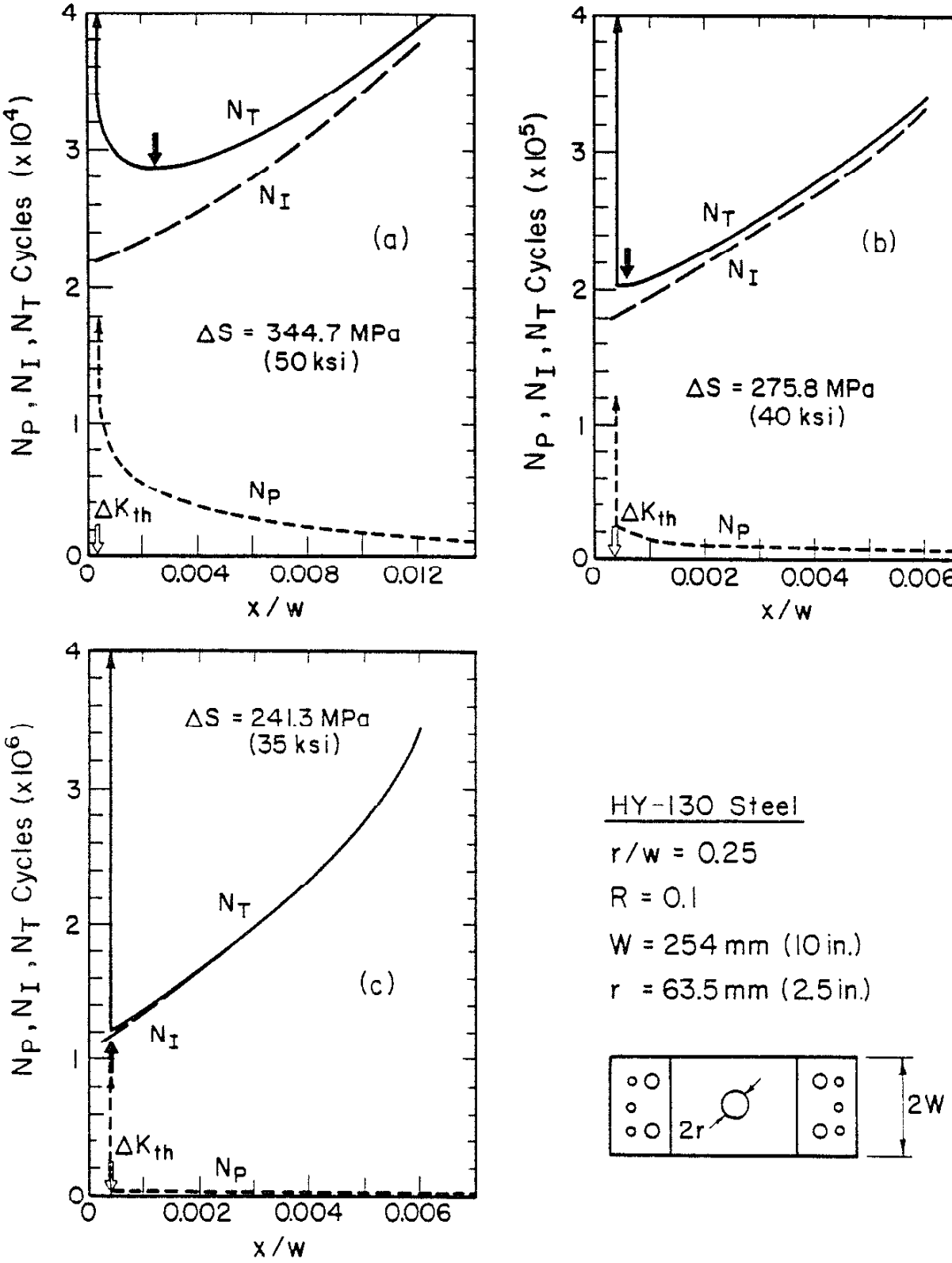

FIGURE 2. APPLICATION OF THE LIFE CALCULATION METHOD TO A CIRCULARLY NOTCHED SPECIMEN AT VARIOUS STRESS LEVELS

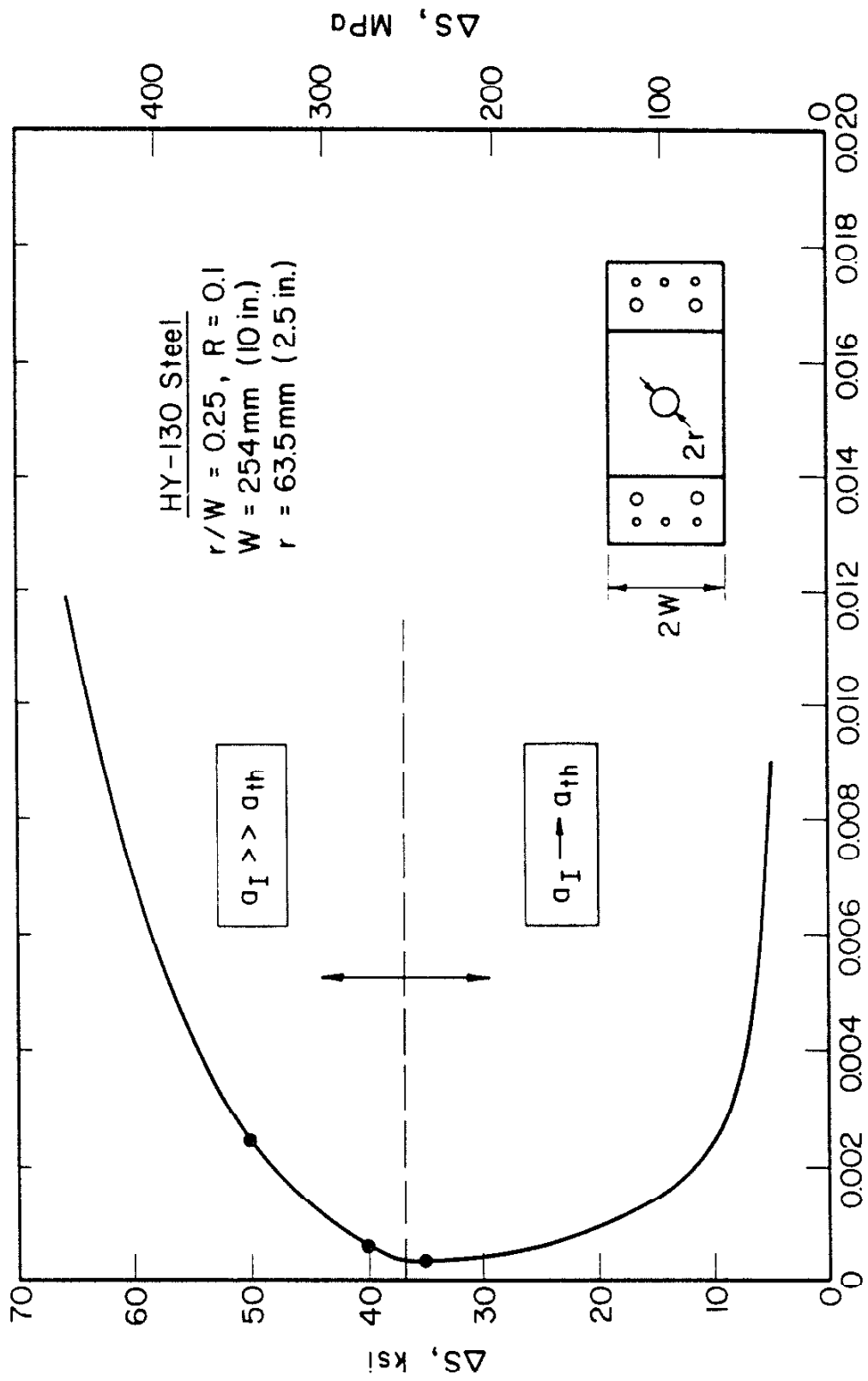

FIGURE 3. PREDICTED CRACK INITIATION LENGTH (a_I) AS A FUNCTION OF APPLIED STRESS FROM FIG. 2

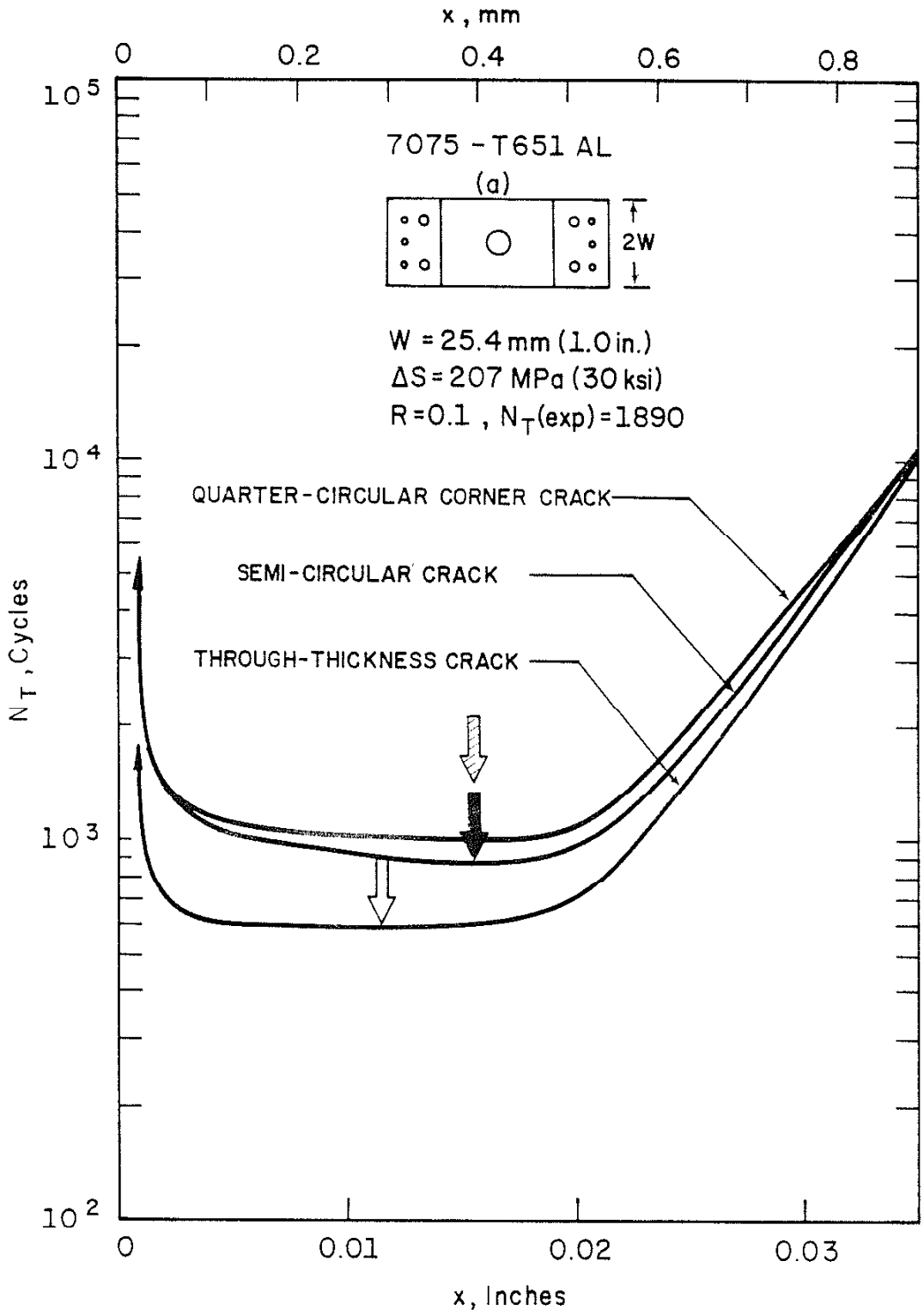

FIGURE 4. EFFECT OF PROPAGATING CRACK SHAPE CORRECTIONS ON THE PREDICTIONS FOR a_I AND N_T

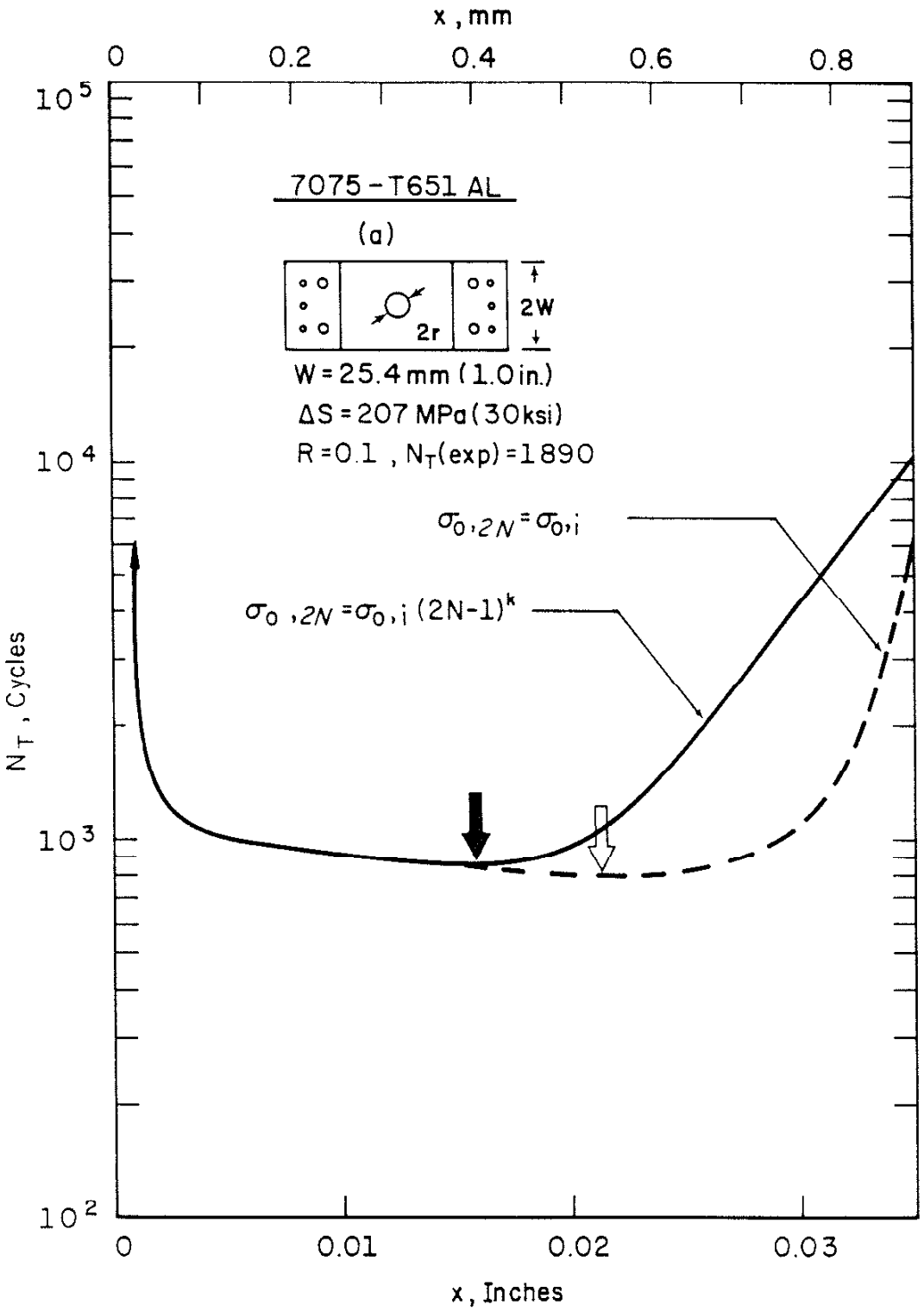

FIGURE 5. EFFECT OF MEAN STRESS RELAXATION ON THE N_T ESTIMATES

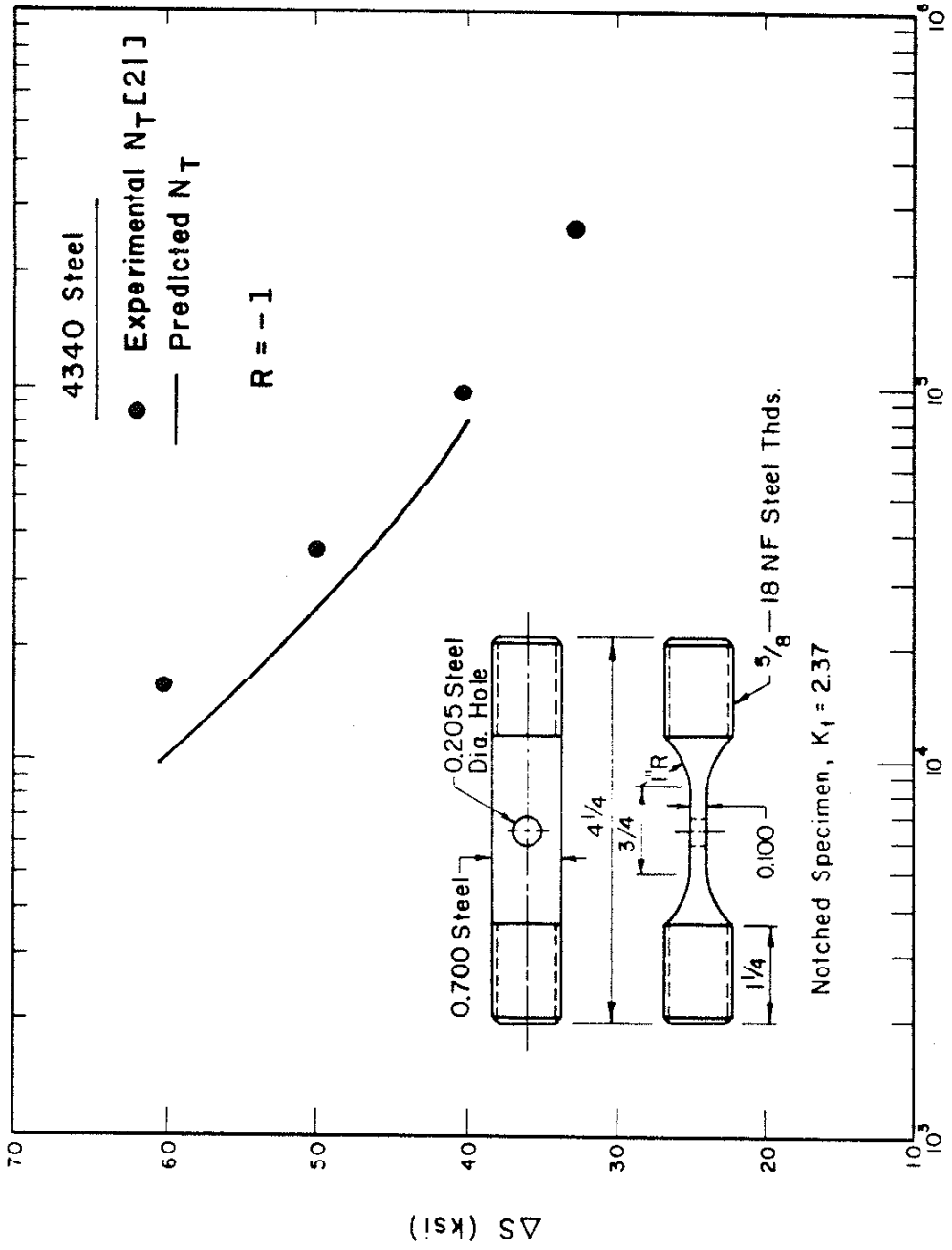

FIGURE 6. PREDICTED AND EXPERIMENTAL LIVES FOR A CIRCULARLY NOTCHED SPECIMEN OF 4340 STEEL

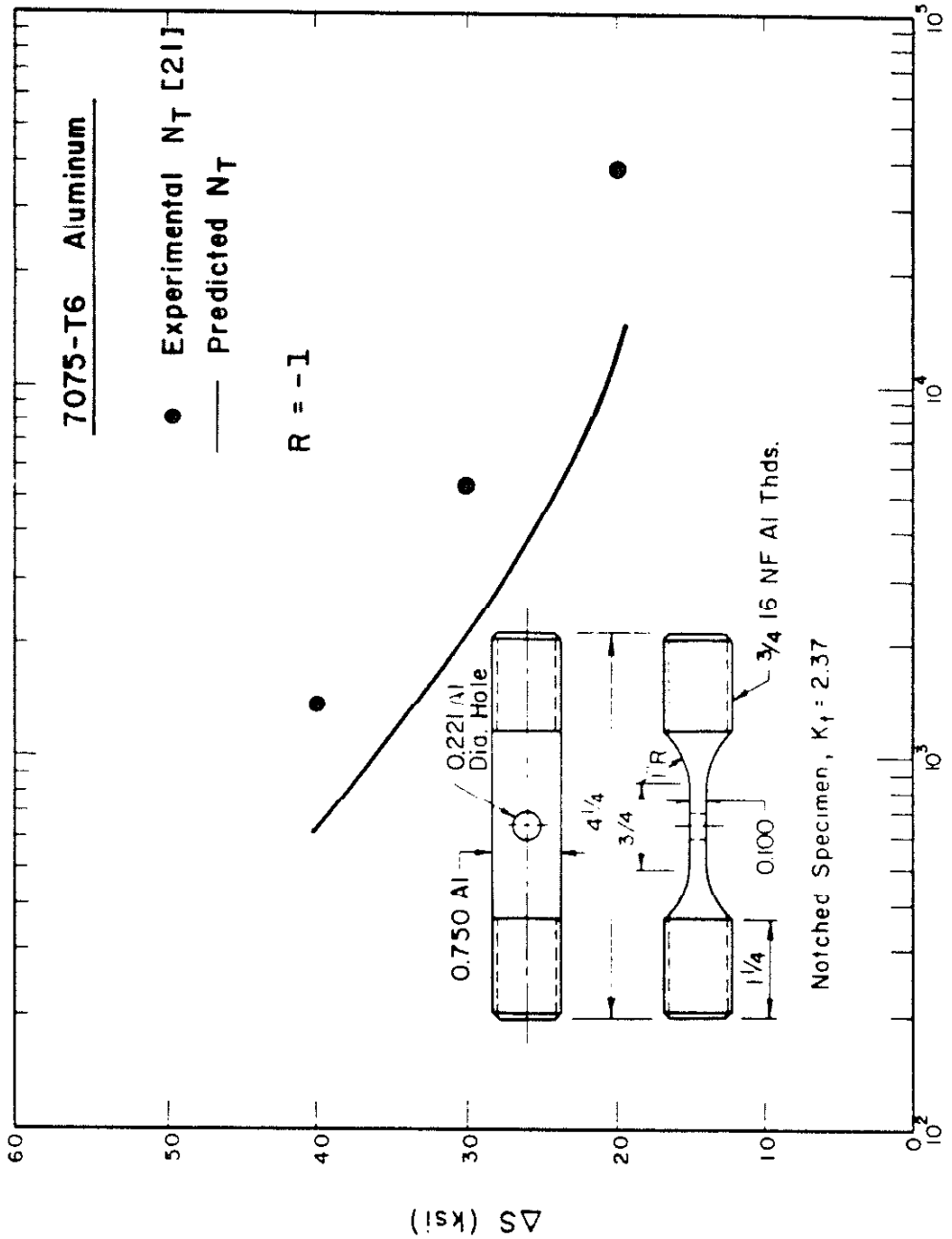

FIGURE 7. PREDICTED AND EXPERIMENTAL LIVES FOR A CIRCULARLY NOTCHED SPECIMEN OF 7075-T6 ALUMINUM ALLOY

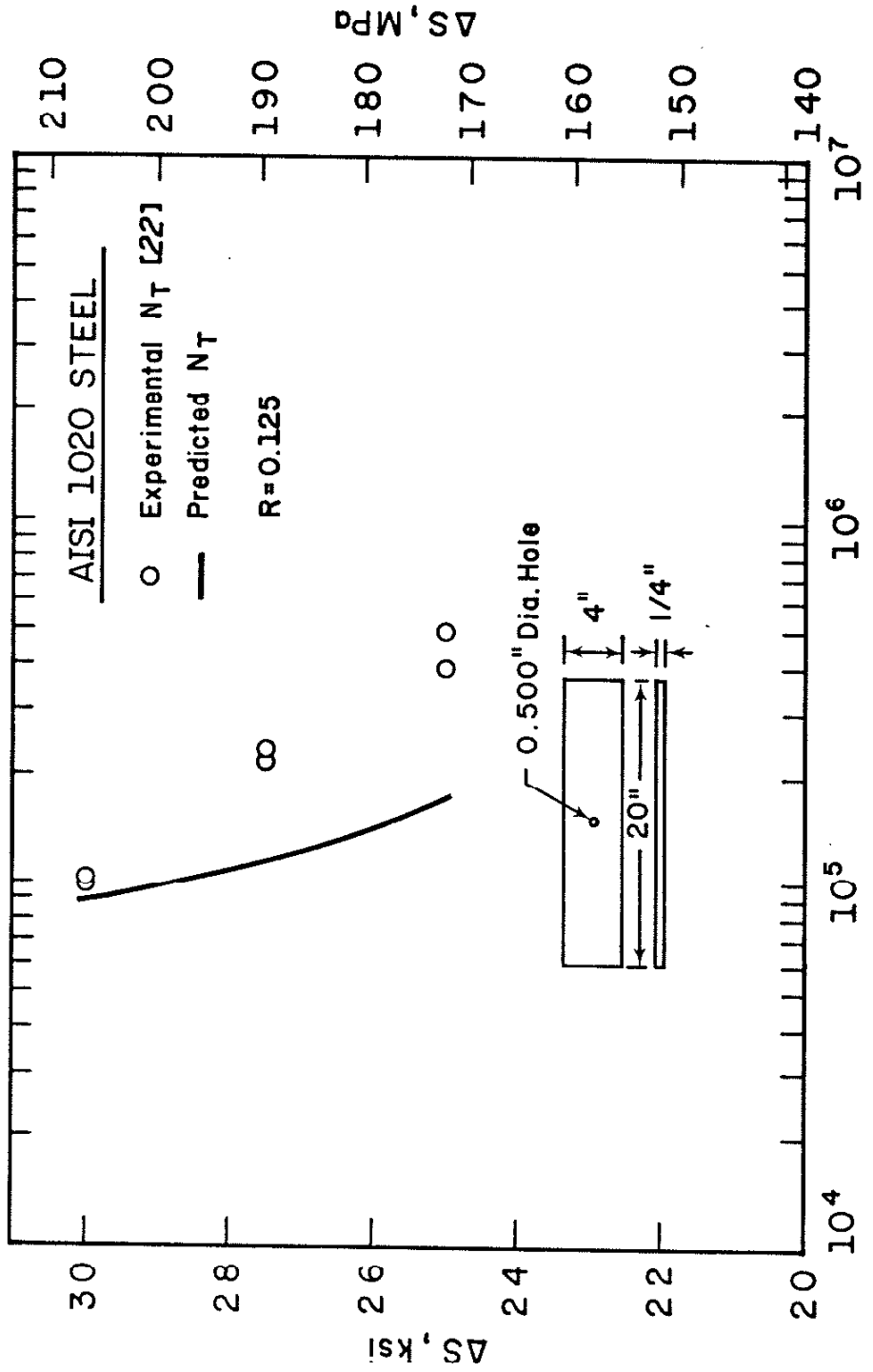

FIGURE 8. PREDICTED AND EXPERIMENTAL LIVES FOR A CIRCULARLY NOTCHED SPECIMEN OF AISI 1020 STEEL

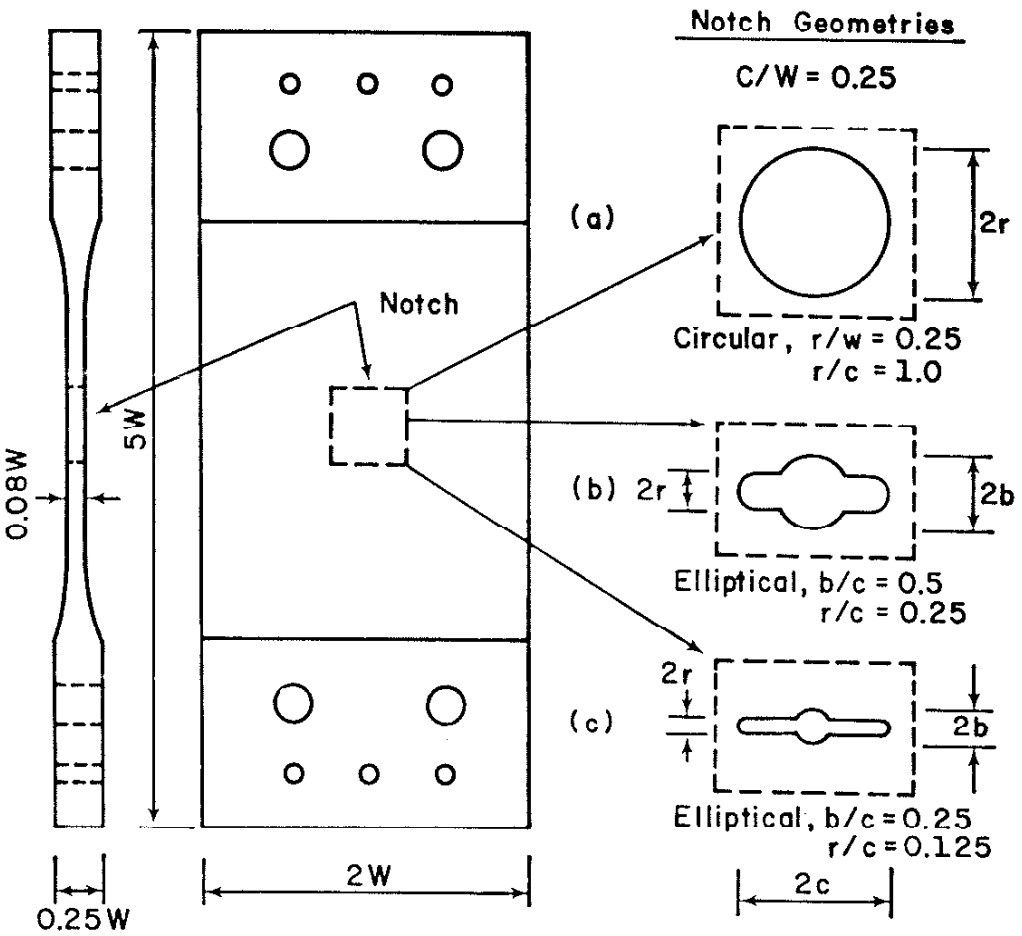

FIGURE 9. NOTCH GEOMETRIES FOR 7075-T651 ALUMINUM ALLOY, HY-130 STEEL AND A-36 STEEL

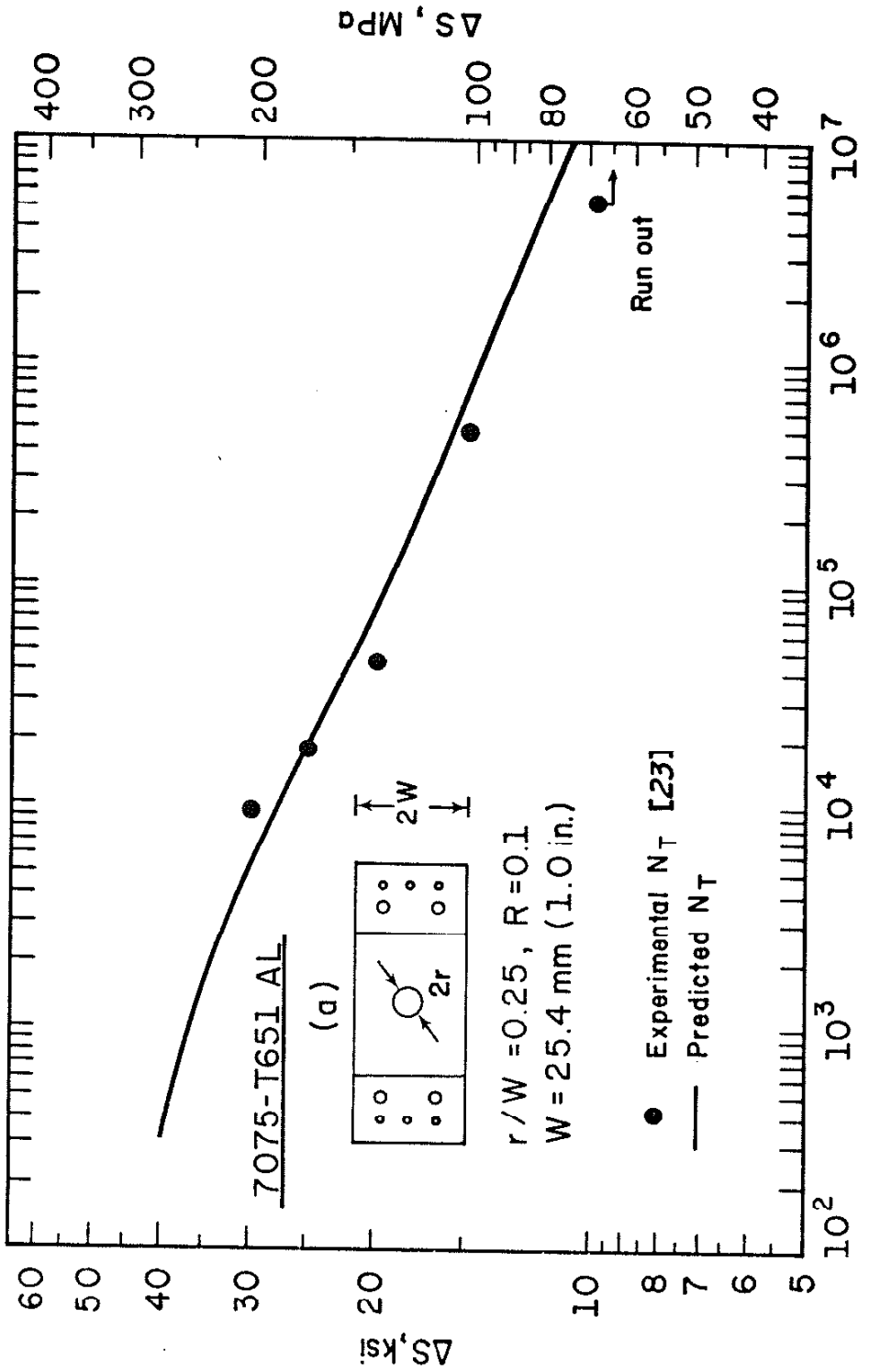

FIGURE 10. PREDICTED AND EXPERIMENTAL LIVES FOR A CIRCULARLY NOTCHED SPECIMEN OF 7075-T651 ALUMINUM ALLOY

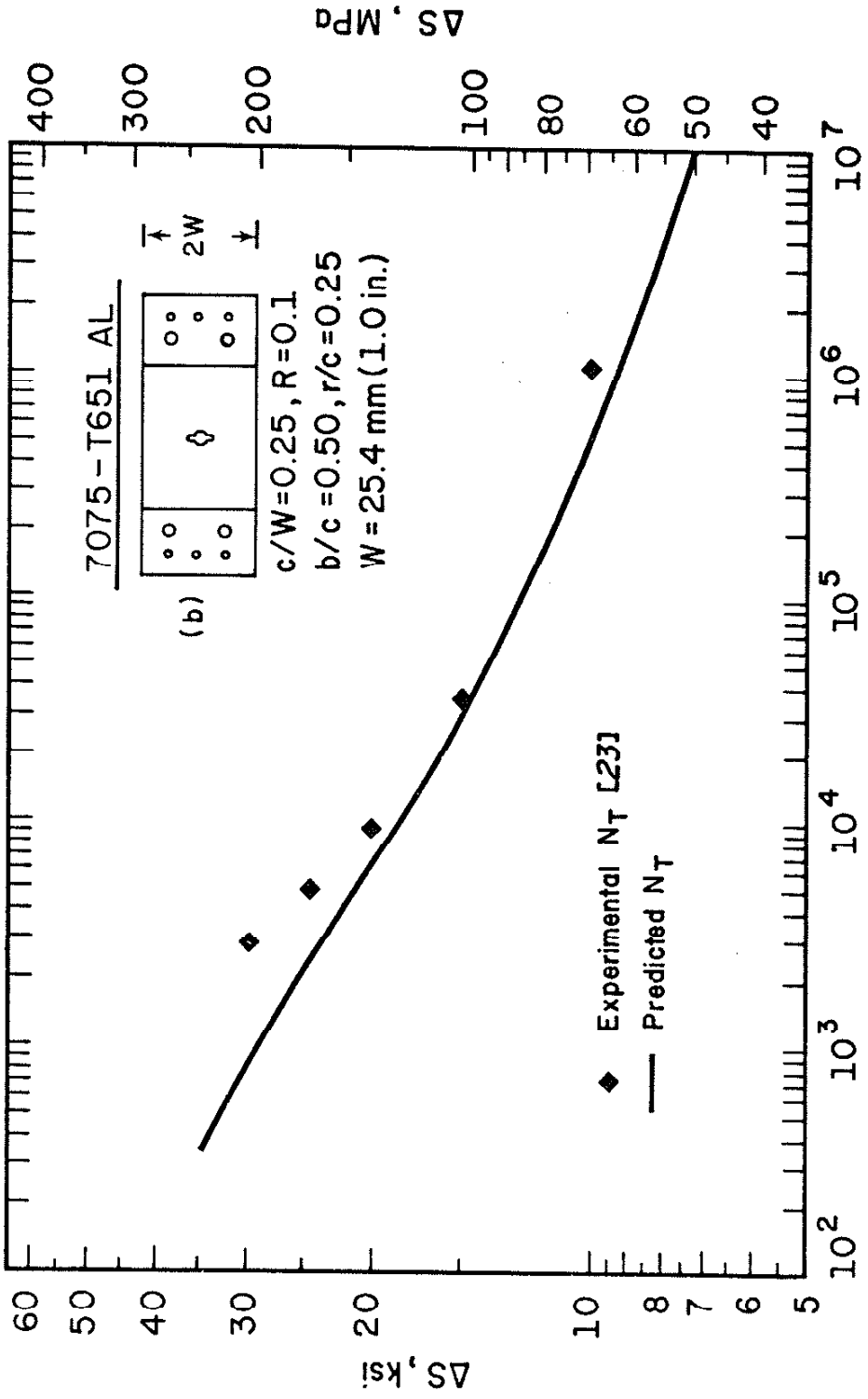

FIGURE 11. PREDICTED AND EXPERIMENTAL LIVES FOR AN ELLIPTICALLY NOTCHED SPECIMEN OF 7075-T651 ALUMINUM ALLOY

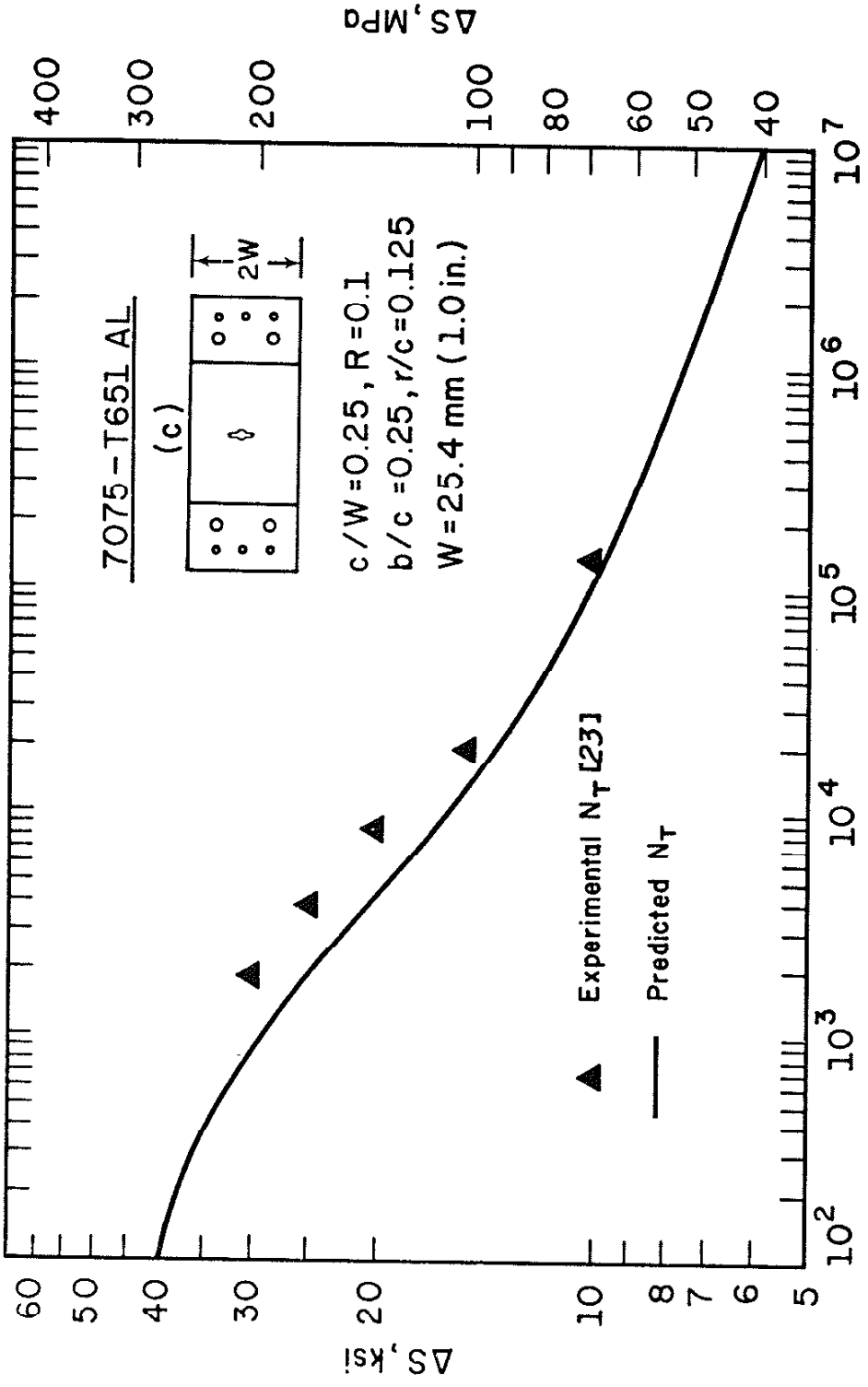

FIGURE 12. PREDICTED AND EXPERIMENTAL LIVES FOR AN ELLIPTICALLY NOTCHED SPECIMEN OF 7075-T651 ALUMINUM ALLOY

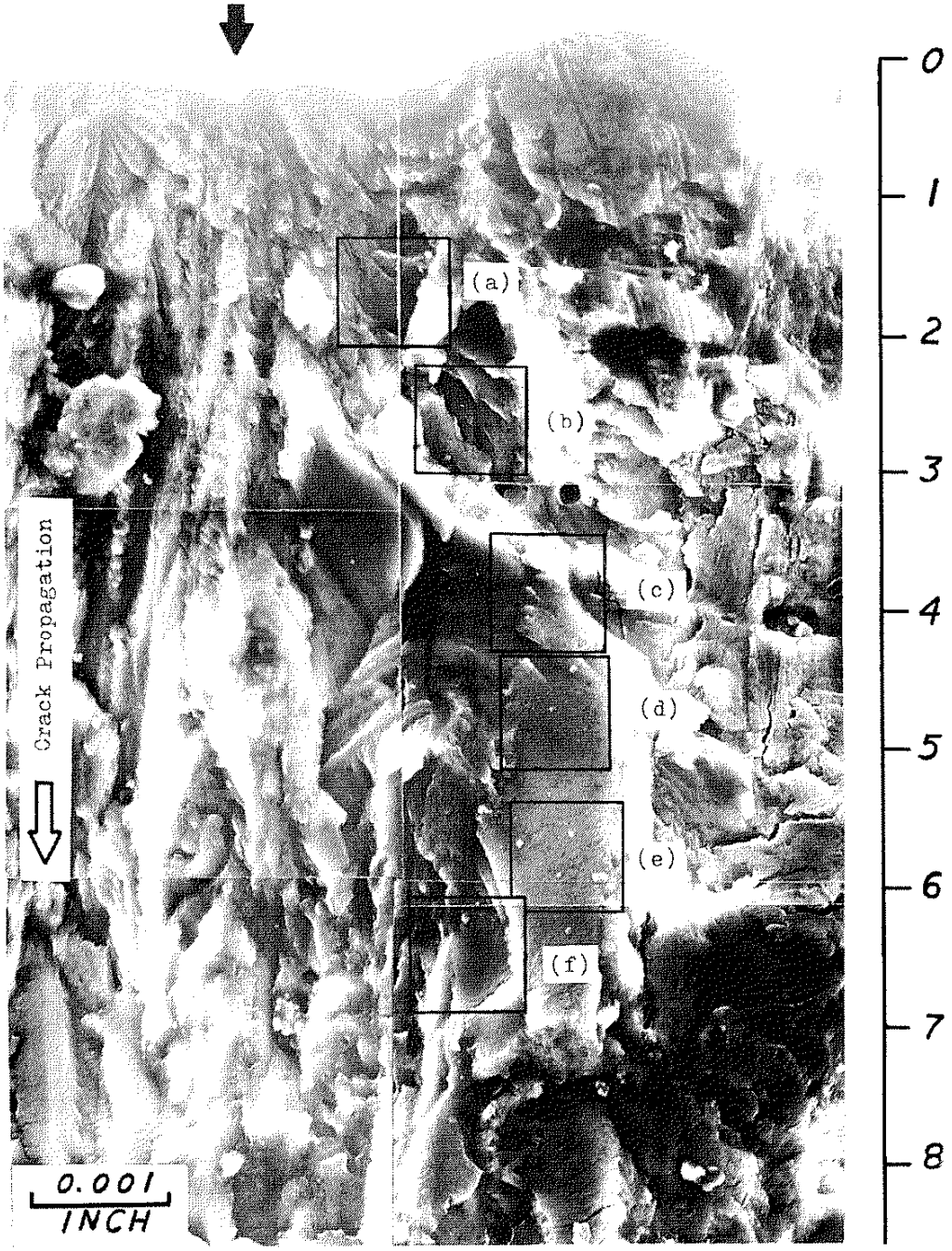

1000X

FIGURE 13. ELECTRON FRACTOGRAPH IN THE VICINITY OF THE CRACK INITIATION SITE (MARKED BY SOLID ARROW) OF AN ELLIPTICALLY NOTCHED SPECIMEN OF 7075-T651 ALUMINUM ALLOY (1000X)

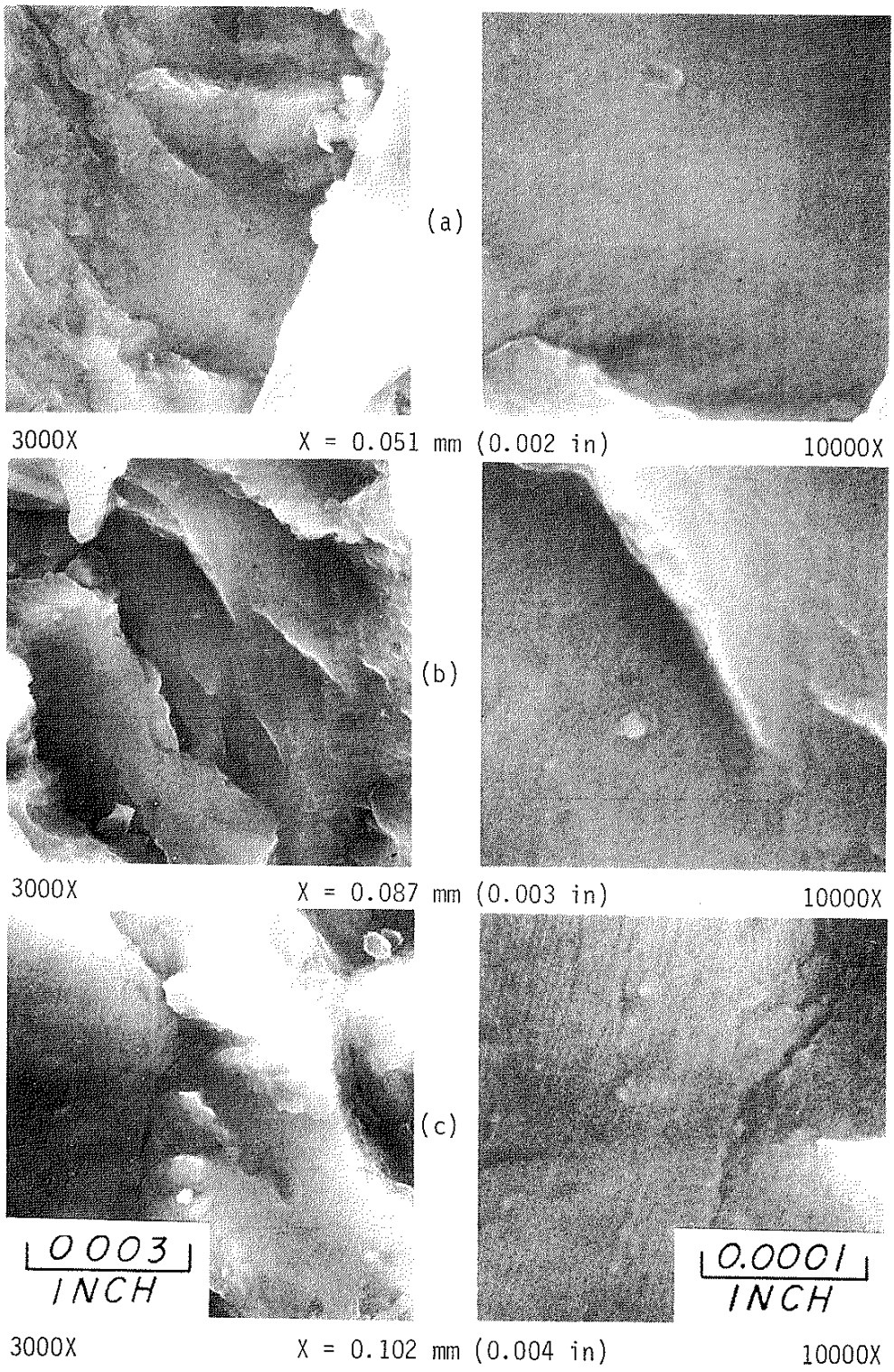

FIGURE 14. ELECTRON FRACTOGRAPHS OF THOSE AREAS MARKED BY SQUARES IN FIG. 13 (3000X AND 10000X)

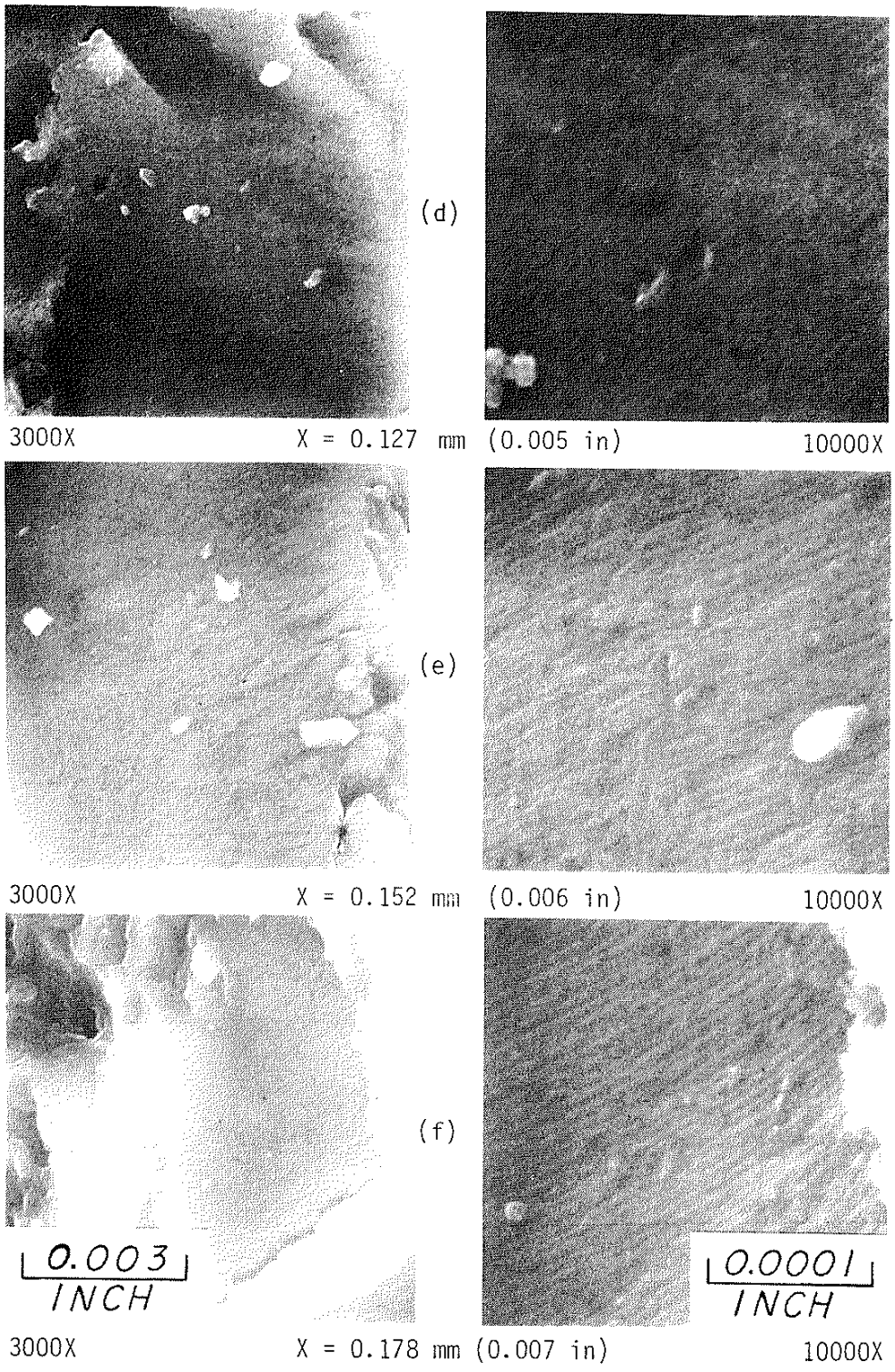

FIGURE 14. (CONTINUED)

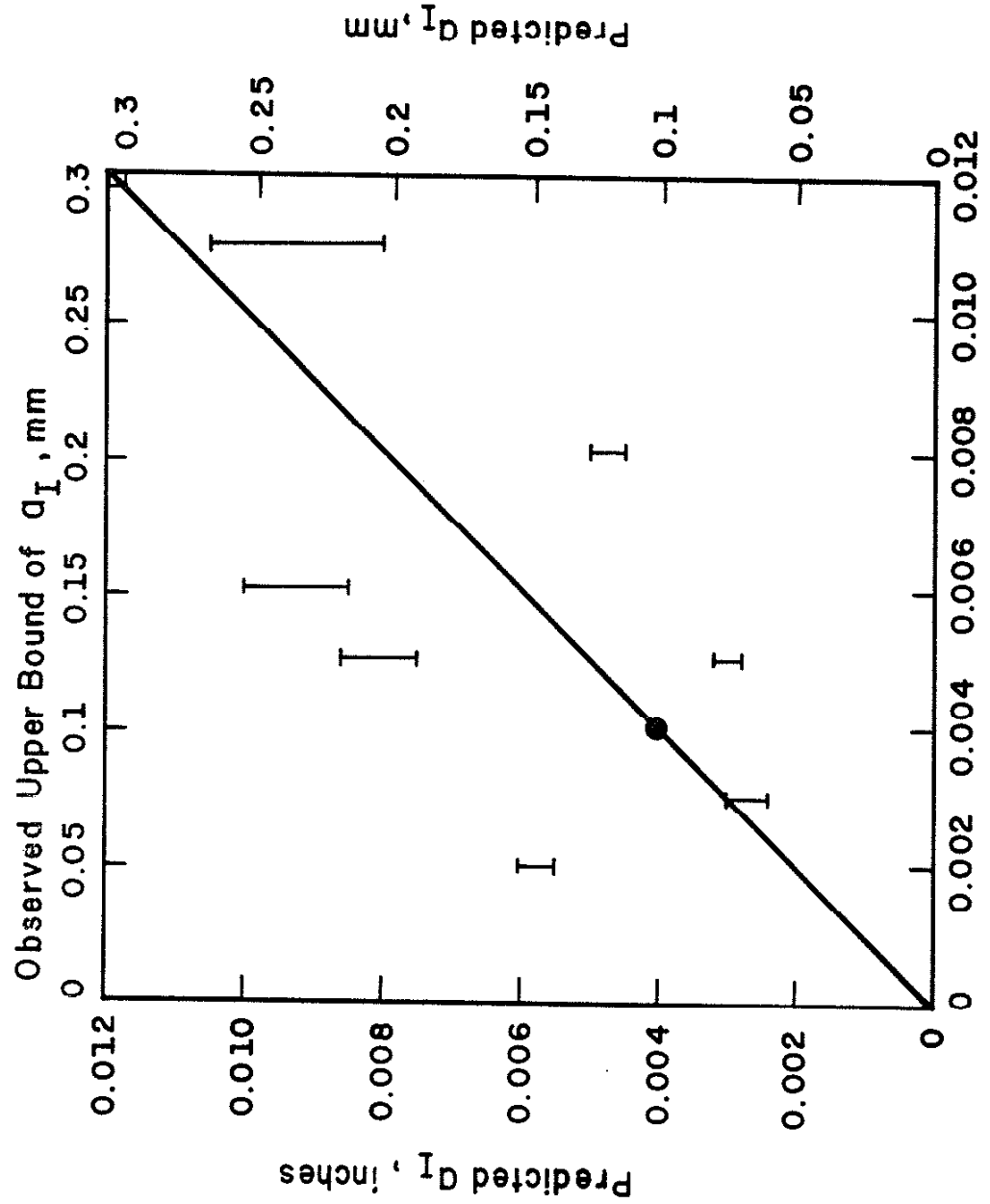

FIGURE 15. COMPARISON OF THE PREDICTED CRACK INITIATION LENGTH TO THE OBSERVED UPPER BOUND OF CRACK INITIATION LENGTH

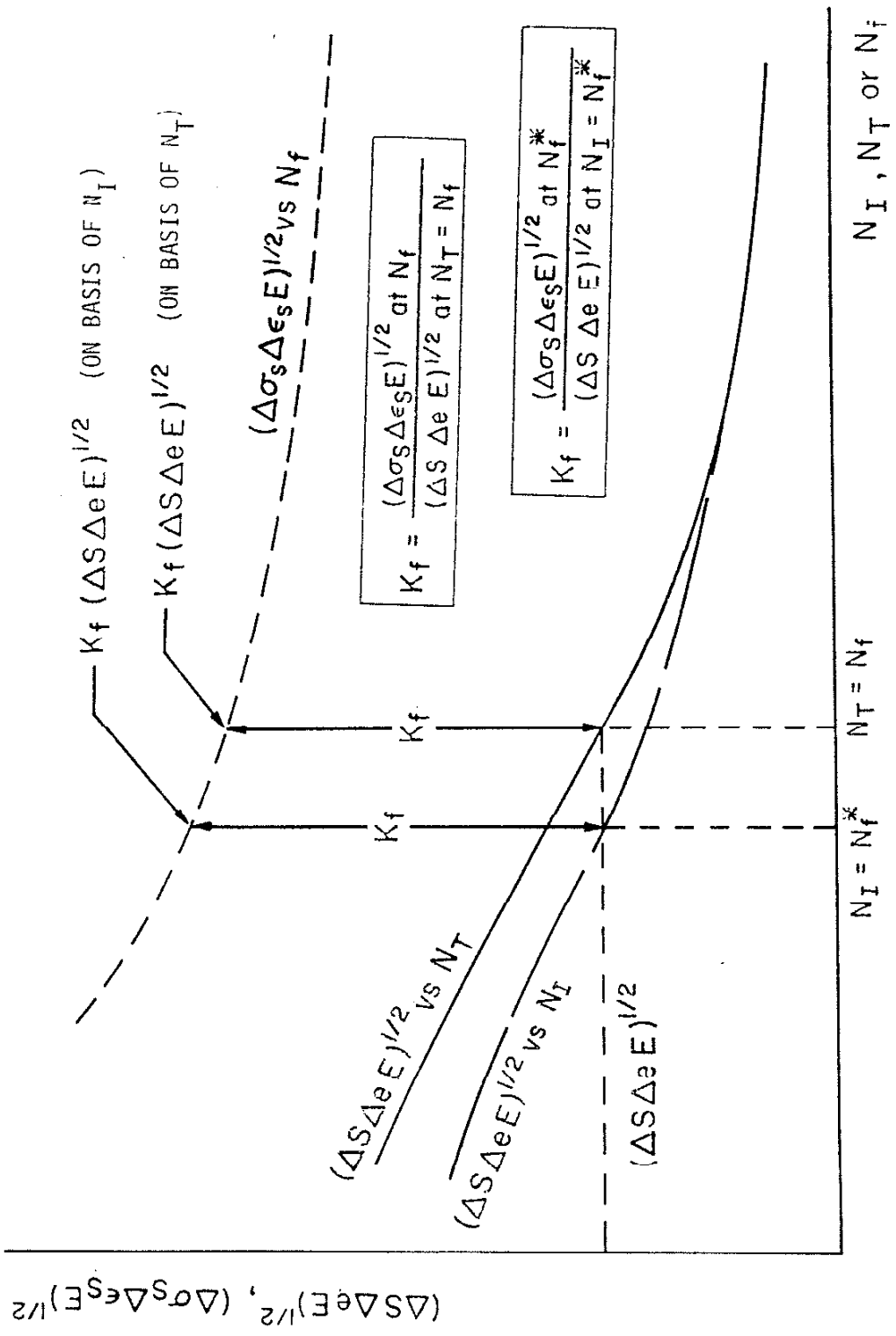

FIGURE 16. TRADITIONAL DEFINITIONS OF K_f ON THE BASES OF BOTH TOTAL LIFE AND CRACK INITIATION LIFE

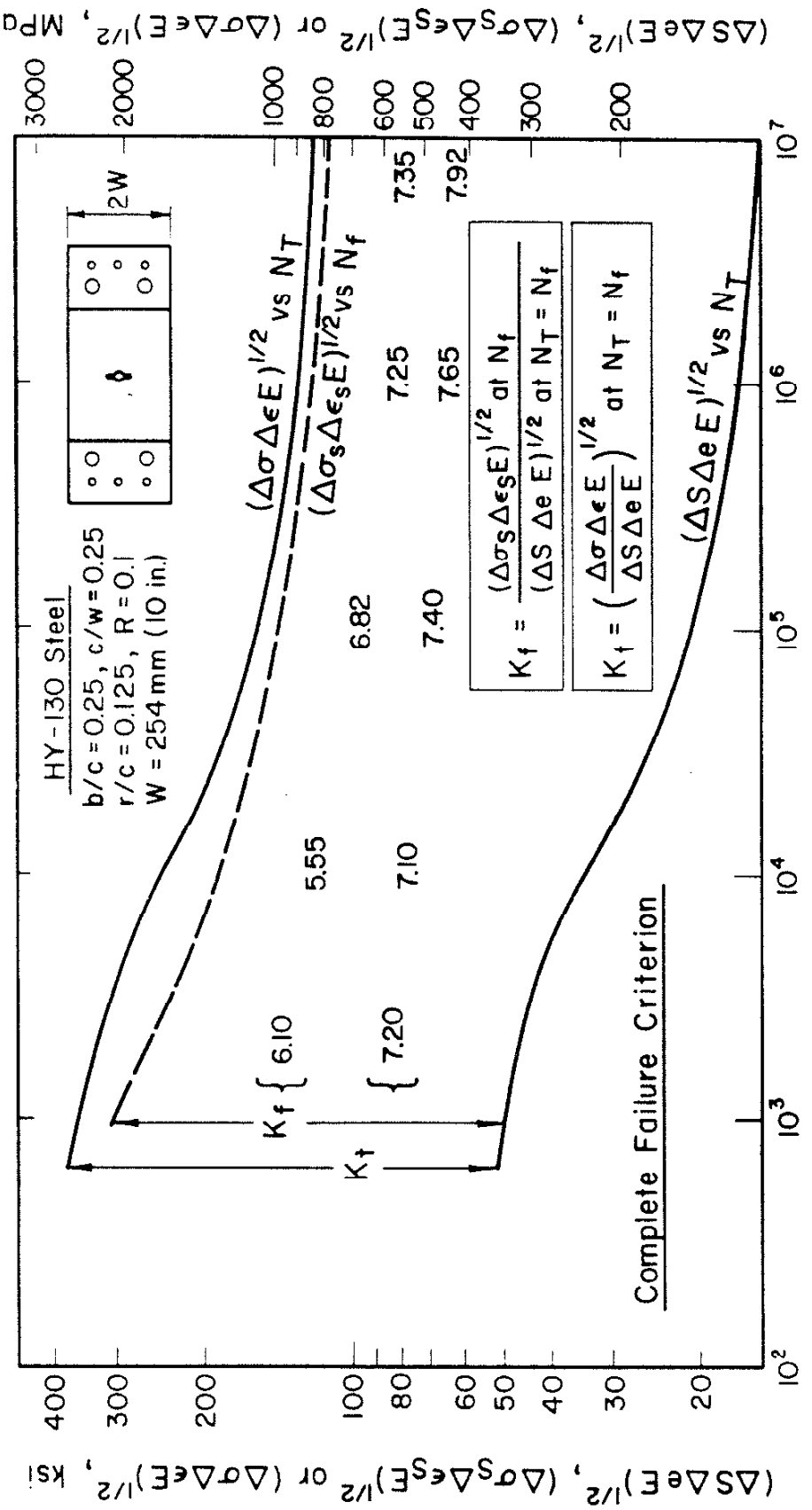

FIGURE 17. ESTIMATION ON BASIS OF TOTAL FATIGUE LIFE OF K_f AND K_t AT VARIOUS N_T

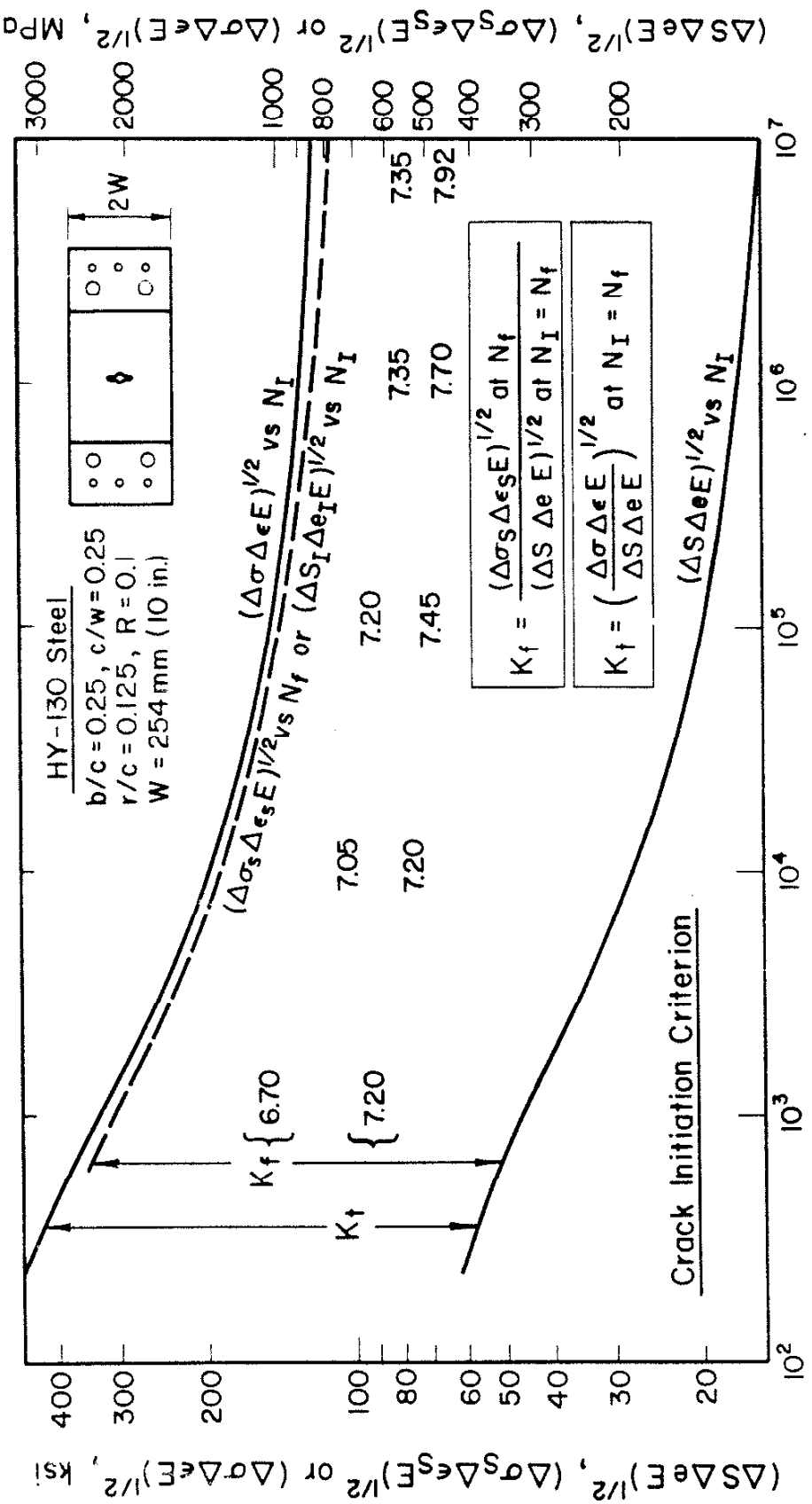

FIGURE 18. ESTIMATION ON BASIS OF CRACK INITIATION LIFE OF K_f AND K_t AT VARIOUS N_I

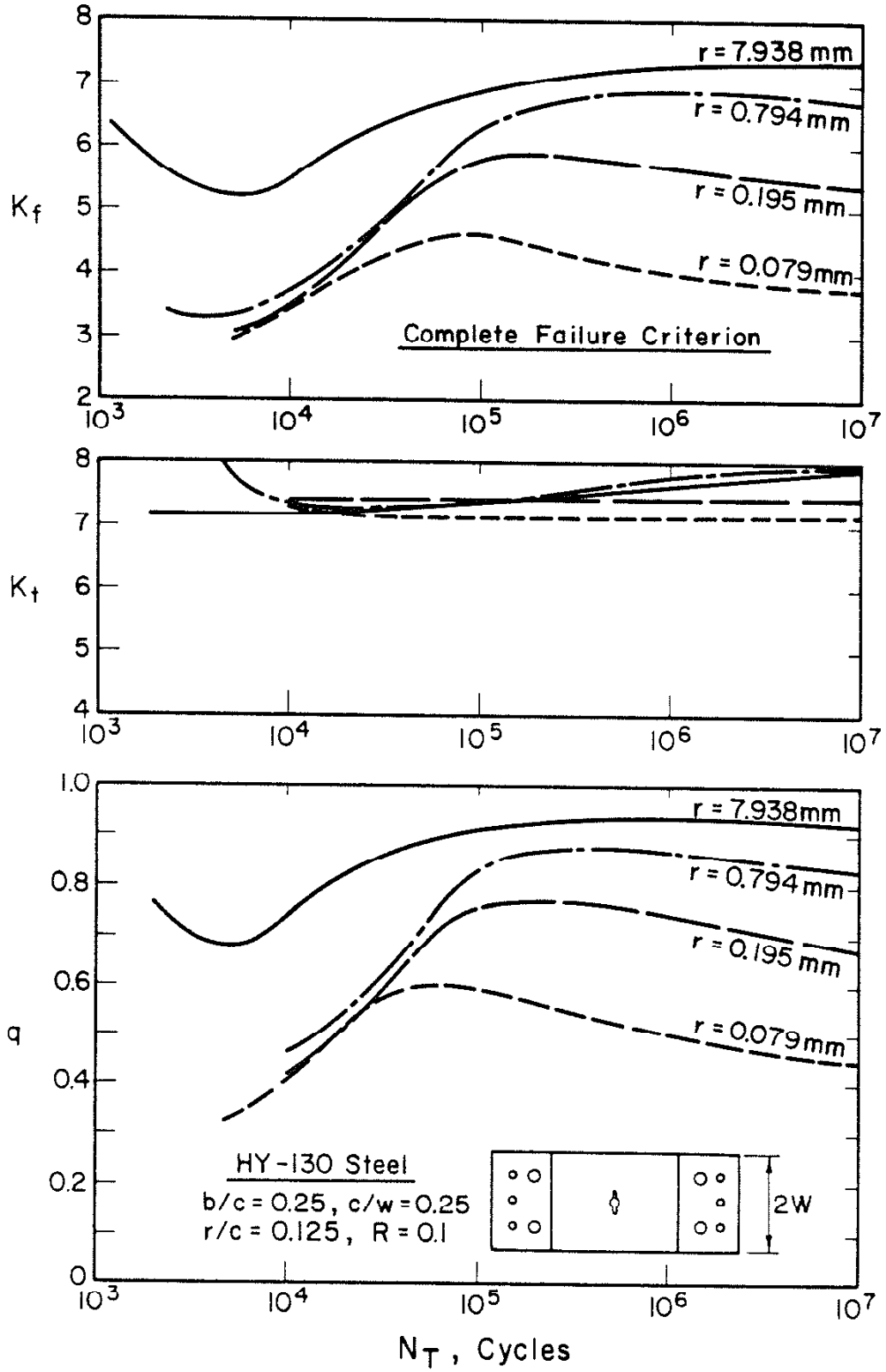

FIGURE 19. K_f, K_t AND q DEFINED ON BASIS OF TOTAL FATIGUE LIFE AS A FUNCTION OF N_T FOR GEOMETRICALLY SIMILAR NOTCHED SPECIMENS

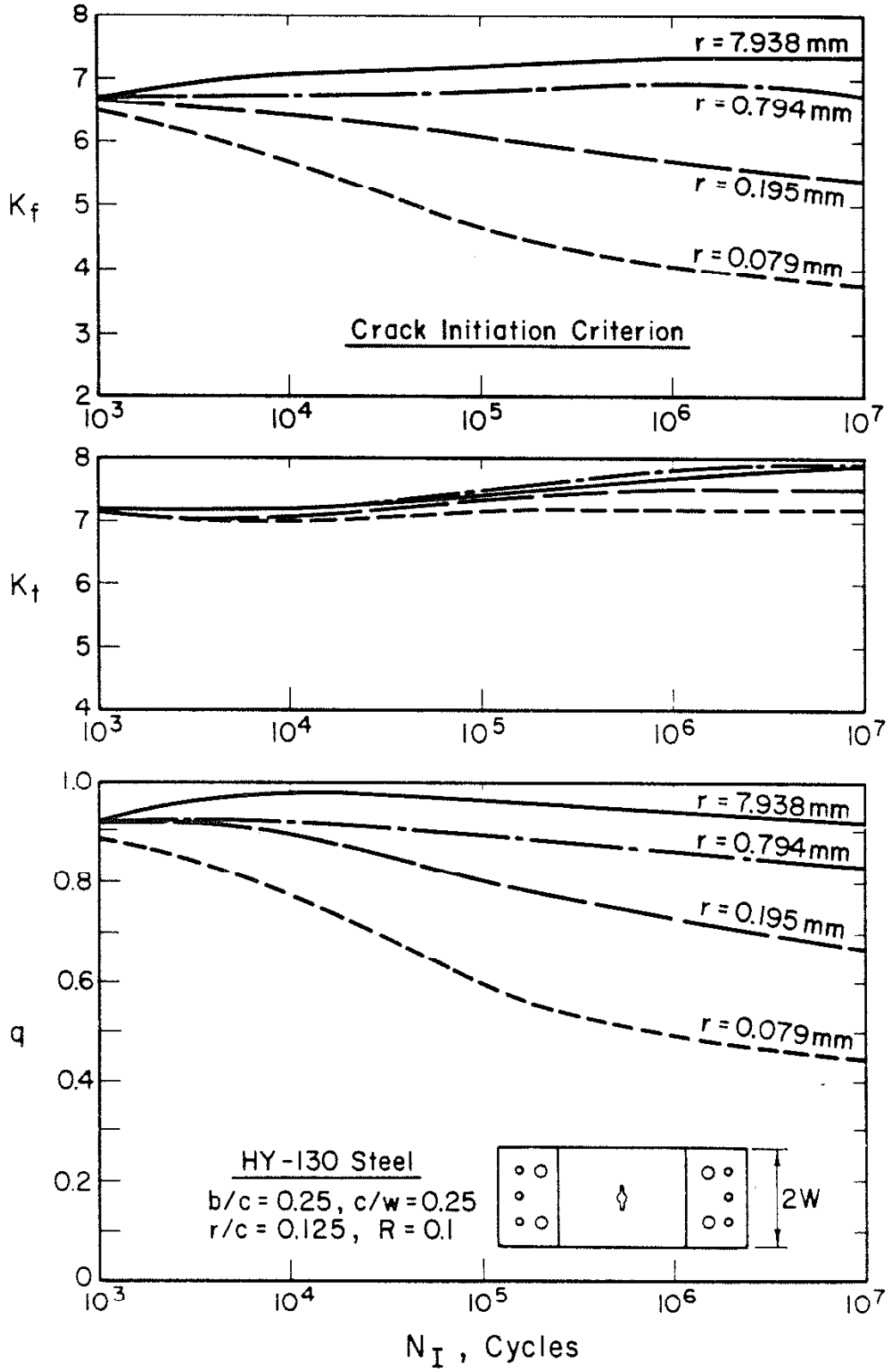

FIGURE 20. K_f, K_t AND q DEFINED ON BASIS OF CRACK INITIATION LIFE AS A FUNCTION OF N_I FOR GEOMETRICALLY SIMILAR NOTCHED SPECIMENS

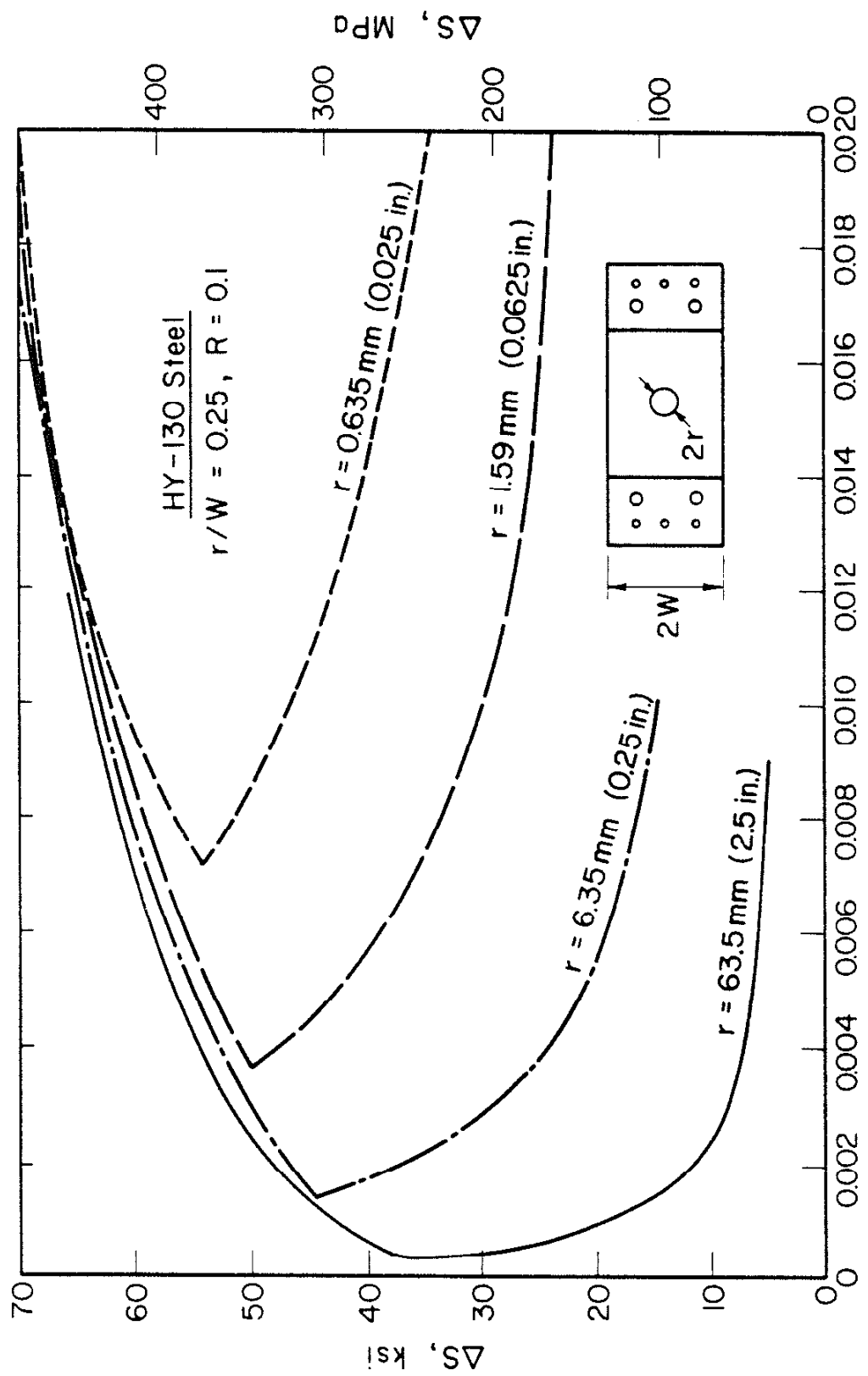

FIGURE 21. THE NORMALIZED CRACK INITIATION LENGTH (a_I/W) AS A FUNCTION OF APPLIED STRESS FOR GEOMETRICALLY SIMILAR NOTCHED SPECIMENS

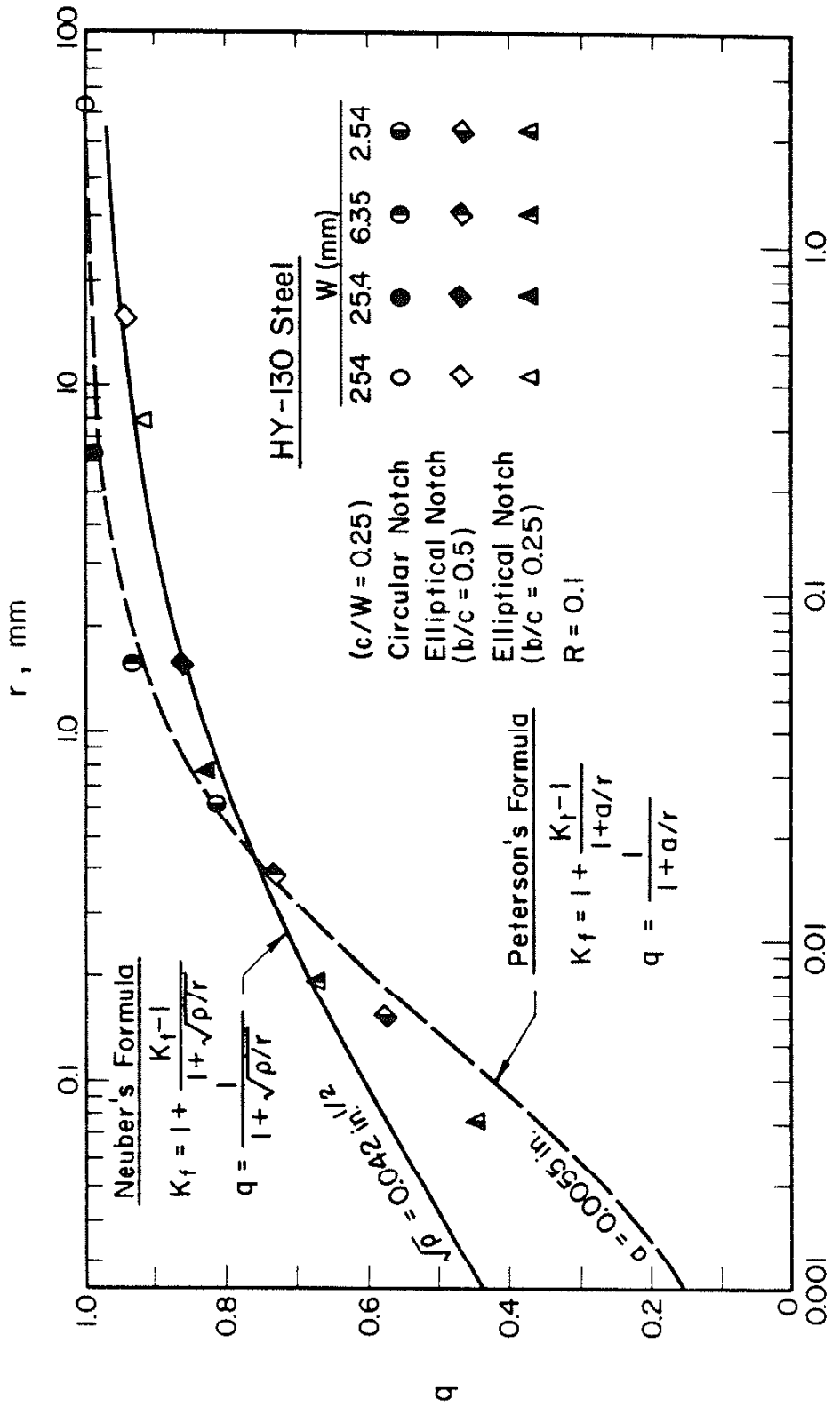

FIGURE 22. NUMERICALLY DETERMINED $\sqrt{\rho}$ AND 'a" FOR HY-130 STEEL AT $N_T = 10^7$ CYCLES

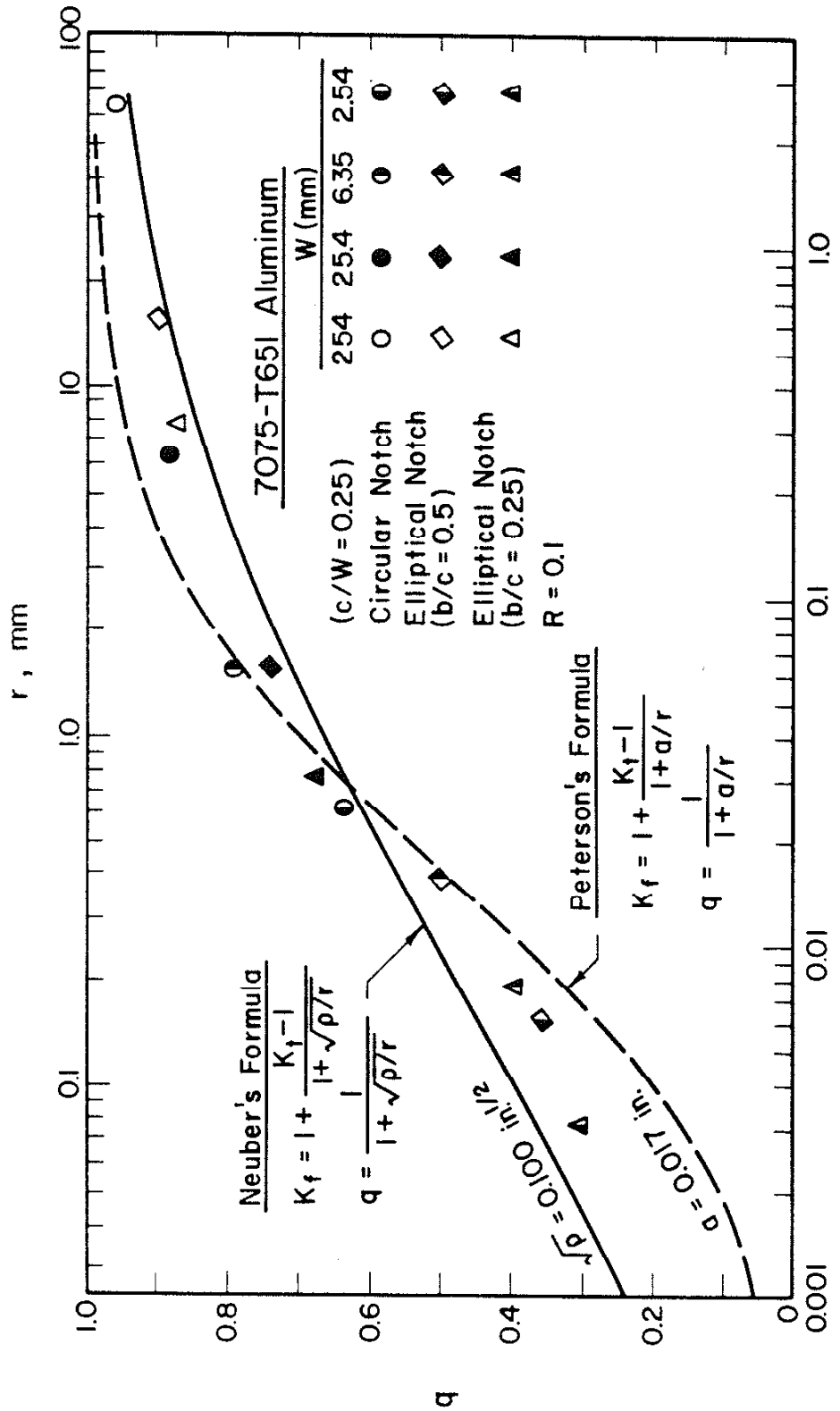

FIGURE 23. NUMERICALLY DETERMINED $\sqrt{\rho}$ AND "a" FOR 7075-T651 ALUMINUM ALLOY AT $N_T = 10^7$ CYCLES

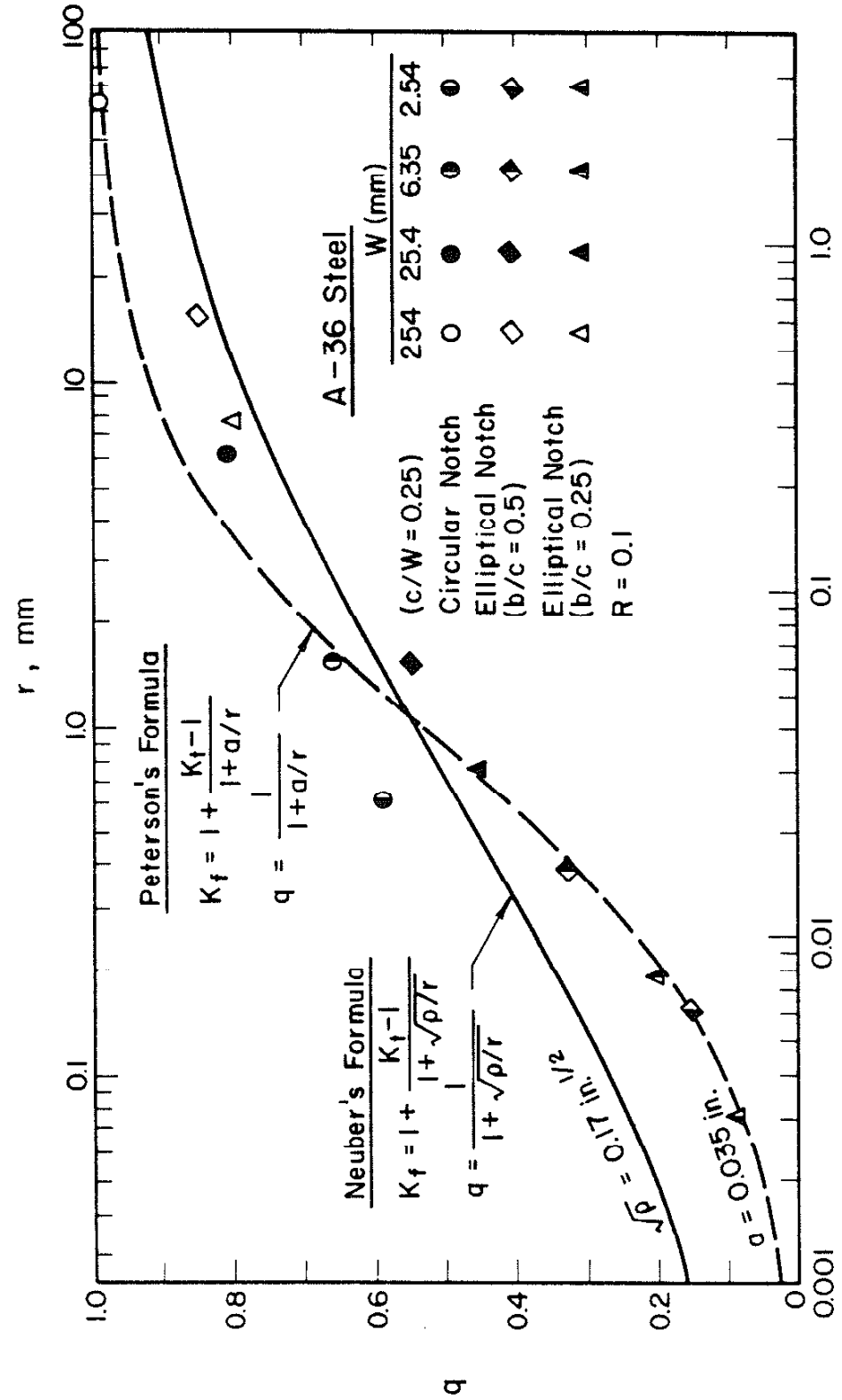

FIGURE 24. NUMERICALLY DETERMINED $\sqrt{\rho}$ AND "a" FOR A-36 MILD STEEL AT $N_T = 10^7$ CYCLES

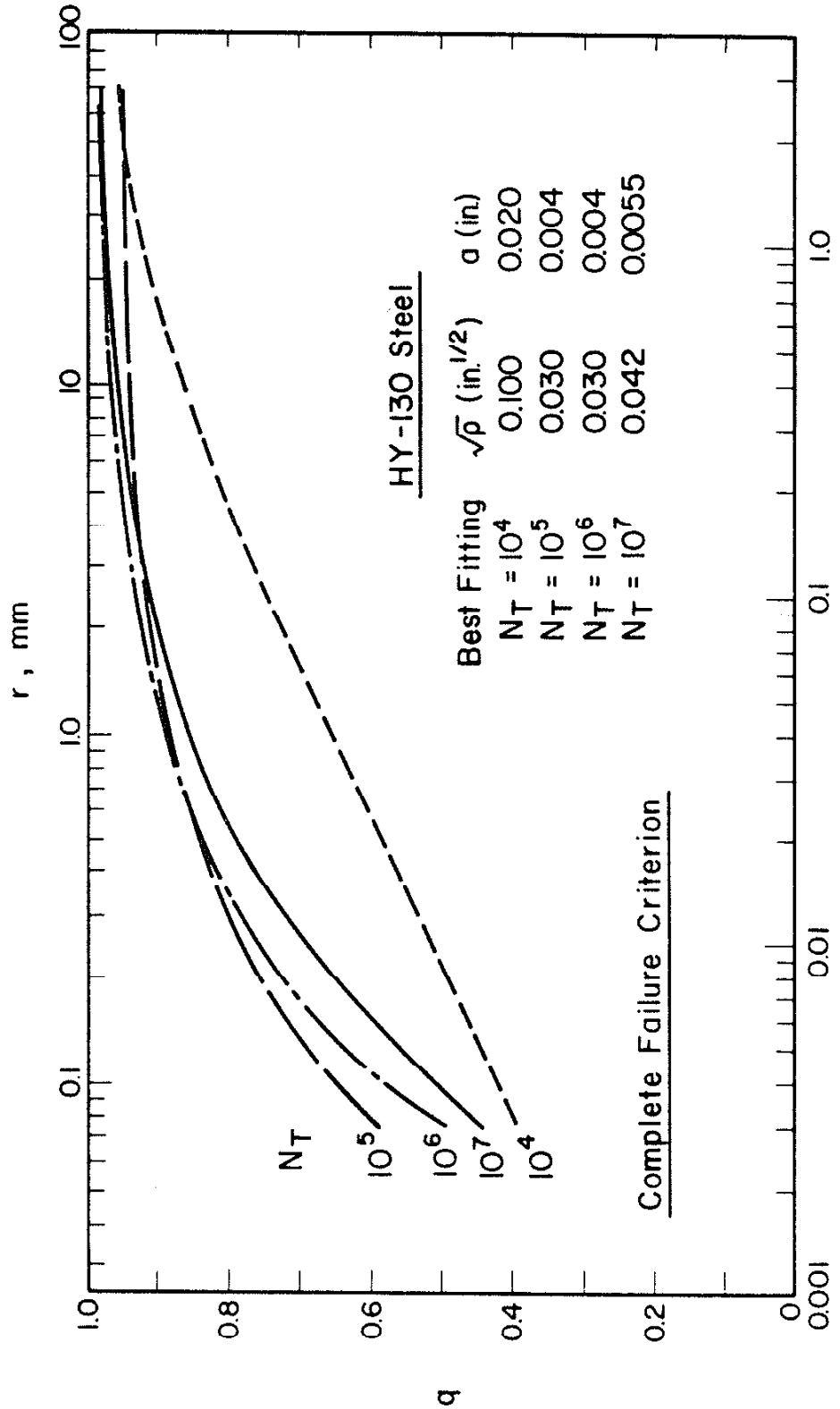

FIGURE 25. VARIATION OF q-r CURVES WITH N_T OF HY-130 STEEL.
q IS DEFINED ON BASIS OF TOTAL FATIGUE LIFE

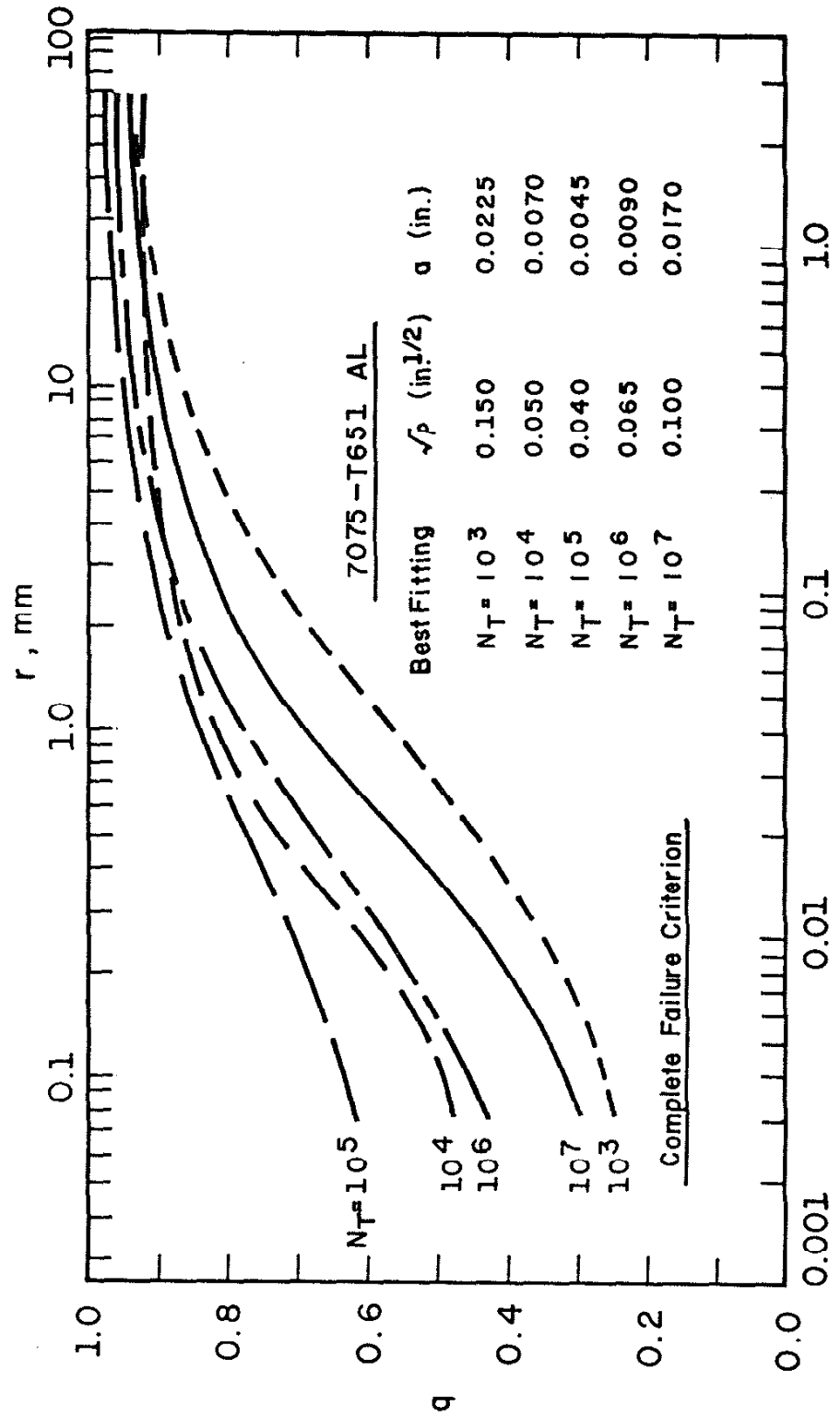

FIGURE 26. VARIATION OF q-r CURVES WITH N_T OF 7075-T651 ALUMINUM ALLOY. q IS DEFINED ON BASIS OF TOTAL FATIGUE LIFE

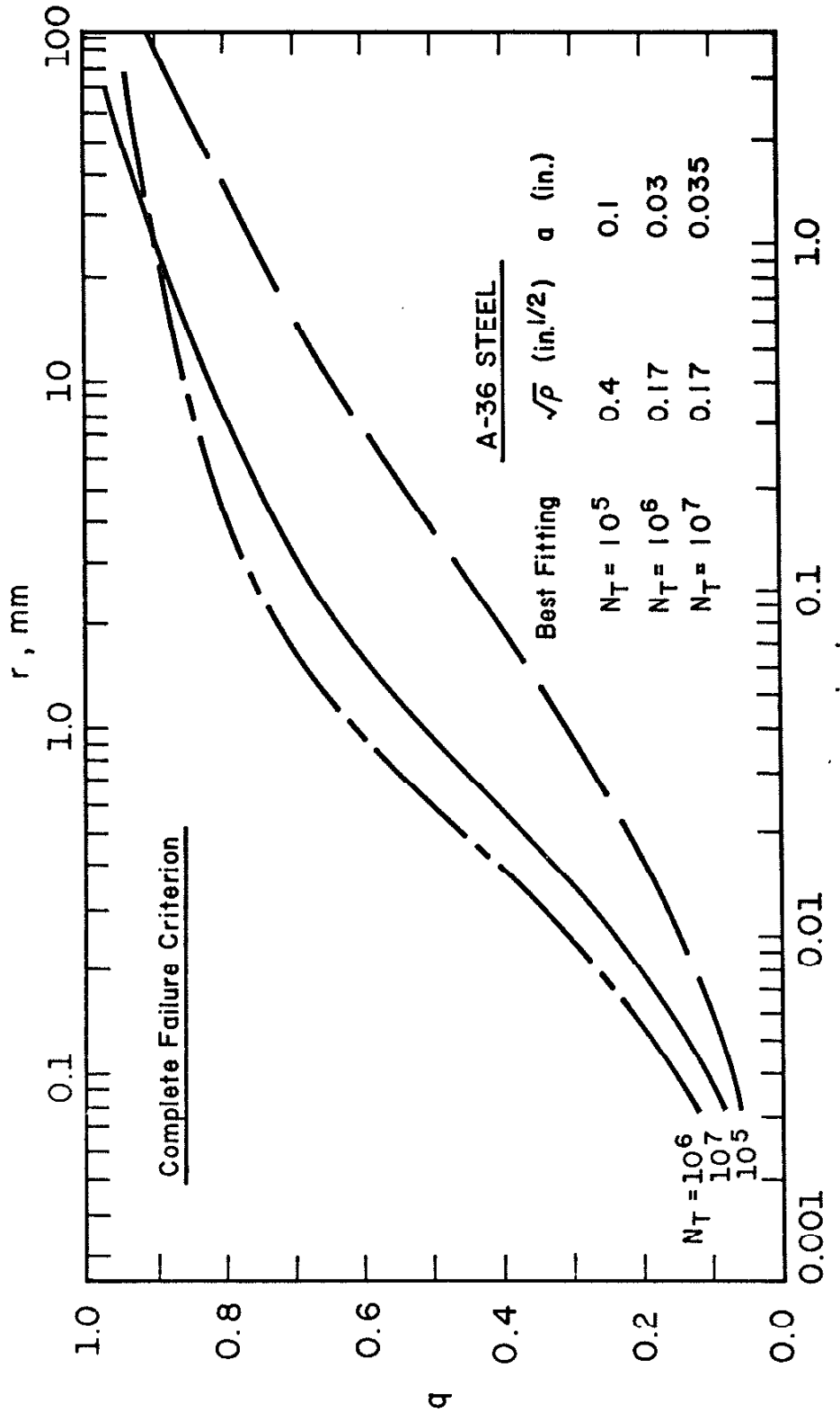

FIGURE 27. VARIATION OF q-r CURVES WITH N- OF A-36 MILD STEEL.
q IS DEFINED ON BASIS OF TOTAL FATIGUE LIFE

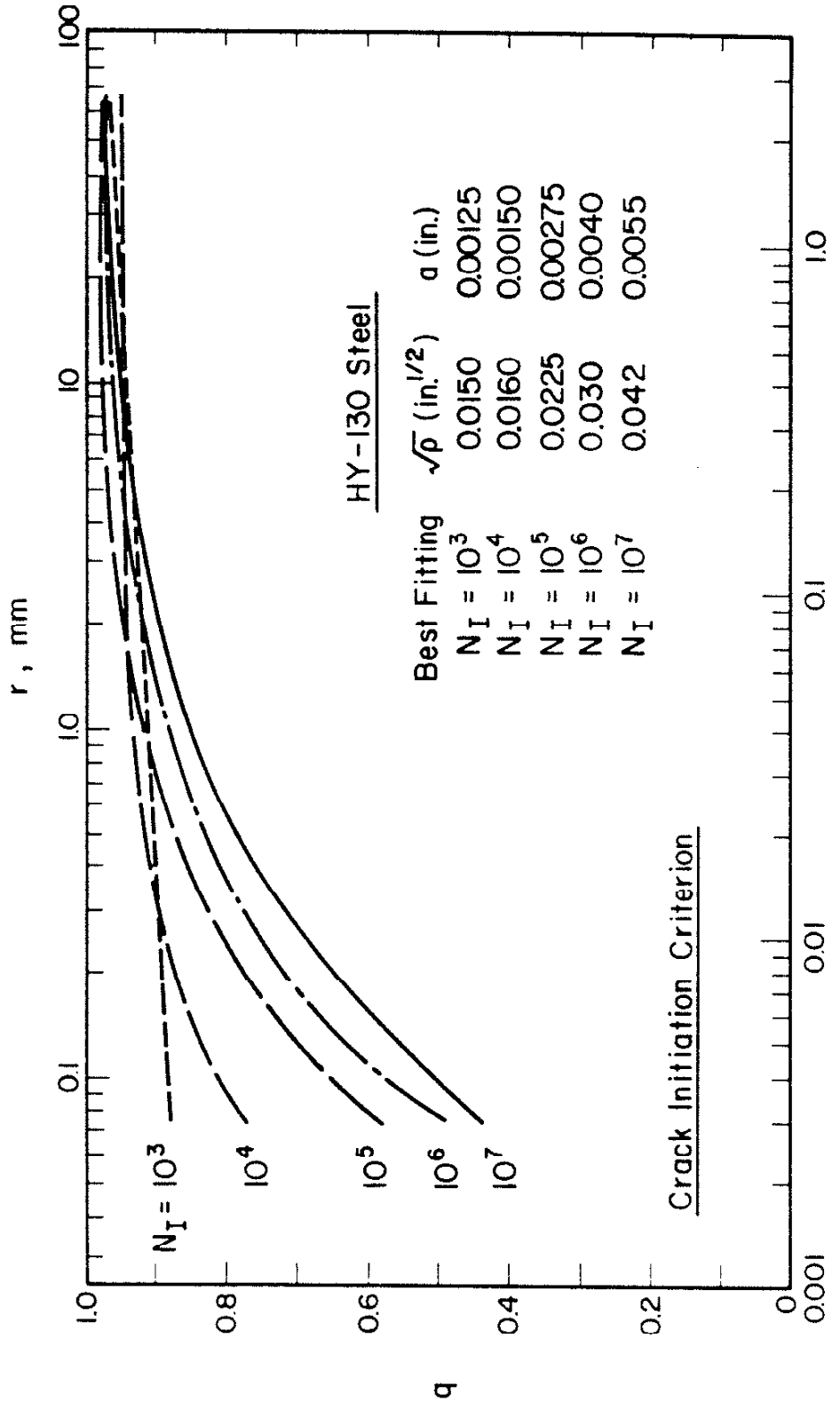

FIGURE 28. VARIATION OF q-r CURVES WITH N_I OF HY-130 STEEL. q IS DEFINED ON BASIS OF CRACK INITIATION LIFE

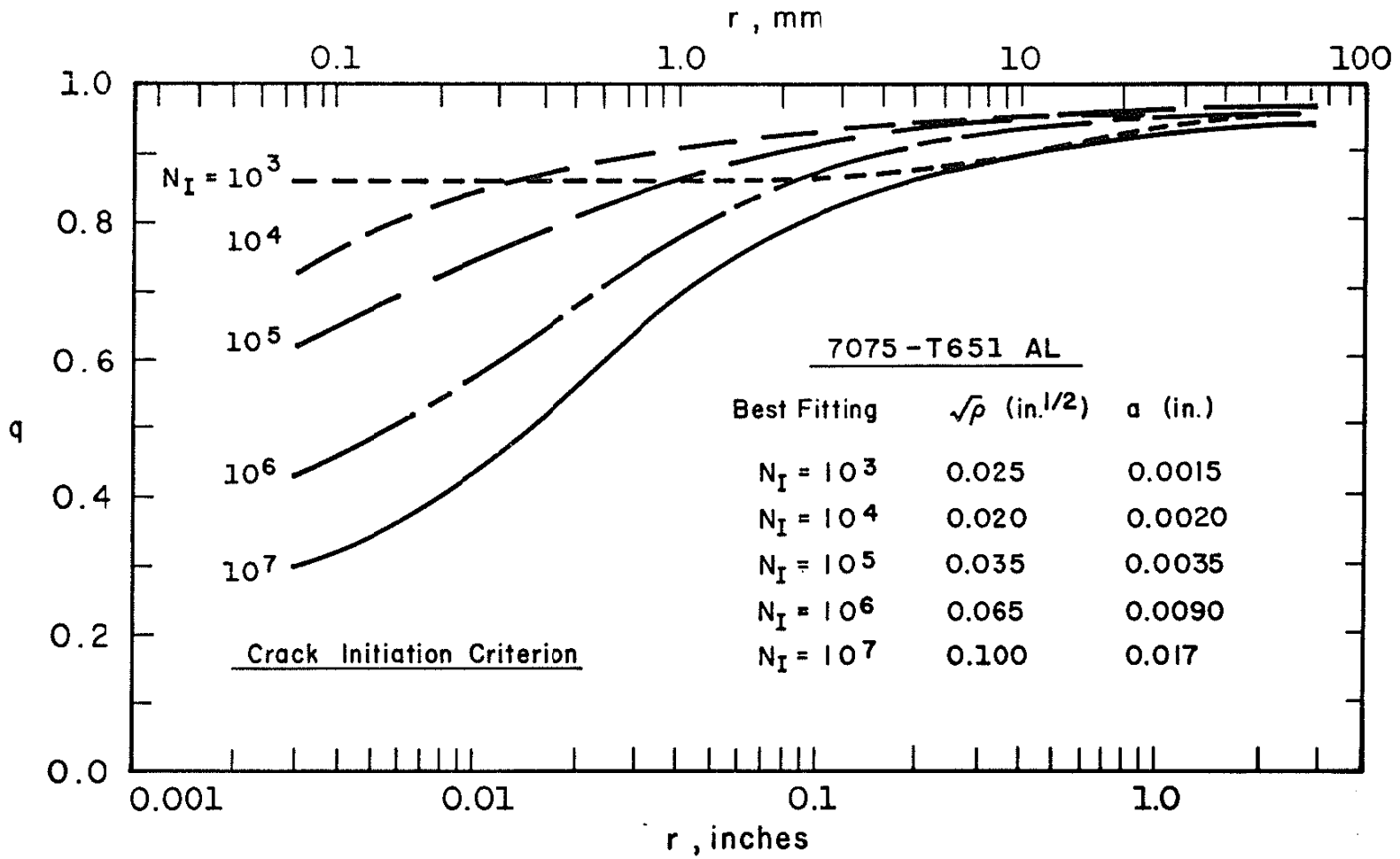

FIGURE 29. VARIATIONS OF q-r CURVES WITH N_I OF 7075-T651 ALUMINUM ALLOY. q IS DEFINED ON BASIS OF CRACK INITIATION LIFE

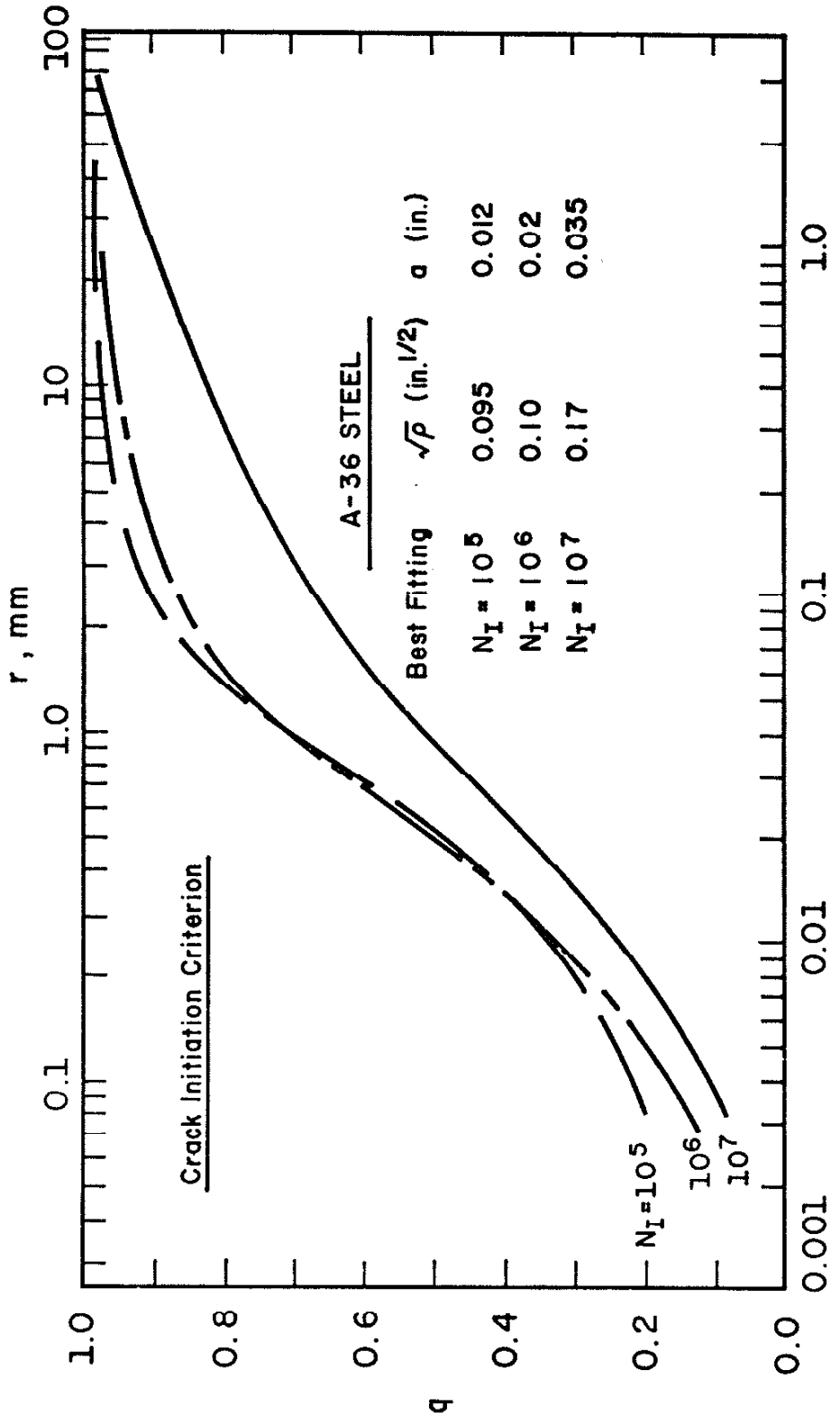

FIGURE 30. VARIATIONS OF q-r CURVES WITH N_I OF A-36 MILD STEEL. q IS DEFINED ON BASIS OF CRACK INITIATION LIFE

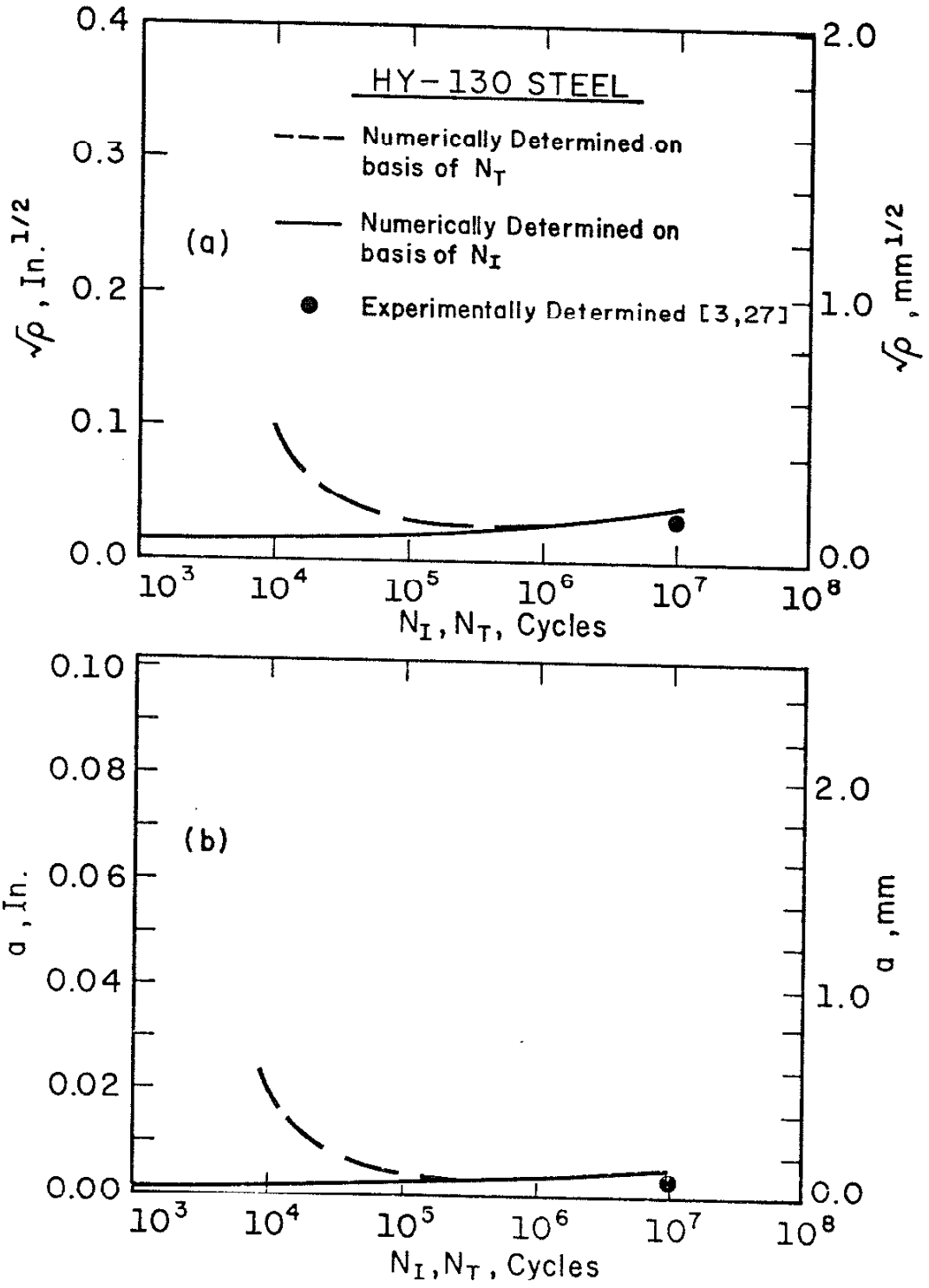

FIGURE 31. VARIATION OF $\sqrt{\rho}$ AND "a" WITH N_I AND N_T FOR HY-130 STEEL

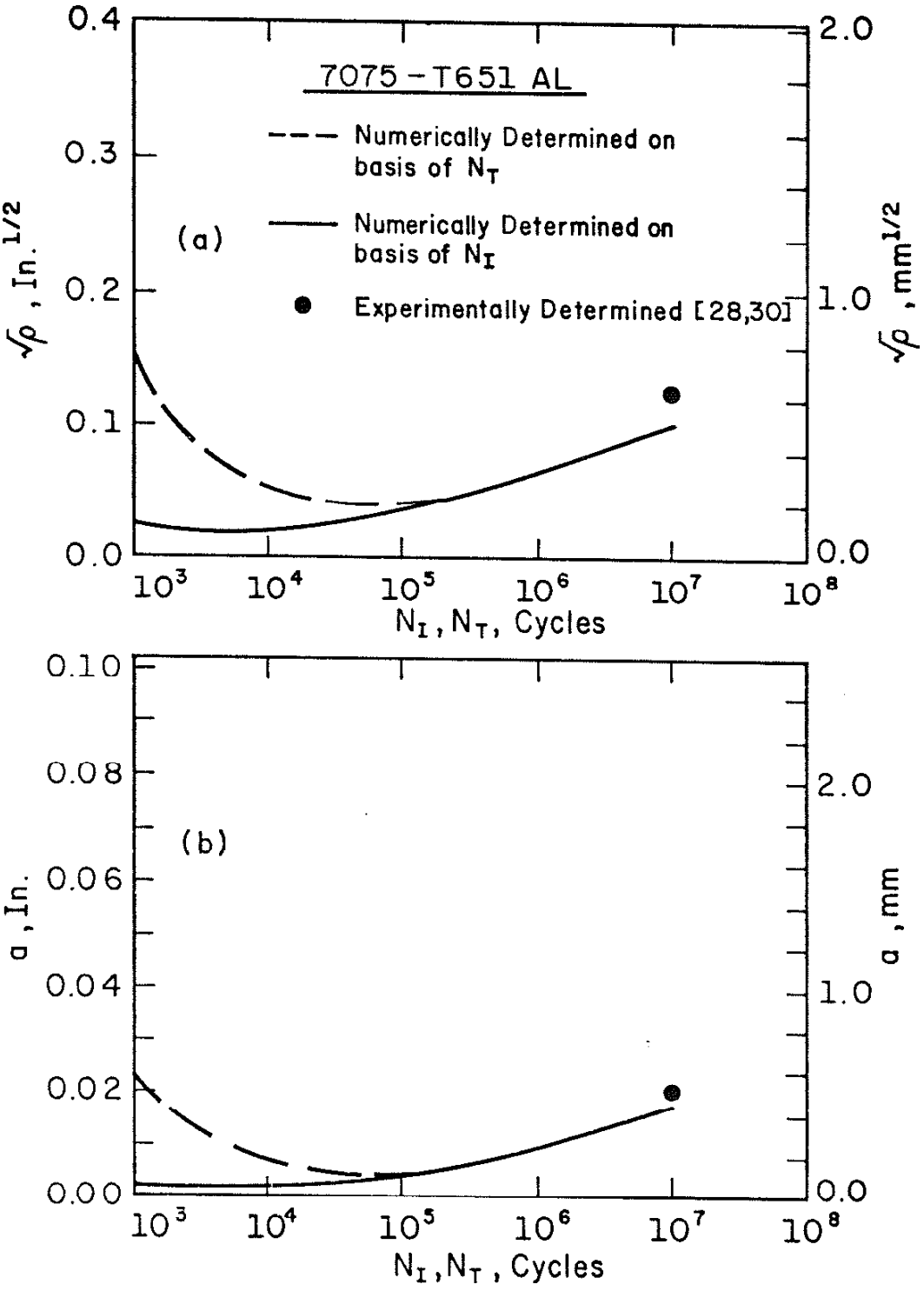

FIGURE 32. VARIATION OF $\sqrt{\rho}$ AND "a" WITH N_I AND N_T FOR 7075-T651 ALUMINUM ALLOY

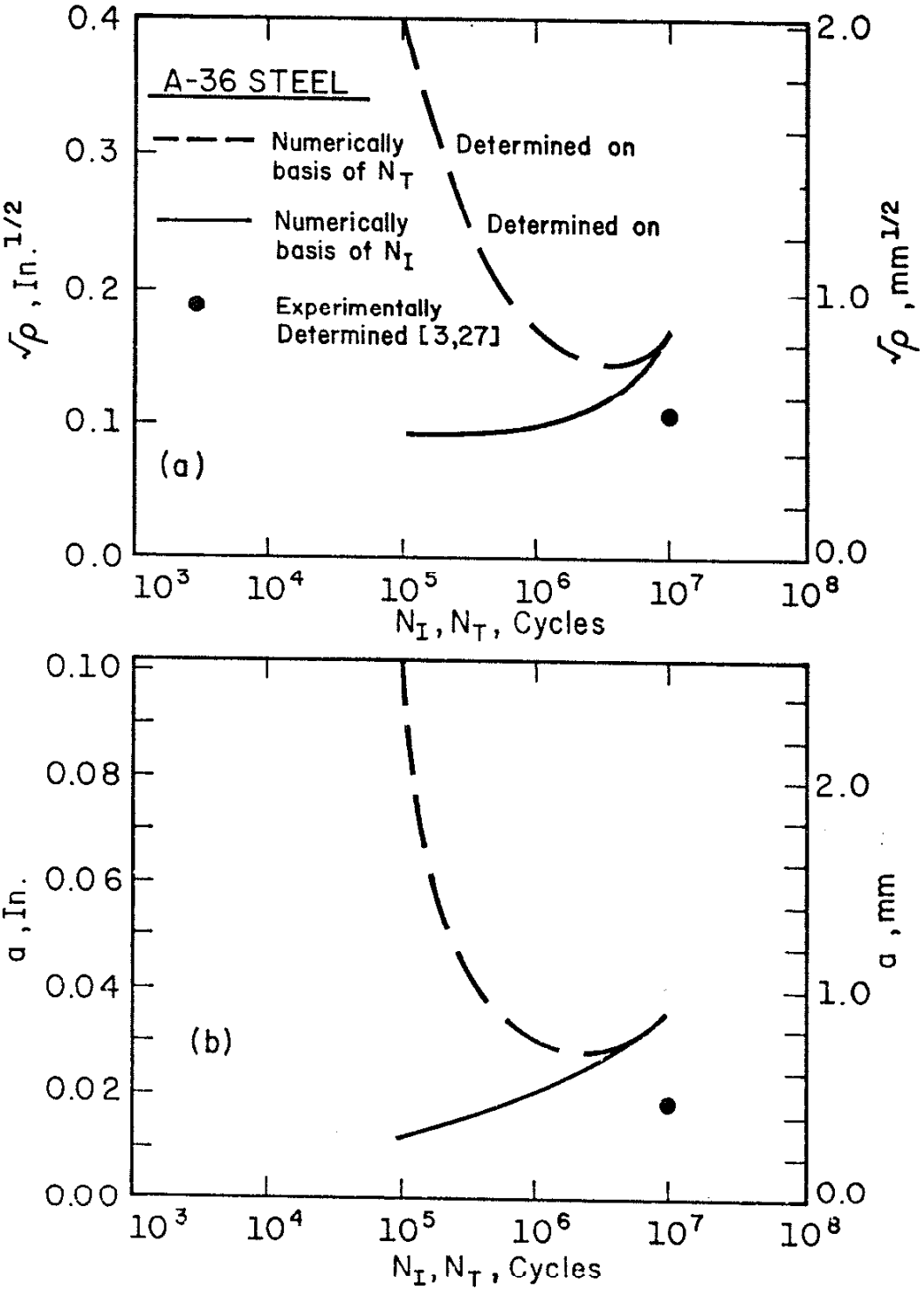

FIGURE 33. VARIATION OF $\sqrt{\rho}$ AND "a" WITH N_I AND N_T FOR A-36 MILD STEEL

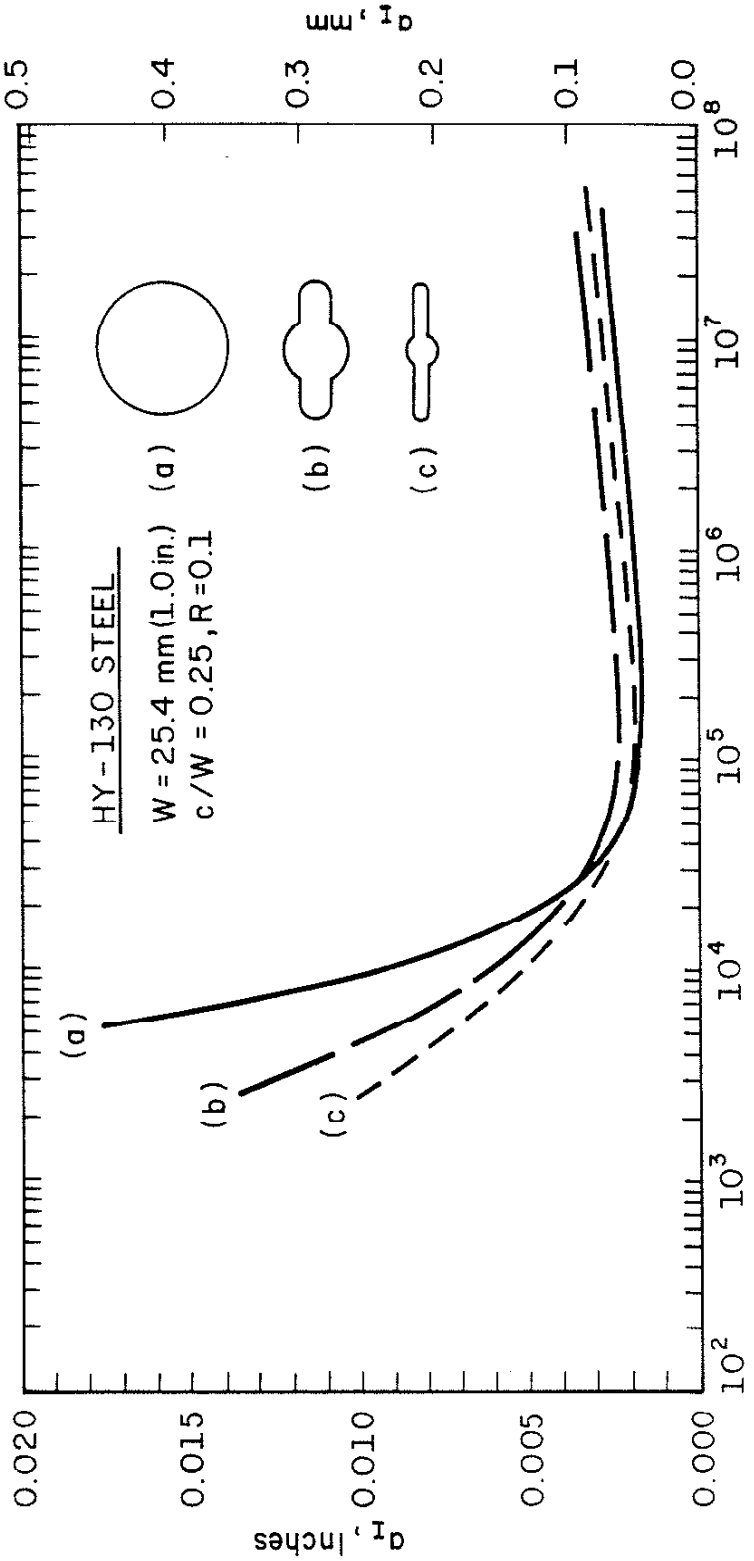

FIGURE 34. VARIATION OF a_I WITH DIFFERENT NOTCH GEOMETRIES (SEE FIG. 9)

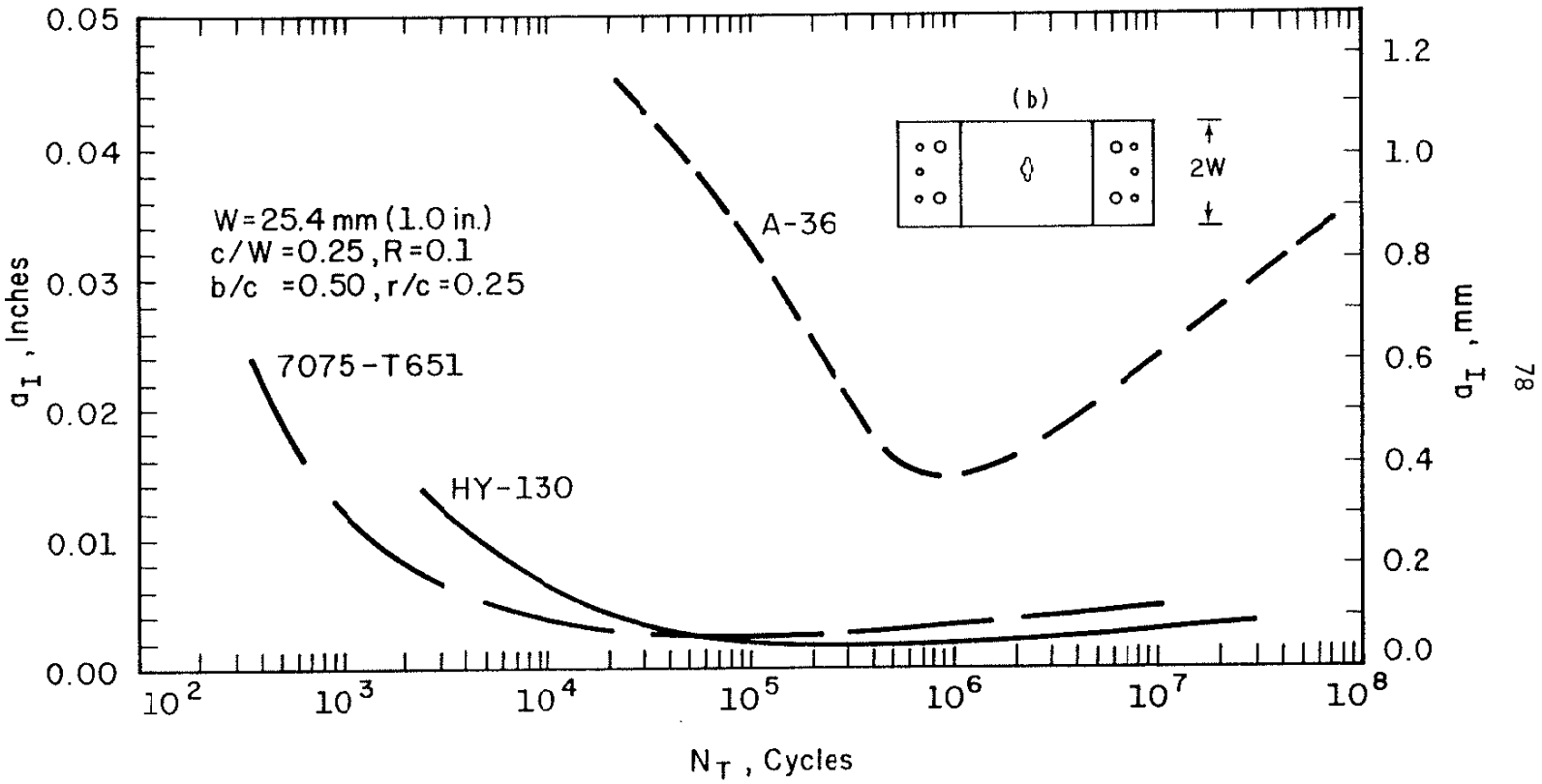

FIGURE 35. VARIATION OF a_I WITH MATERIAL

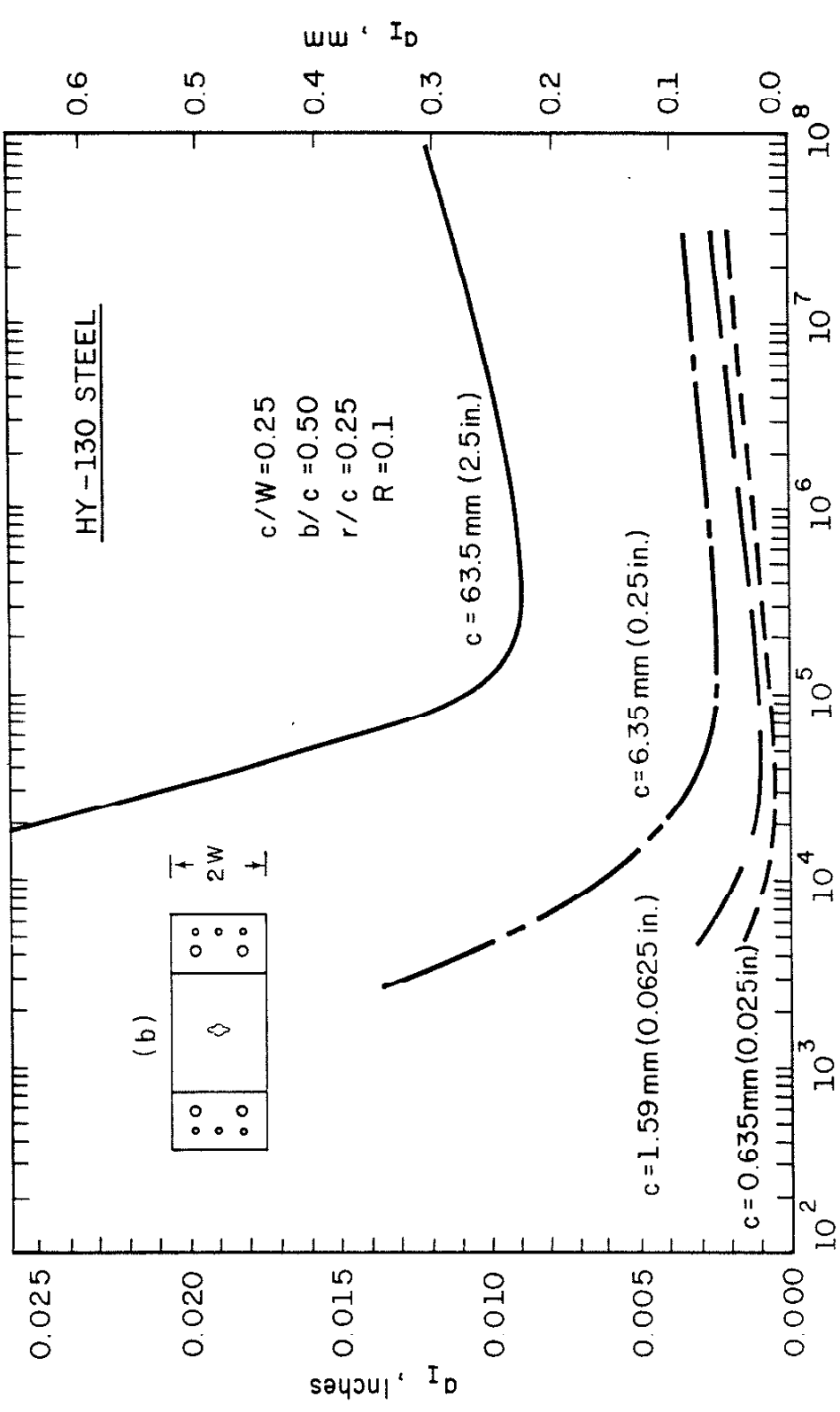

FIGURE 36. VARIATION OF a_I WITH DIFFERENT NOTCH SIZES

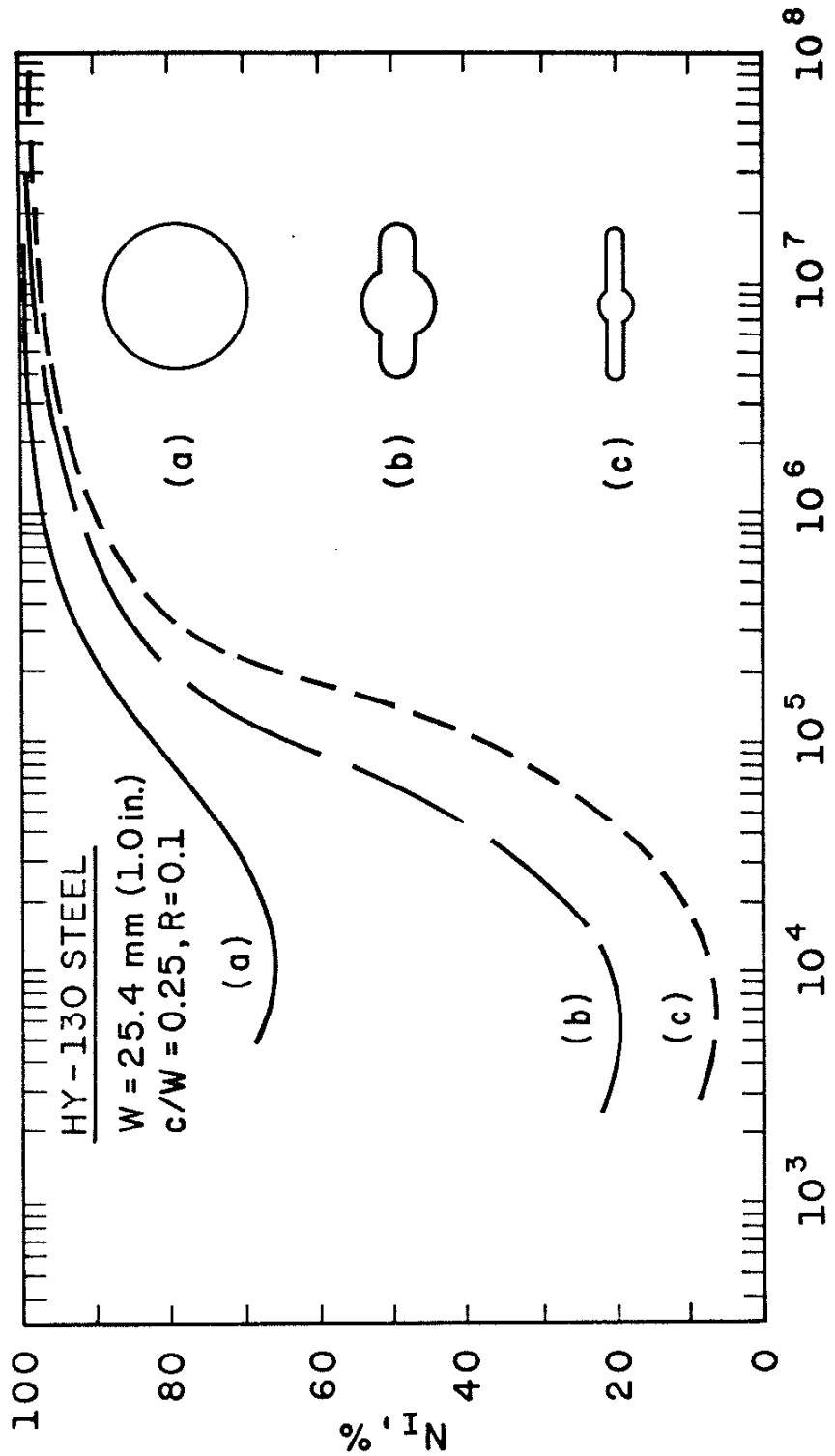

FIGURE 37. VARIATION OF N_I % WITH DIFFERENT NOTCH GEOMETRIES FOR HY-130 STEEL

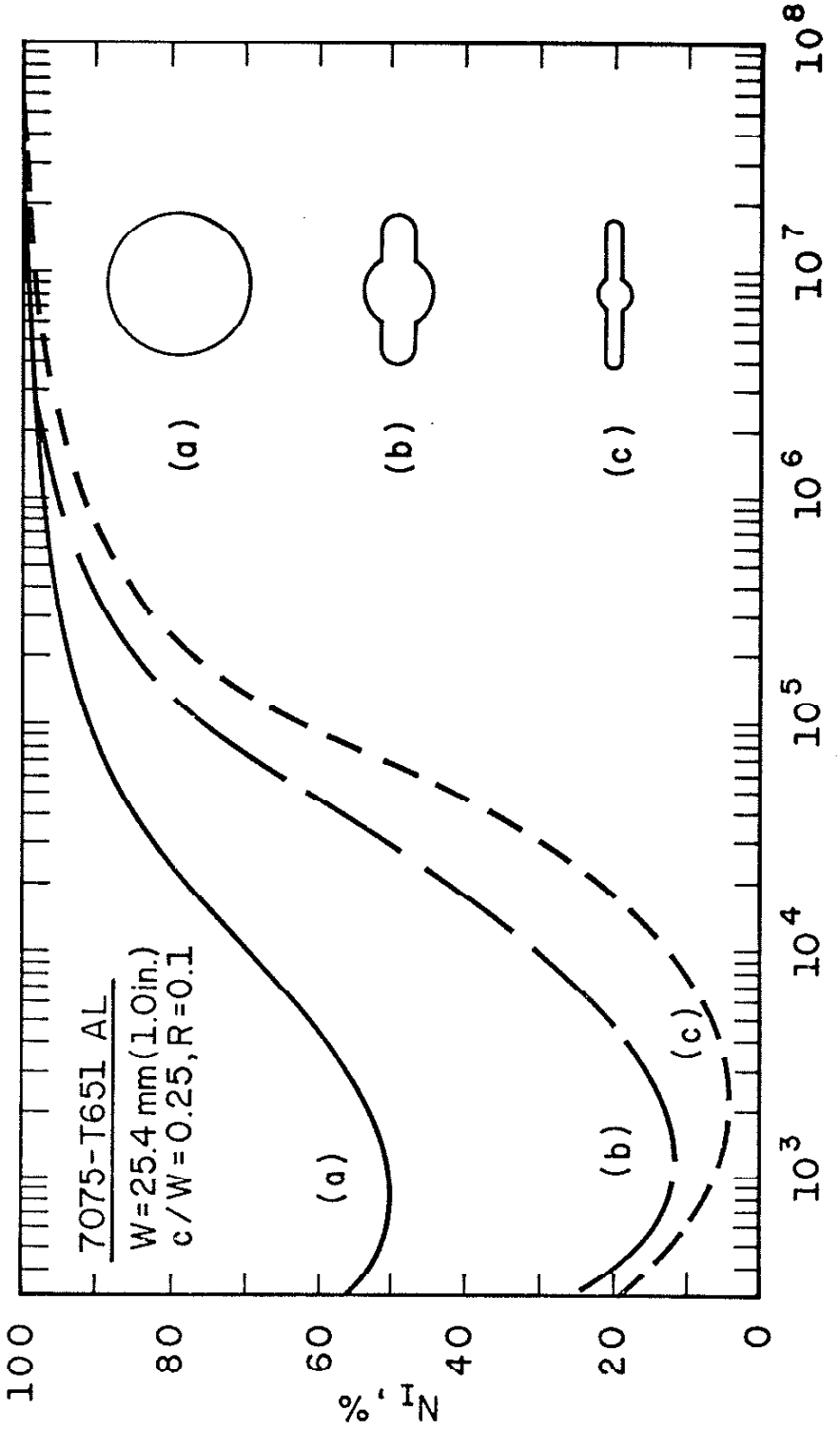

FIGURE 38. VARIATION OF N_I % WITH DIFFERENT NOTCH GEOMETRIES FOR 7075-T651 ALUMINUM ALLOY

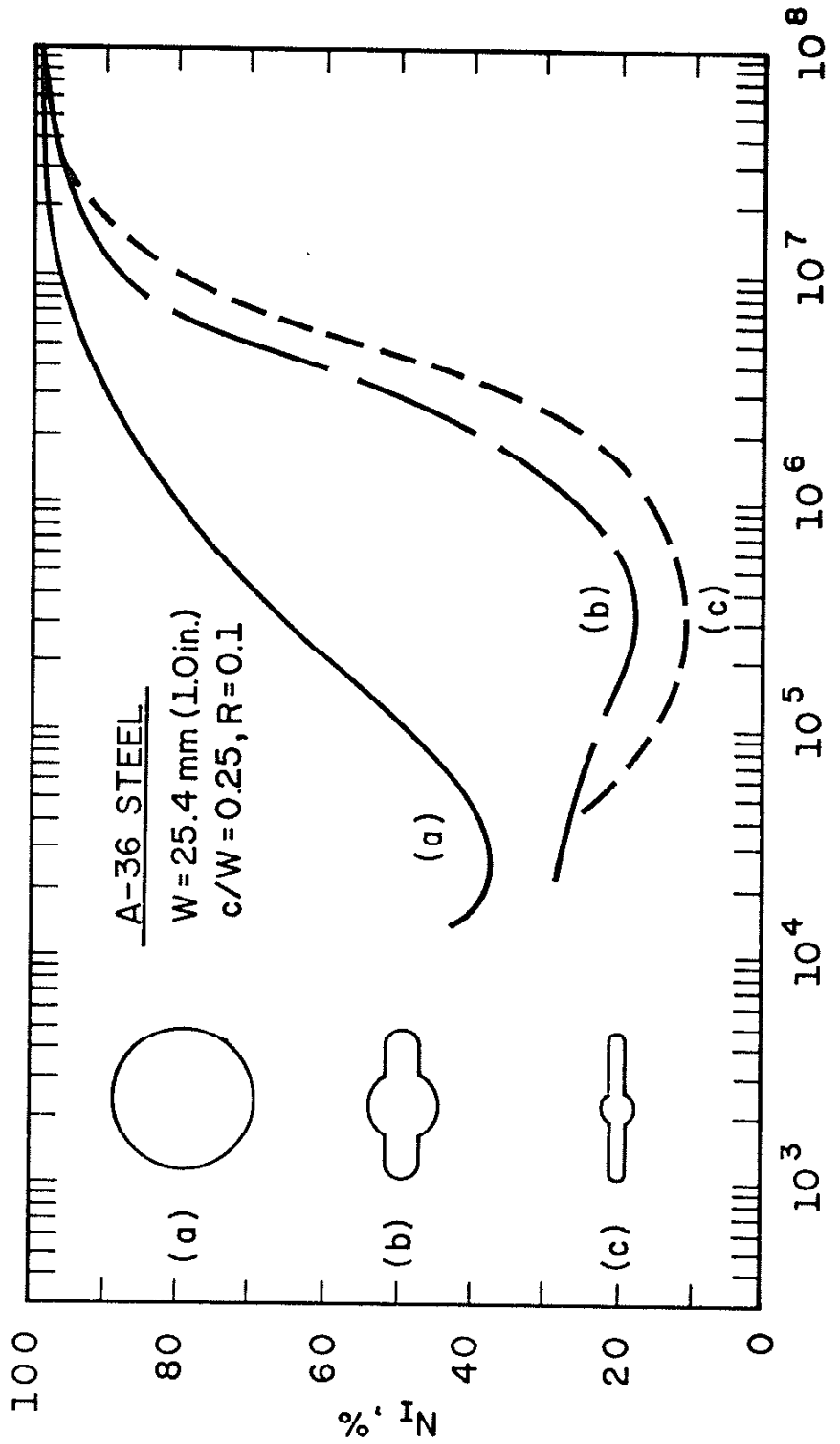

FIGURE 39. VARIATION OF N_I % WITH DIFFERENT NOTCH GEOMETRIES FOR A-36 MILD STEEL

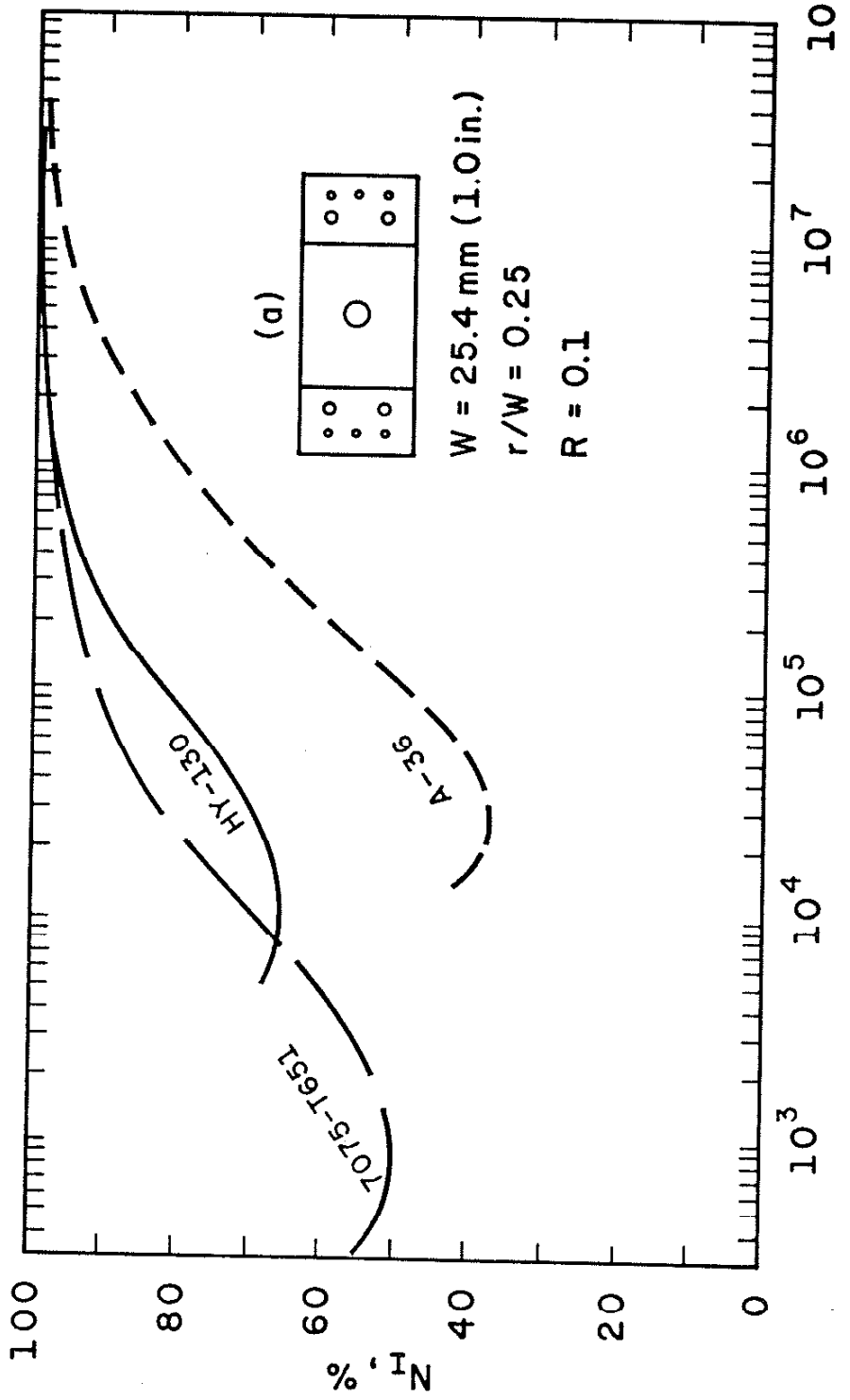

FIGURE 40. VARIATION OF N_I % OF A CIRCULARLY NOTCHED SPECIMEN OF DIFFERENT MATERIALS

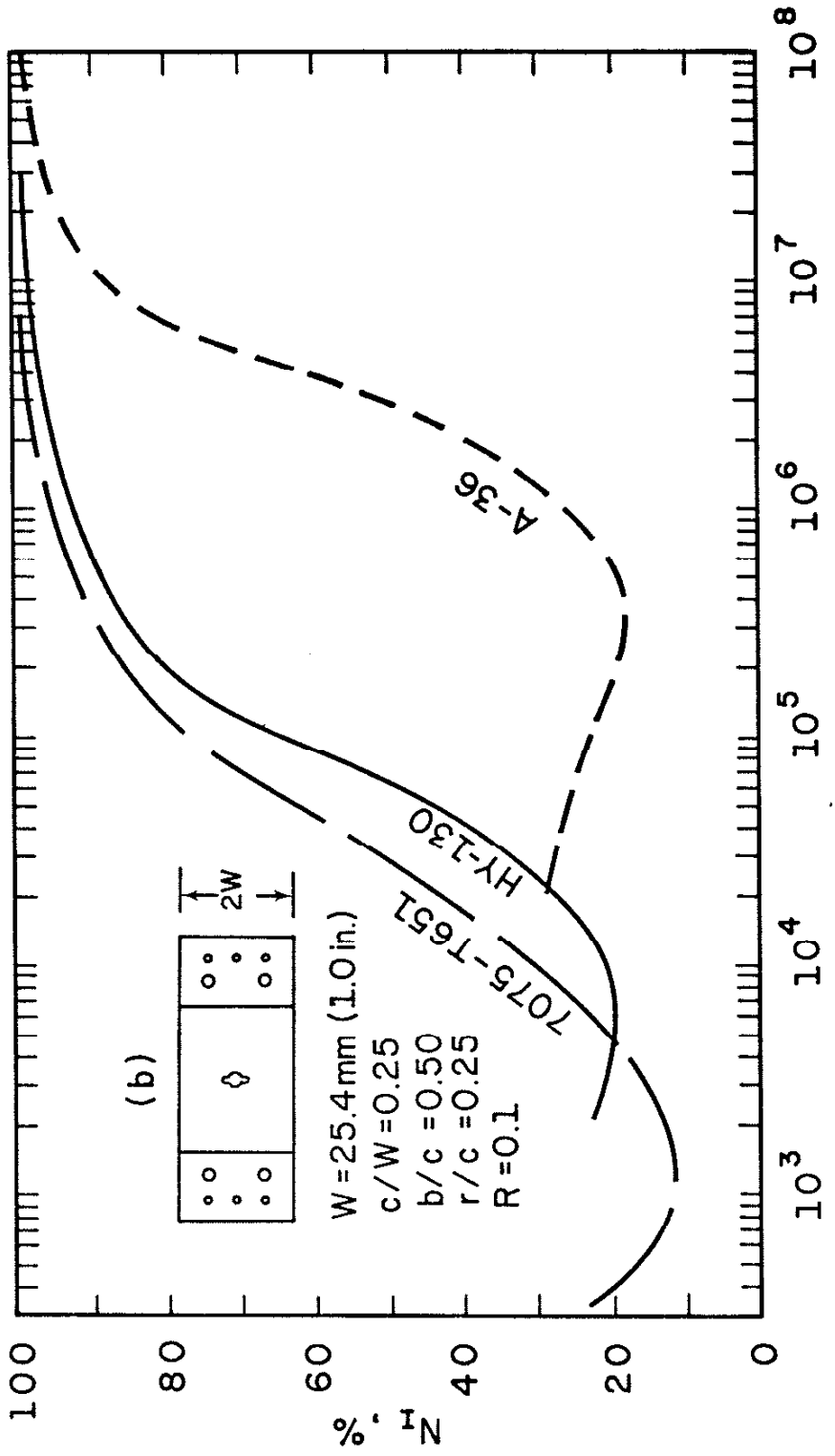

FIGURE 41. VARIATION OF N_I % OF AN ELLIPTICALLY NOTCHED SPECIMEN OF DIFFERENT MATERIALS

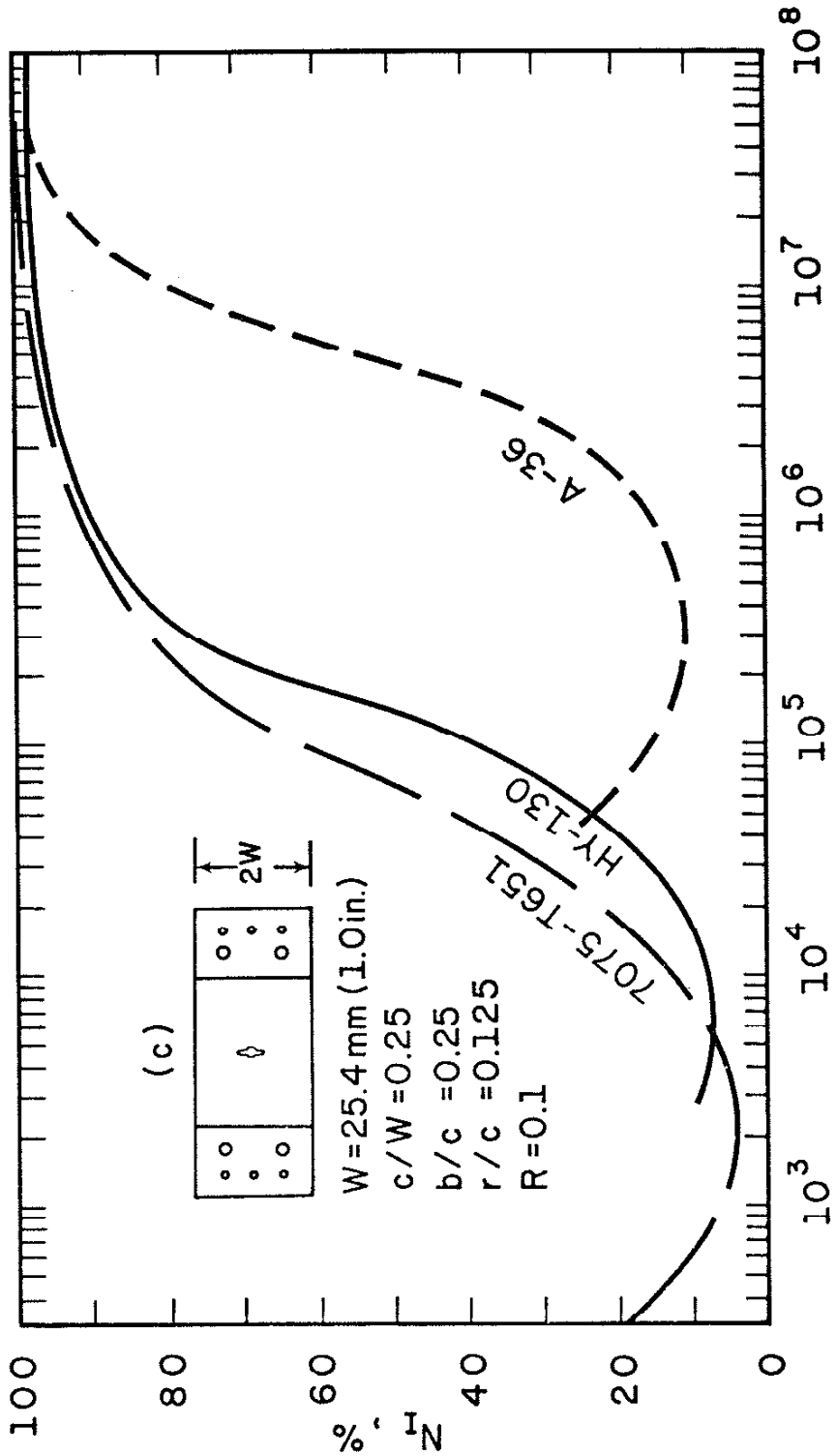

FIGURE 42. VARIATION OF N_I % OF AN ELLIPTICALLY NOTCHED SPECIMEN OF DIFFERENT MATERIALS

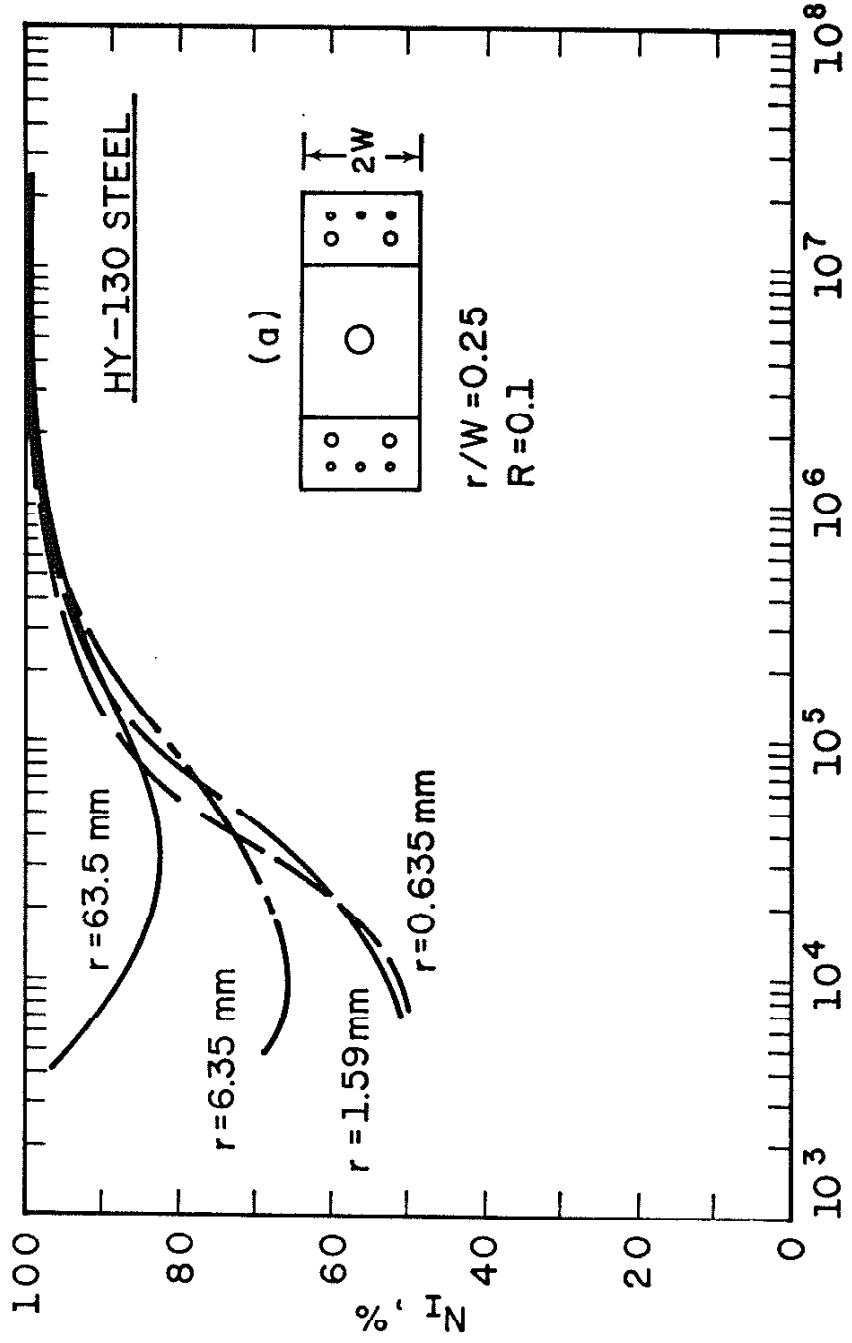

FIGURE 43. VARIATION OF N_I % WITH NOTCH SIZE FOR CIRCULARLY NOTCHED SPECIMENS OF HY-130 STEEL

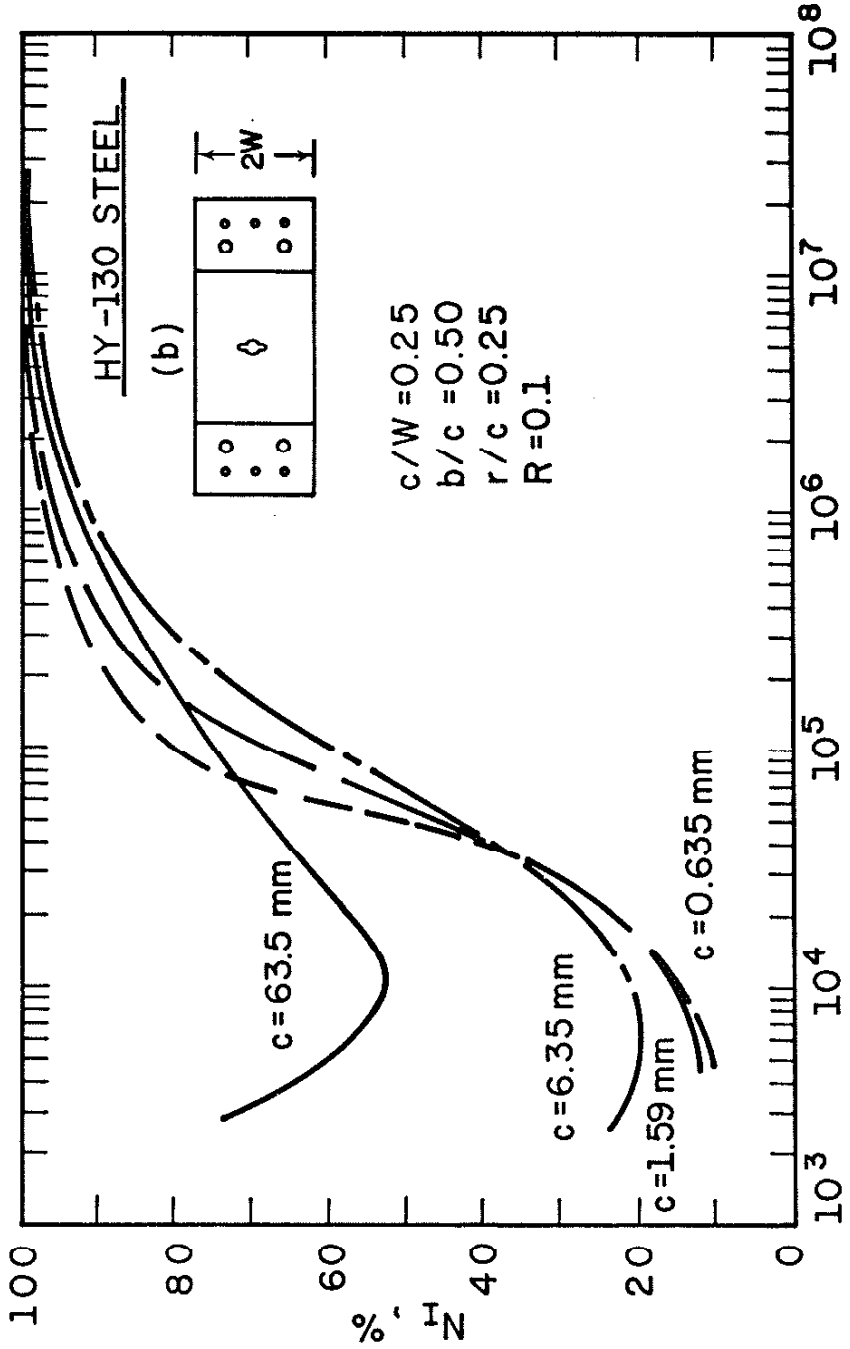

FIGURE 44. VARIATION OF N_I % WITH NOTCH SIZE FOR ELLIPTICALLY NOTCHED SPECIMEN OF HY-130 STEEL

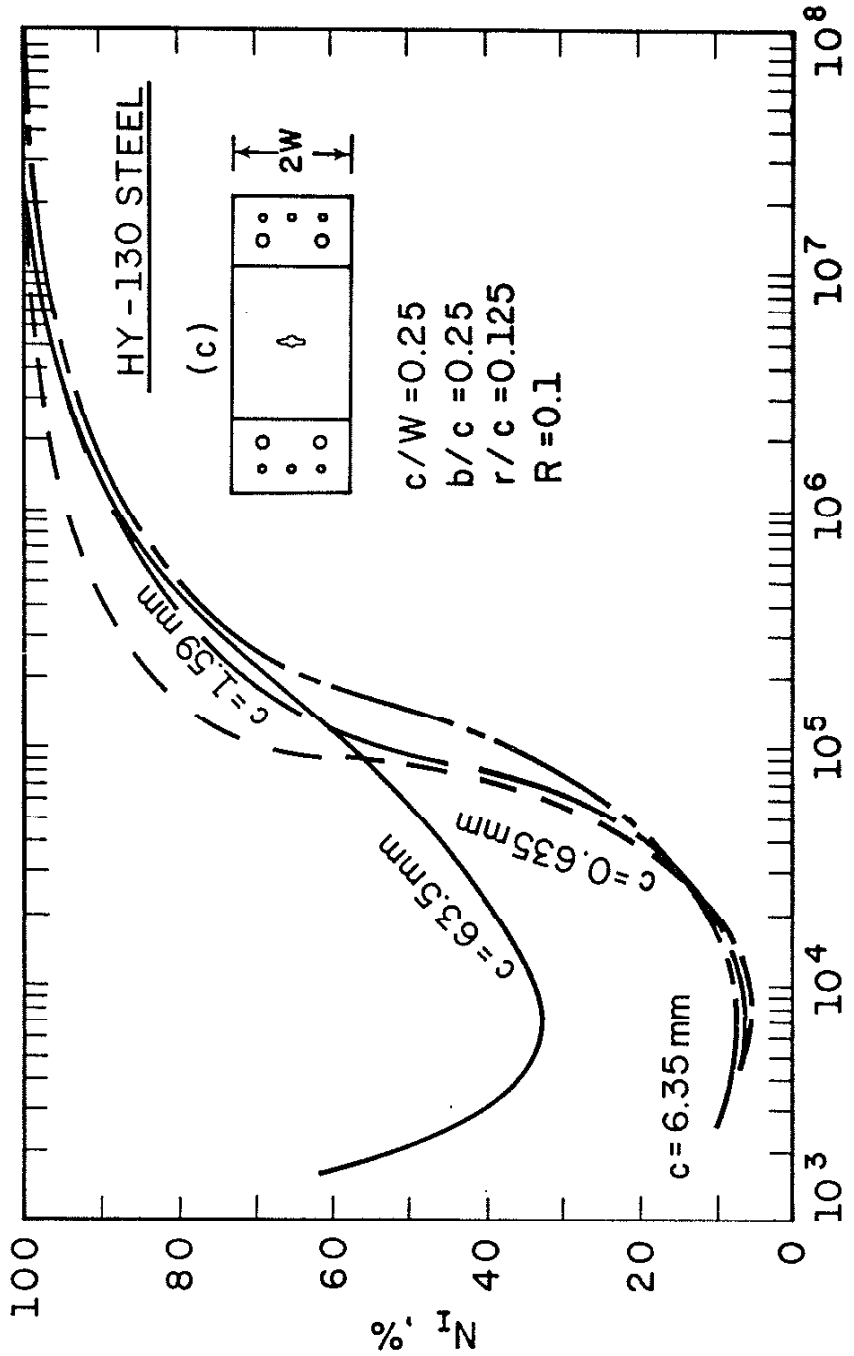

FIGURE 45. VARIATION OF N_I % WITH NOTCH SIZE FOR ELLIPTICALLY NOTCHED SPECIMENS OF HY-130 STEEL

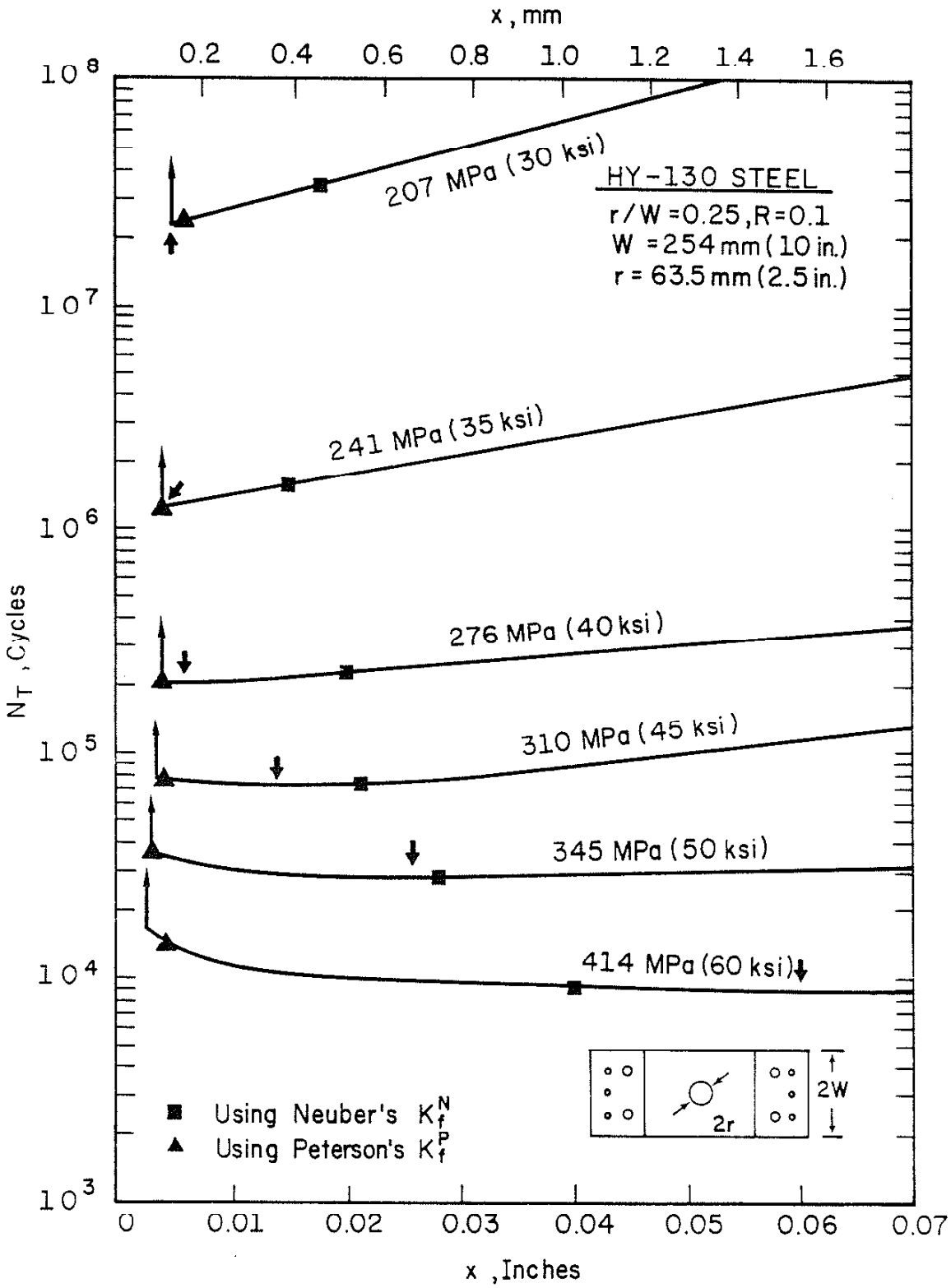

FIGURE 46. EFFECT OF ASSUMED CRACK INITIATION LENGTH x ON N_T ESTIMATIONS OF A CIRCULARLY NOTCHED SPECIMEN (W = 254 mm) AT VARIOUS STRESS LEVELS

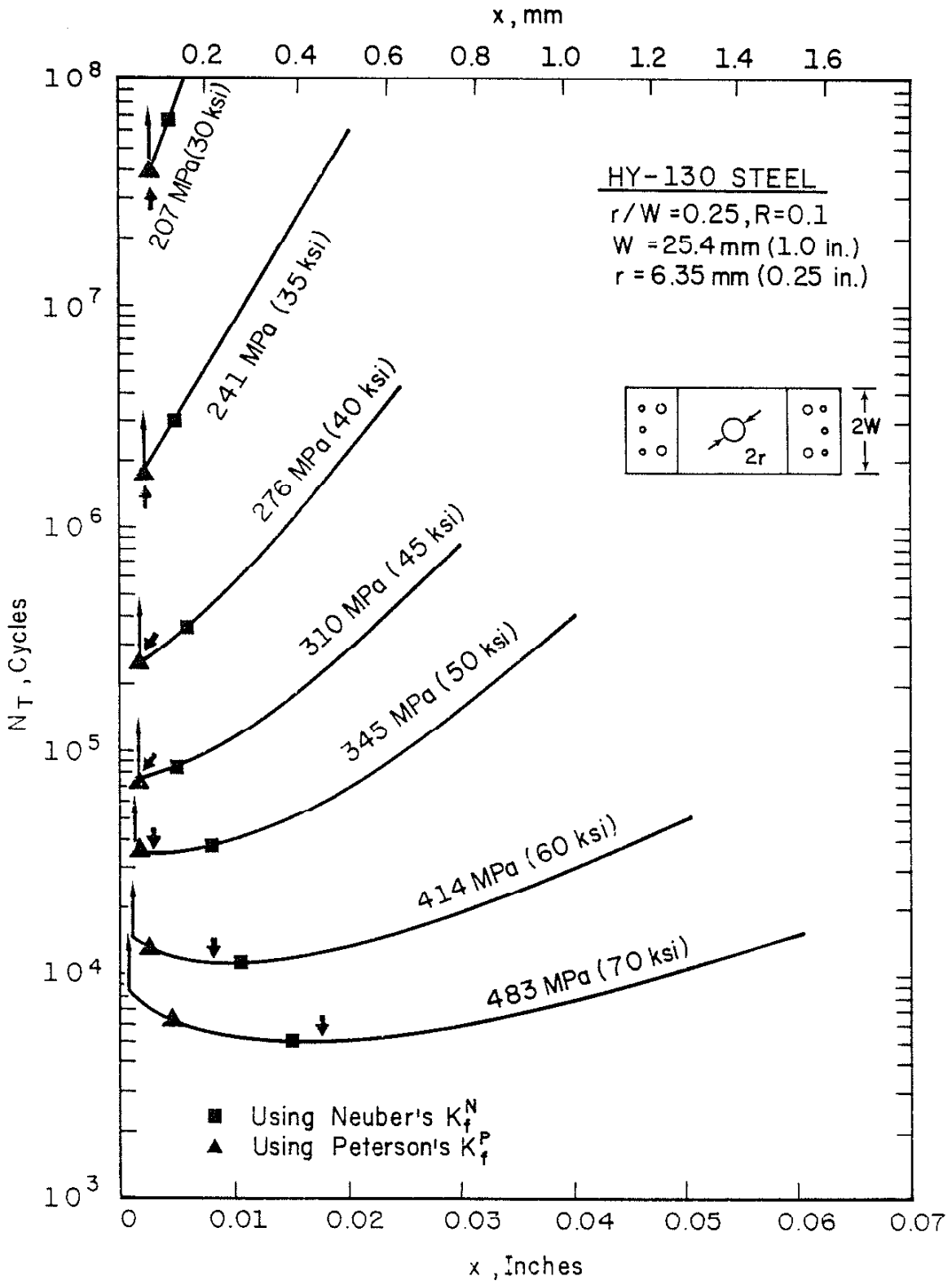

FIGURE 47. EFFECT OF ASSUMED CRACK INITIATION LENGTH x ON N_T ESTIMATIONS OF A CIRCULARLY NOTCHED SPECIMEN (W = 25.4 mm) AT VARIOUS STRESS LEVELS

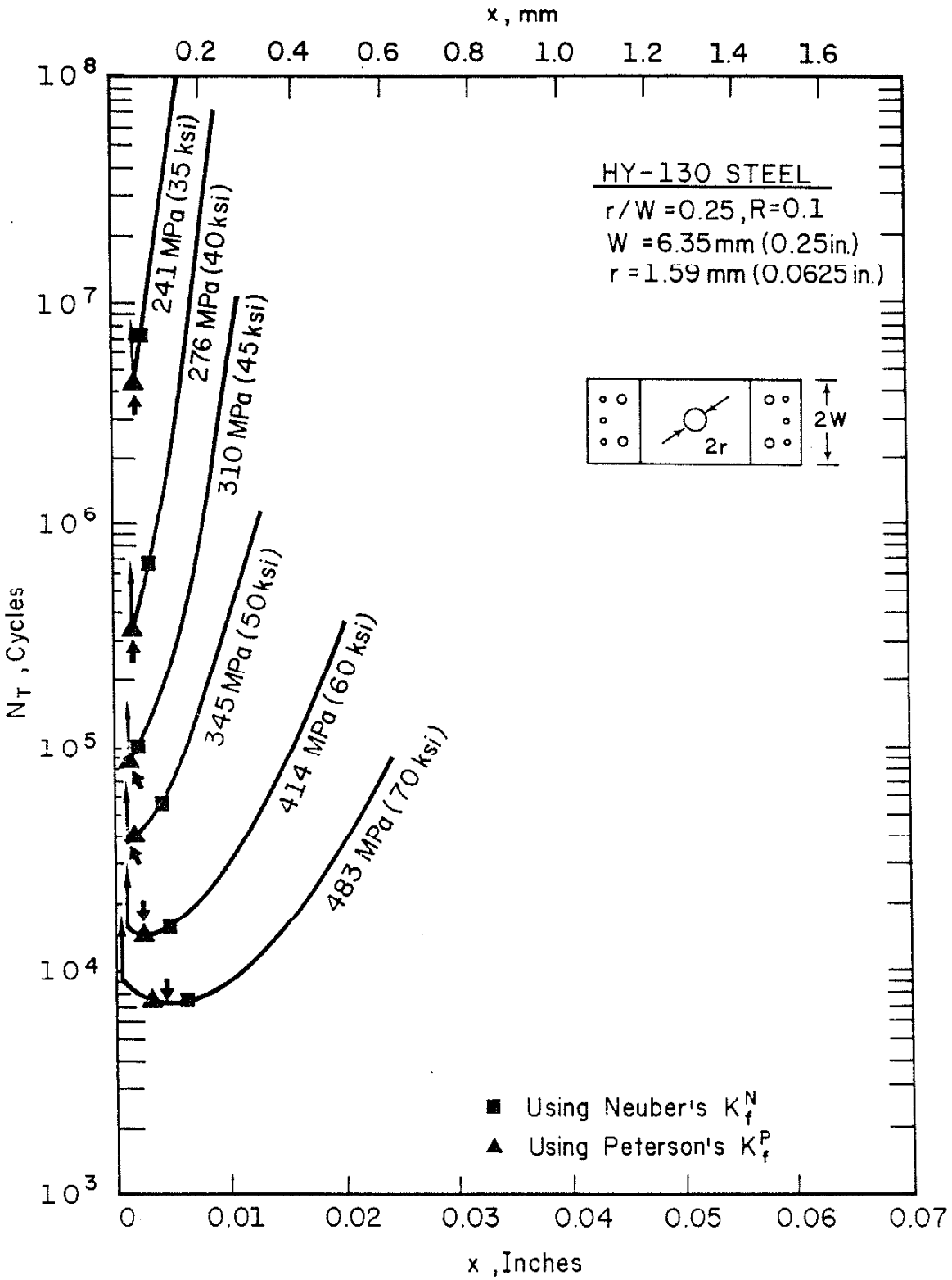

FIGURE 48. EFFECT OF ASSUMED CRACK INITIATION LENGTH x ON N_T ESTIMATIONS OF A CIRCULARLY NOTCHED SPECIMEN (W = 6.35 mm) AT VARIOUS STRESS LEVELS

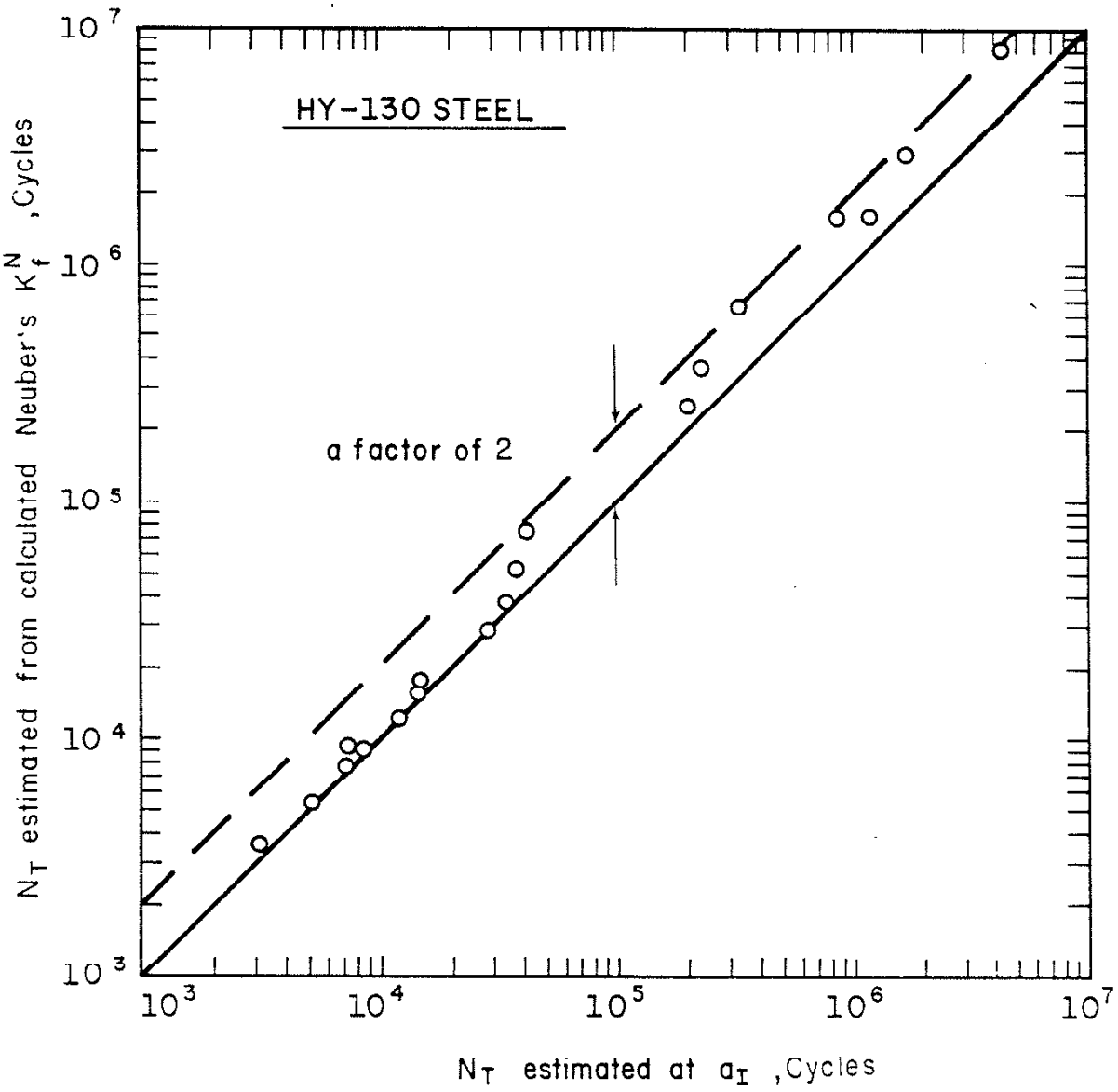

FIGURE 49. COMPARISON OF N_T ESTIMATED FROM THE CALCULATED K_f^N WITH THE PREDICTED N_T USING THE ANALYTICAL MODEL

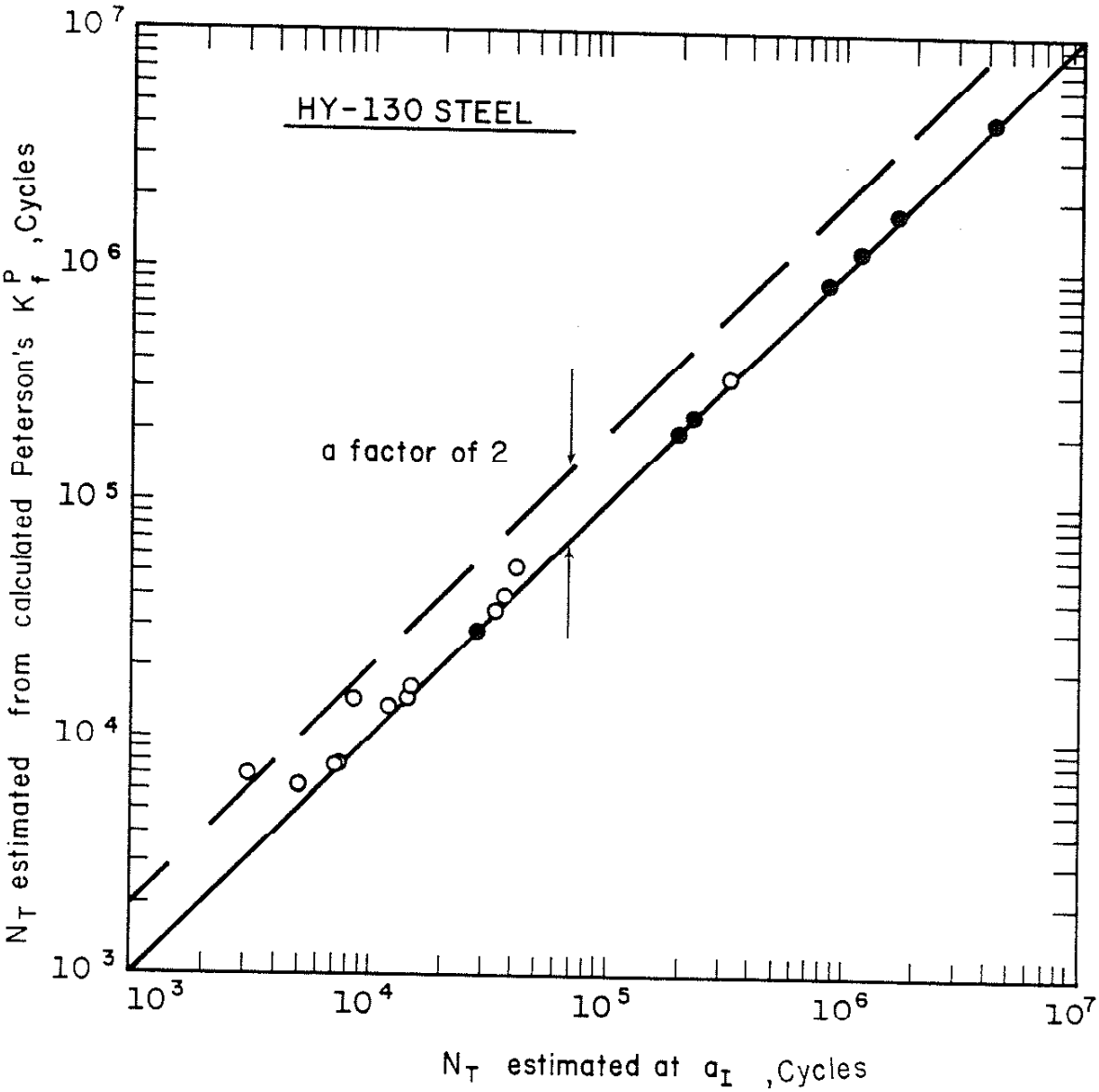

FIGURE 50. COMPARISON OF N_T ESTIMATED FROM THE CALCULATED K_f^P WITH THE PREDICTED N_T USING THE ANALYTICAL MODEL

APPENDIX I: RATE-CALCULATION METHOD[17]

The rate-calculation method was first proposed by Socie et al.[17] using concepts developed by Morrow.

In the absence of a fatigue crack, the stress and strain experienced by each element in front of the notch root can be determined using an elasto-plastic finite element analysis[19]. The fatigue life of each element can be calculated from the stress and strain ranges experienced by the element and the stress-life and strain-life relationships[2,3] (Eqs. (1) through (4)), as shown in Fig. A-1(b) and (c). To account for the actual mean stress effect on the fatigue life estimations of the micro-elements, Eq. (5) in combination with Eqs. (3) and (4) may be employed. The estimated fatigue life (N_f) of the micro-element as a function of the distance (x) of that element from the notch root gives a plot shown in Fig. A-1(d). The reciprocal of the derivative of this curve at a specific point represents the damage rate due to crack initiation mechanisms at that particular point. This crack initiation rate may be interpreted as the rate of the crack advancing due to low cycle fatigue mechanisms.

The crack propagation rate (da/dN) can be calculated for the presence of a small fatigue crack which has developed to some distance from the notch root on the basis of fracture mechanics concepts. Newman's results[20] of stress intensity correction factors (F) for cracks emanating from circular and elliptical holes are employed for the calculations of the stress intensity factor: see Fig. A-1(e). Paris' crack-propagation-rate law[7] for a specific load ratio R, Eq. (7), or Forman's crack-propagation-rate

law[9], Eq. (9), is employed to calculate the crack propagation rate of any crack propagating along the potential crack advancing path.

The competition of the damage rates due to crack initiation and due to crack propagation can be examined by superimposing the plots of the crack initiation rate and the crack propagation rate as a function of the distance that the crack has advanced from the notch root, as shown in Fig. A-1(g). The crack initiation rate decreases, and the crack propagation rate increases with increasing the distance from the notch root or the crack length. The equality of the crack initiation rate and the crack propagation rate determines the crack initiation length (a_I), Fig. A-1(g).

The crack initiation life (N_I) and crack propagation life (N_p) can now be estimated. The crack initiation life (N_I) is taken as the fatigue life of the micro-element at a distance equal to a_I from the notch root. The crack propagation life is calculated from a_I to an appropriate final crack length (a_f) which may be determined from fracture toughness or limit load. The summation of the crack initiation life and the crack propagation life gives the total fatigue life (N_T).

The application of this method to a circularly notched specimen of HY-130 steel is shown in Fig. A-2. The solid arrow indicates the crack initiation length (a_I) defined by the model, and the open arrow denotes the crack size (a_{th}) determined by the threshold stress intensity ΔK_{th}. The crack propagation rate becomes infinitesimal as x approaches a_{th} (ΔK approaches ΔK_{th})[11,12]. At low stresses, ΔK_{th} determines a_I: the model predicts that a_I approaches a_{th} at low stresses (see Fig. A-2(d) and (c)).

For the comparison of the Rate-calculation method with the Life-calculation method in the aspects of calculation procedures and of prediction results, a brief summary of calculation procedures of the Life-calculation method, which is described in detail in Section 2.2, is illustrated in Fig. A-3 and the application of the Life-calculation method to the same circularly notched specimen of HY-130 steel as in Fig. A-2 is shown in Fig. A-4.

RATE-CALCULATION METHOD

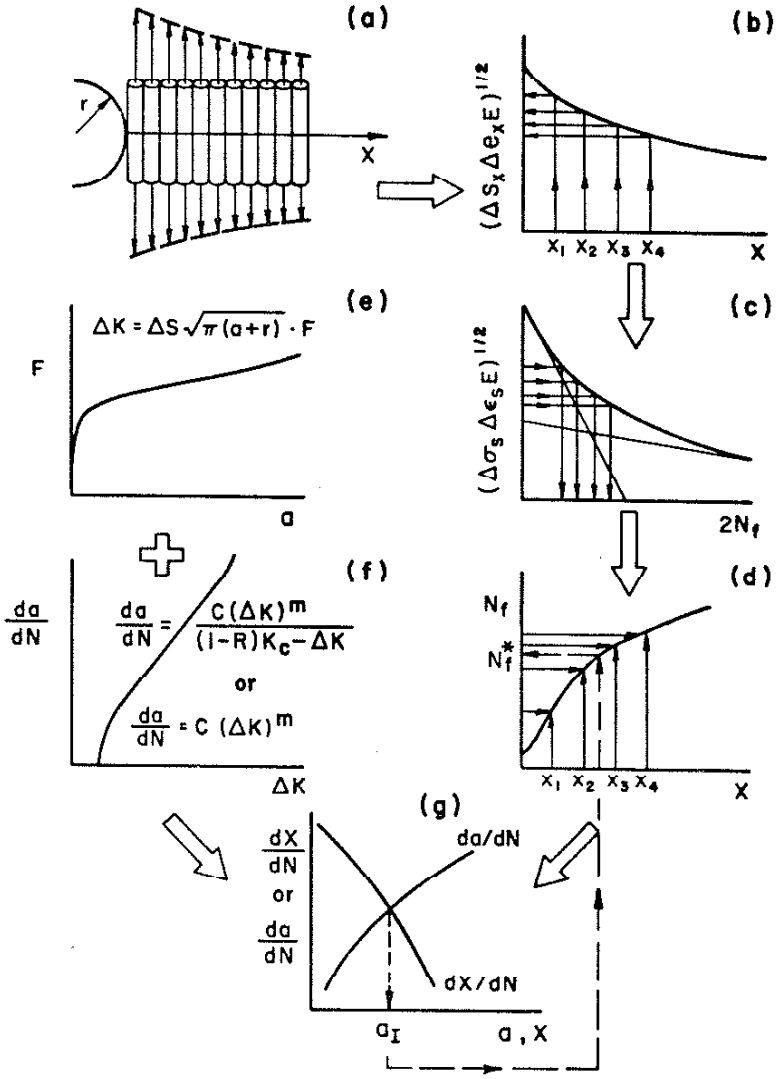

$$N_I = N_f^* \ , \ N_P = \int_{a_I}^{a_f} \frac{dN}{da} \, da \ , \ N_T = N_I + N_P$$

FIGURE A-1. PROCEDURES OF THE RATE-CALCULATION METHOD FOR DEFINING THE CRACK INITIATION LENGTH a_I AND PREDICTING THE TOTAL FATIGUE LIFE N_T FOR A NOTCHED MEMBER

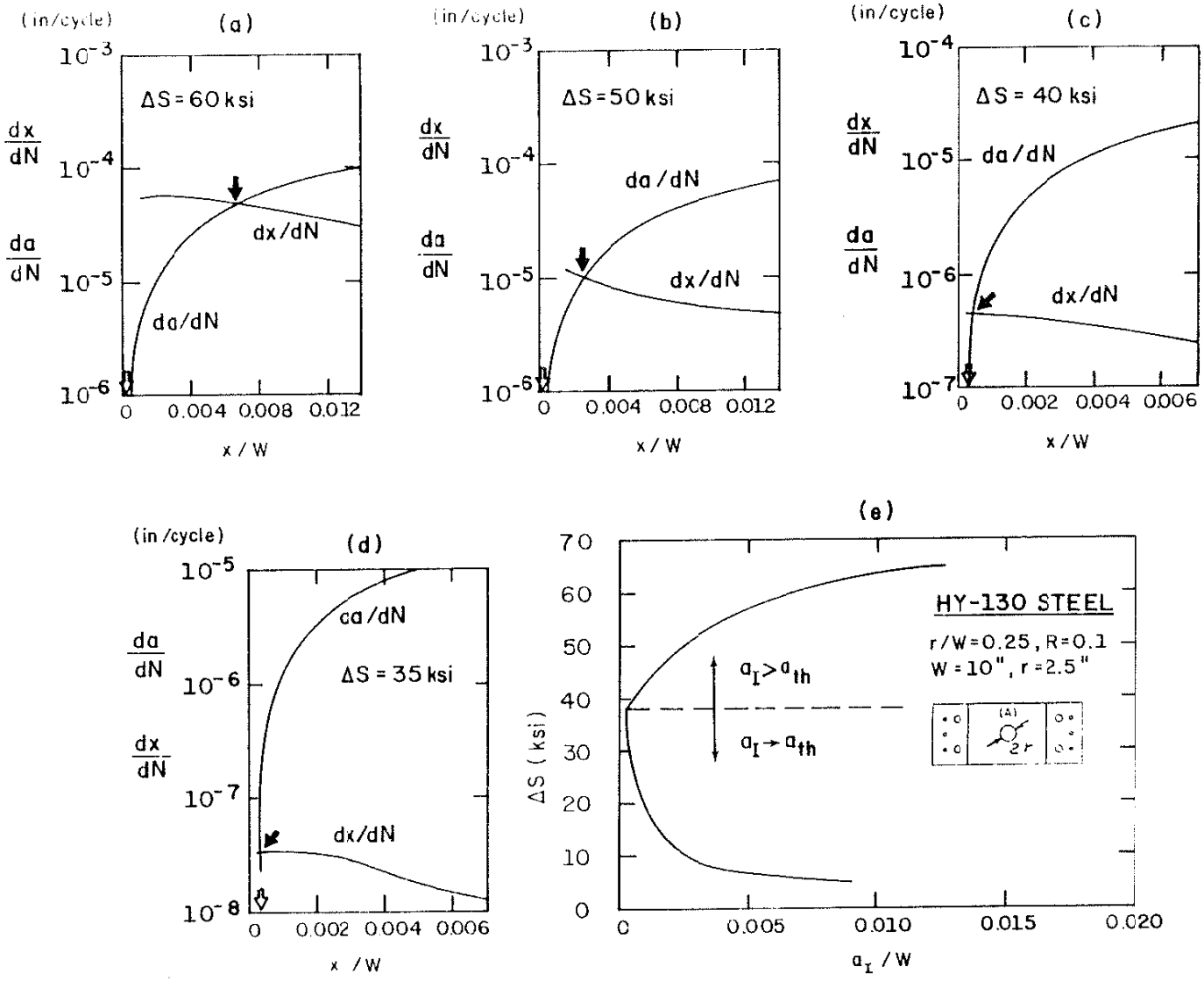

FIGURE A-2. ILLUSTRATIONS OF DETERMINING THE CRACK INITIATION LENGTH a_I FOR A CIRCULARLY NOTCHED SPECIMEN AT VARIOUS STRESS LEVELS USING THE RATE-CALCULATION METHOD

LIFE CALCULATION METHOD

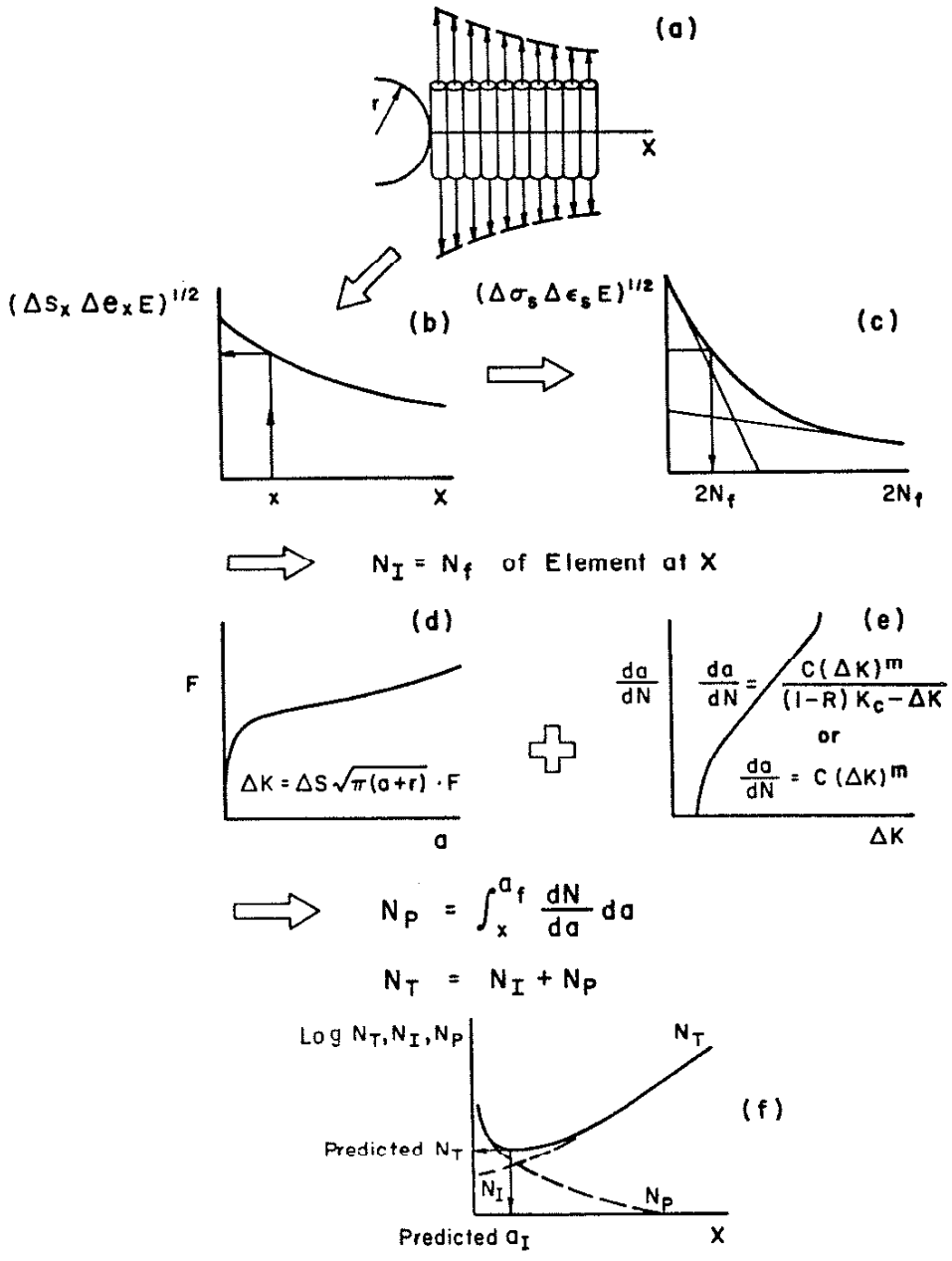

FIGURE A-3. PROCEDURES OF THE LIFE-CALCULATION METHOD FOR DEFINING THE CRACK INITIATION LENGTH a_I AND PREDICTING THE TOTAL FATIGUE LIFE N_T FOR A NOTCHED MEMBER

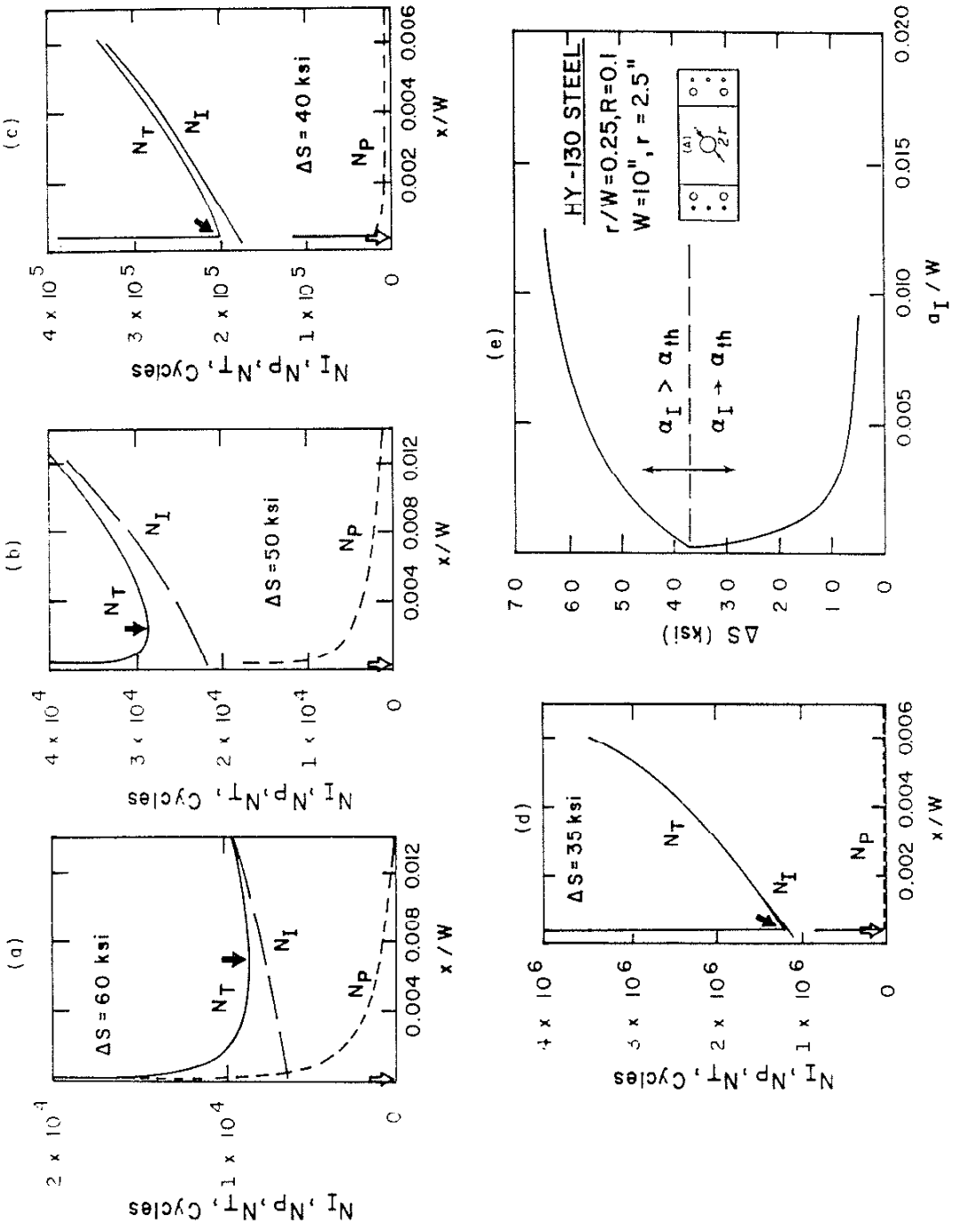

FIGURE A-4. DETERMINING THE CRACK INITIATION LENGTH a_I FOR A CIRCULARLY NOTCHED SPECIMEN AT VARIOUS STRESS LEVELS USING THE LIFE-CALCULATION METHOD

APPENDIX II: NUMERICAL EQUIVALENCE OF RATE-CALCULATION AND LIFE-CALCULATION METHODS

As seen in Fig. A-2(e) and A-4(e), the Rate-calculation method and the Life-calculation method predict the same crack initiation length a_I for a notched member. Fig. A-5 illustrates that these two methods are numerically equivalent, and differ only in procedure. The crack propagation life N_P for a particular choice of the element (a_I^*) in Fig. A-5(a) is the remaining crack propagation life N_P that an initiated crack propagates from a_I^* to a_f in Fig. A-5(b). Since the total fatigue life of a notched member of a specific notch geometry, dimension, loading and material is a constant, N_T^*. The remaining crack propagation life is:

$$N_P = N_T^* - N \tag{A-1}$$

where N is the number of cycles to develop a crack of a size equal to a_I^*. Differentiating against x, the distance from the notch root, or a, the crack length, Eq. (A-1) becomes:

$$\frac{dN_P}{dx} = -\frac{dN}{dx} \tag{A-2}$$

$$\text{i.e.,} \qquad \frac{dx}{dN_P} = -\frac{da}{dN} \tag{A-2'}$$

Now, the Life-calculation method defines the crack initiation length a_I as the minimum of the N_T vs. x curve as shown in Fig. A-5(a). The slope of that curve at a_I should be zero, i.e.,

$$\frac{dN_T}{dx} = \frac{dN_I}{dx} + \frac{dN_P}{dx} = 0 \tag{A-3}$$

From Eqs. (A-2) and (A-3), we have

$$\frac{dN_I}{dx} = -\frac{dN_P}{dx} \tag{A-4}$$

$$\text{i.e.,} \quad \frac{dx}{dN_I} = \frac{da}{dN} \tag{A-4'}$$

Eq. (A-4) indicates that the equality of the increment rate of N_I (dN_I/dx) and the decrement rate of N_P ($-dN_P/dx$) at a_I results in a minimum value of the estimated N_T as a function of the choice of element (x). Eq. (A-4'), which is mathematically equivalent to Eq. (A-4), indicates that when the crack embryo initiates to its crack initiation length a_I the damage rate due to crack propagation mechanism equals to the damage rate due to crack initiation mechanism. This means that the statement in Life-calculation Method that the fatigue crack propagation phase beings when the increment of N_I exceeds the decrement of N_P with increasing x (see Fig. A-5(a)) is equivalent to the statement in Rate-calculation Method that the fatigue crack propagation phase begins when the damage rate due to crack propagation mechanism exceeds the damage rate due to crack initiation mechanism (see Fig. A-5(c)). Therefore, as we can see in Figs. A-2(e) and A-4(e), these two methods give the identical predictions for the crack initiation length, and hence, the fatigue life of a notched member.

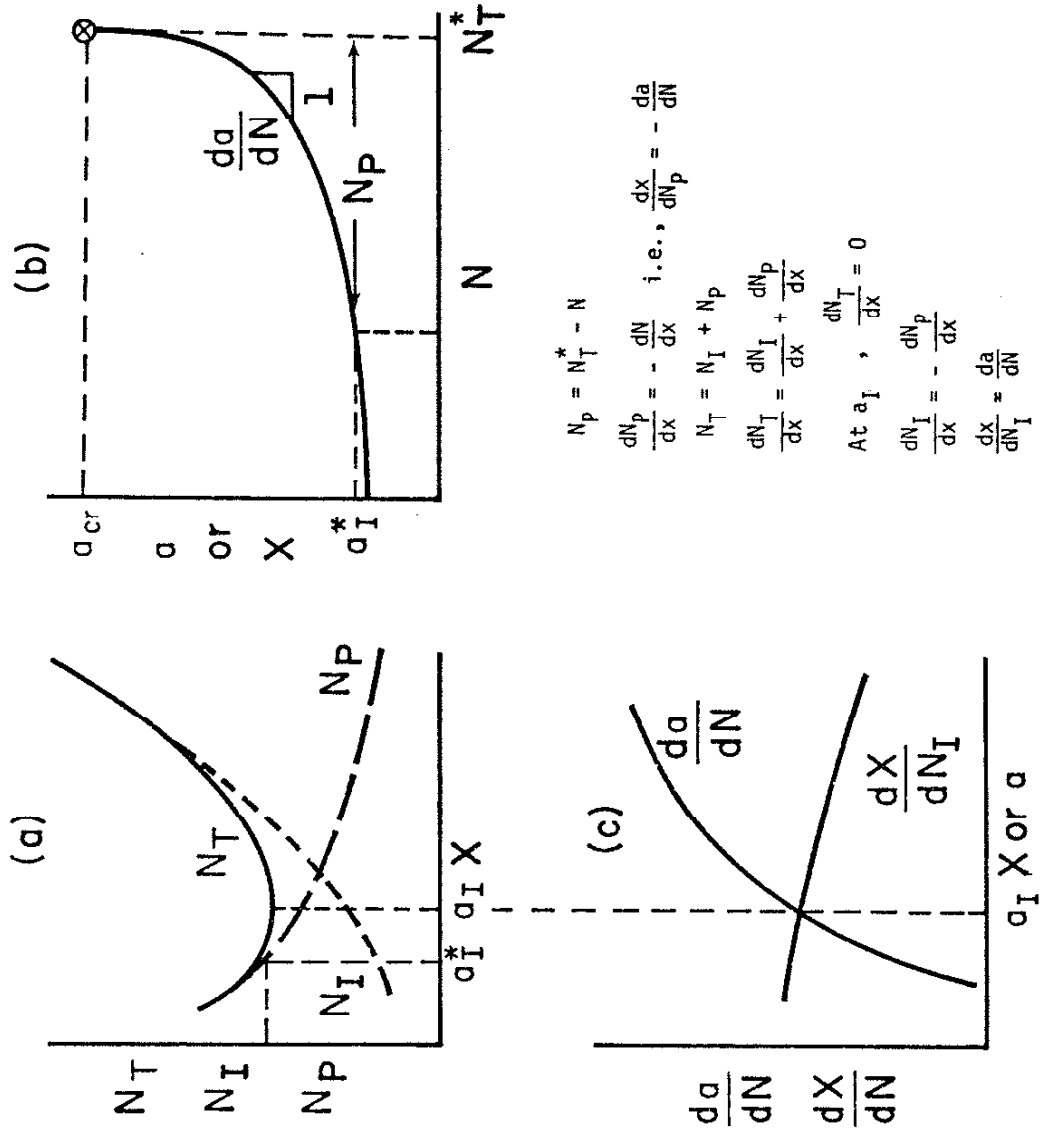

FIGURE A-5. THE NUMERICAL EQUIVALENCE BETWEEN THE LIFE-CALCULATION METHOD AND THE RATE-CALCULATION METHOD

APPENDIX III: SAMPLE CALCULATION OF N_I, N_P AND N_T VS. X CURVES

N_I vs. x Curve

The mechanical properties needed in this calculation are σ_f', b, ε_f', c and E, from which $2N_t$ and ε_{tr} can be calculated. To calculate the fatigue life $2N_f$ of the micro-element (x) subjected to a stress ΔS_x and strain Δe_x, a combination of Eqs. (3) and (4) is employed,

$$\frac{\Delta S_x \Delta e_x}{4} = \frac{(\sigma_f' - \sigma_o)^2}{E} (2N_f)^{2b} + (\sigma_f' - \sigma_o)\, \varepsilon_f' \, (2N_f)^{b} + c \qquad \text{(A-5)}$$

If the micro-element experiences no plastic strain, the initial mean stress $\sigma_{o,i}$ is concerned prevailing the whole life and no mean stress relaxation occurs. Eq. (A-5) can be solved for $2N_f$ of that element using Newton's method. If the element is subjected to a non-zero plastic strain amplitude, σ_o will relax. Thus Eq. (A-5) can not be directly solved for $2N_f$. In this case, an increment-life method is employed. The fatigue life of the element is the accumulation of the repeatedly applied increments of cycles ($\Delta 2N$) until the damage summation exceeds unity. The operational details are given in the following program listing and the programming flow chart shown in Fig. A-7.

The names of variables used in the program are as follows:

Λ = x

CYC2N = accumulation of reversals (2N in flow chart)

CY2NP = 2N in Eq. (5) (2N' in flow chart)

D = accumulation of damage

DAE = Δe_x

DAEE = $\Delta \epsilon_e$

DAEP = $\Delta \epsilon_p$

DAS = ΔS_x

DATAS = ΔS

E = E

EF = ϵ_f'

ETR = ϵ_{tr}

EXPK = k

FLNF = N_f

FL2NF = $2N_f$

GES2N = $2N_f$ (guessed)

IDA2N = $\Delta 2N$, increment of loading reversals

R = R

SB = b

SC = c

SIGF = σ_f'

SIGOI = $\sigma_{o,i}$

TR2NT = $2N_t$

PROGRAM LISTING

```
      DIMENSION DAE(20),DAS(20),GES2N(20),ILA2N(20),DATAS(20),A(20)
      DIMENSION DAEE(20),DAEP(20),SIGOI(20),EXPK(20)
      DIMENSION CYC2N(20),CY2NP(20),D(20),FL2NF(20),FLNF(20)
      DIMENSION X(20),B(20),FX(20),FPX(20),Y(20),Z(20),W(20)
            DATA E,SIGF,SB,EF,SC,R/28000.,216.,-0.06,0.9,-0.64,0.1/
      TR2NT=(EF*E/SIGF)**(1./(SB-SC))
      ETR=SIGF/E*TR2NT**SB+EF*TR2NT**SC
      READ (5,10) (DATAS(I),A(I),DAE(I),DAS(I),GES2N(I),I=1,20)
   10 FORMAT (5F10.0)
      WRITE (6,20)
   20 FORMAT ('1H1,2X,'DATAS',5X,'A',7X,'STRAIN',6X,'STRESS',6X,'GES2N',
     *          ///)
      WRITE (6,30) (DATAS(I),A(I),DAE(I),DAS(I),GES2N(I),I=1,20)
   30 FORMAT (1H ,2X,F4.1,3X,F6.4,F13.6,F10.2,F12.0)
      WRITE (6,40)
   40 FORMAT ('1H1,1X,'DATAS',6X,'A',7X,'STRAIN',6X,'STRESS',8X,'K',9X,
     *       'D',11X,'2NP',10X,'NP',9X,'DA2N',///)
      DO 500 I=1,20
      DAEE(I)=DAS(I)/E
      DAEP(I)=DAE(I)-DAEE(I)
      SIGOI(I)=(1+R)*DAS(I)/2./(1-R)
      B(I)=SIGF-SIGOI(I)
      X(I)=GES2N(I)
  100 FX(I)=B(I)**2./E*X(I)**(2.*SB)+B(I)*EF*X(I)**(SB+SC)-DAE(I)*DAS(I)
     */4.
      FPX(I)=B(I)**2./E*2.*SB*X(I)**(2.*SB-1)+B(I)*EF*(SB+SC)*X(I)**(SB
     *+SC-1.)
      Y(I)=FX(I)/FPX(I)
      X(I)=X(I)-Y(I)
      Z(I)=ABS(Y(I))
      W(I)=X(I)/1000.
      IF(Z(I).LE.W(I)) GO TO 200
      GO TO 100
  200 IF(DAEP(I).LE.0.0) GO TO 450
      EXPK(I)=-4625.*DAEP(I)/2./E/ETR
      IDA2N(I)=X(I)/1000.
      IF(IDA2N(I).LE.3) GO TO 300
      GO TO 350
  300 IDA2N(I)=3
  350 CYC2N(I)=0.
      D(I)=0.
  400 CY2NP(I)=CYC2N(I)+(IDA2N(I)+1)/2.
      B(I)= SIGF-SIGOI(I)*(CY2NP(I)-1)**EXPK(I)
  410 FX(I)=B(I)**2./E*X(I)**(2.*SB)+B(I)*EF*X(I)**(SB+SC)-DAE(I)*DAS(I)
     */4.
      FPX(I)=B(I)**2./E*2.*SB*X(I)**(2.*SB-1.)+B(I)*EF*(SB+SC)*X(I)**(SB
     *+SC-1.)
      Y(I)=FX(I)/FPX(I)
      X(I)=X(I)-Y(I)
      Z(I)=ABS(Y(I))
      W(I)=X(I)/1000.
      IF(Z(I).LE.W(I)) GO TO 420
      GO TO 410
  420 D(I)=D(I)+IDA2N(I)/X(I)
      CYC2N(I)=CYC2N(I)+IDA2N(I)
      IF(D(I).GE.1.0) GO TO 430
      GO TO 400
  430 FL2NF(I)=CYC2N(I)
      FLNF(I)=FL2NF(I)/2.
      GO TO 470
  450 FL2NF(I)=X(I)
      FLNF(I)=FL2NF(I)/2.
      EXPK(I)=0.
      D(I)=1.
  470 WRITE (6,60) DATAS(I),A(I),DAE(I),DAS(I),EXPK(I),D(I),FL2NF(I),
     *                FLNF(I),IDA2N(I)
   60 FORMAT (1H ,F6.1,F9.4,F13.6,F10.2,F13.5,F9.5,F13.0,F13.0,I10)
  500 CONTINUE
      STOP
      END
```

INPUT/OUTPUT

DATAS	A	STRAIN	STRESS	GES2N
60.0	0.0010	0.052800	173.00	100.
60.0	0.0020	0.052000	172.00	100.
60.0	0.0040	0.047000	170.50	100.
60.0	0.0060	0.039600	168.00	100.
60.0	0.0080	0.033000	166.00	100.
60.0	0.0100	0.028000	163.50	700.
60.0	0.0120	0.024000	160.50	900.
60.0	0.0140	0.021000	158.00	1000.
60.0	0.0160	0.018700	157.00	1600.
60.0	0.0180	0.016600	153.00	1800.
60.0	0.0200	0.014700	151.20	3000.
60.0	0.0220	0.013100	149.00	4000.
60.0	0.0240	0.012000	147.20	5000.
60.0	0.0260	0.011200	145.50	5000.
60.0	0.0280	0.010500	144.00	5000.
60.0	0.0300	0.010000	142.10	5000.
60.0	0.0320	0.009200	140.60	10000.
60.0	0.0340	0.008600	139.00	10000.
60.0	0.0360	0.007900	137.60	10000.
60.0	0.0380	0.007200	136.20	10000.

DATAS	A	STRAIN	STRESS	K	D	2NF	NF	DA2N
60.0	0.0010	0.052800	173.00	-0.40832	1.00265	861.	431.	3
60.0	0.0020	0.052000	172.00	-0.40163	1.00209	894.	447.	3
60.0	0.0040	0.047000	170.50	-0.35831	1.00035	1077.	539.	3
60.0	0.0060	0.039600	168.00	-0.29428	1.00115	1485.	743.	4
60.0	0.0080	0.033000	166.00	-0.23710	1.00042	2070.	1035.	5
60.0	0.0100	0.028000	163.50	-0.19409	1.00014	2832.	1416.	7
60.0	0.0120	0.024000	160.50	-0.16000	1.00042	3870.	1935.	9
60.0	0.0140	0.021000	158.00	-0.13450	1.00002	5091.	2546.	11
60.0	0.0160	0.018700	157.00	-0.11467	1.00014	6303.	3152.	13
60.0	0.0180	0.016600	153.00	-0.09753	1.00004	8577.	4289.	17
60.0	0.0200	0.014700	151.20	-0.08145	1.00019	11127.	5564.	21
60.0	0.0220	0.013100	149.00	-0.06813	1.00015	14625.	7313.	27
60.0	0.0240	0.012000	147.20	-0.05906	1.00017	18276.	9138.	33
60.0	0.0260	0.011200	145.50	-0.05258	1.00014	22224.	11112.	39
60.0	0.0280	0.010500	144.00	-0.04692	1.00012	26802.	13401.	46
60.0	0.0300	0.010000	142.10	-0.04313	1.00031	32329.	16165.	55
60.0	0.0320	0.009200	140.60	-0.03660	1.00009	41250.	20625.	69
60.0	0.0340	0.008600	139.00	-0.03184	1.00019	52000.	26000.	87
60.0	0.0360	0.007900	137.60	-0.02615	1.00030	68068.	34034.	114
60.0	0.0380	0.007200	136.20	-0.02046	1.00002	92127.	46064.	154

The fatigue life of the element x is taken as the crack initiation life (N_I) corresponding to the choice of that element (x) as the assumed boundary between crack initiation and propagation. The calculation is made for several choices of the elements. The results of life-estimates for these elements are plotted against their locations from the notch root (x) to give a N_I vs. x curve, as shown in Fig. A-7.

N_P vs. x Curve

For the choice of the element x as the assumed boundary between crack initiation and propagation, the corresponding crack propagation life (N_P) is calculated by integrating Eq. (8) from x to a_f. This calculation is also repeated for those choices of the elements x as in the N_I estimations. The results of N_P estimates are plotted against x in Fig. A-7.

N_T vs. x Curve

Summation of N_I and N_P gives the total fatigue life N_T. N_T vs. x curve can be obtained directly from summing up the N_I vs. x and N_P vs. x curves: see Fig. A-7.

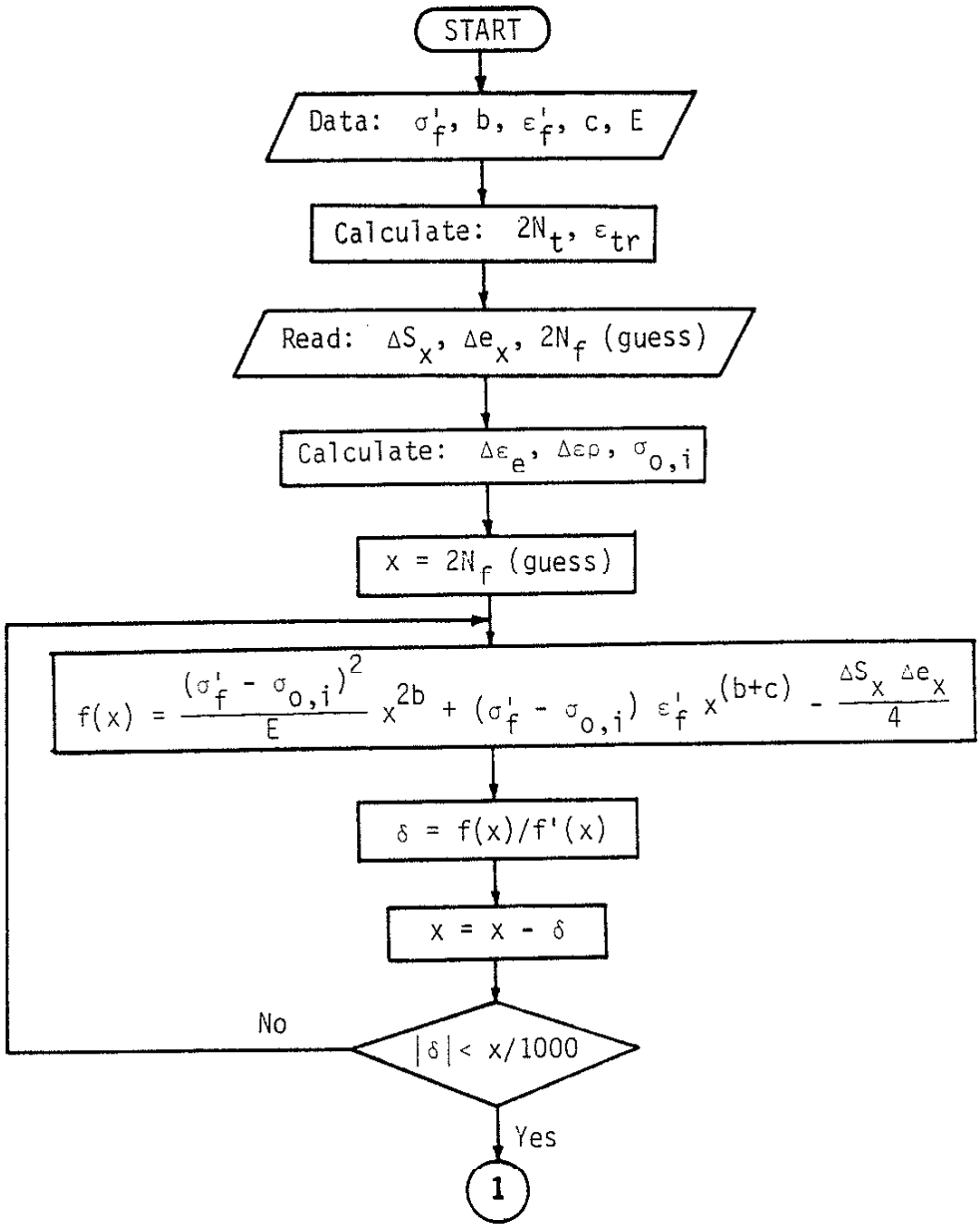

FIGURE A-6. FLOW CHART FOR DETERMINING THE FATIGUE LIFE $2N_f$ OF THE SIMULATED MICRO-ELEMENT

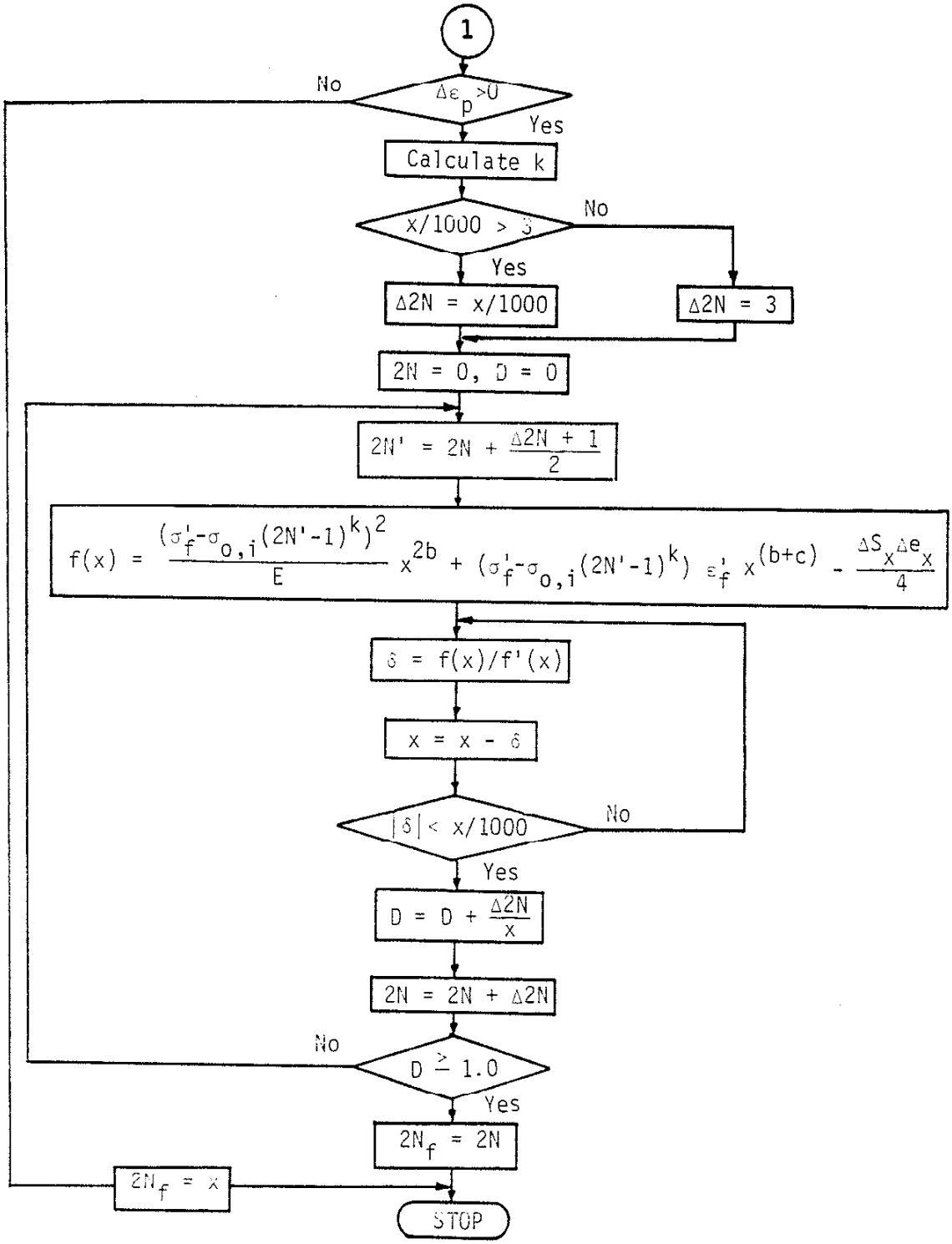

FIGURE A-6. (CONT'D)

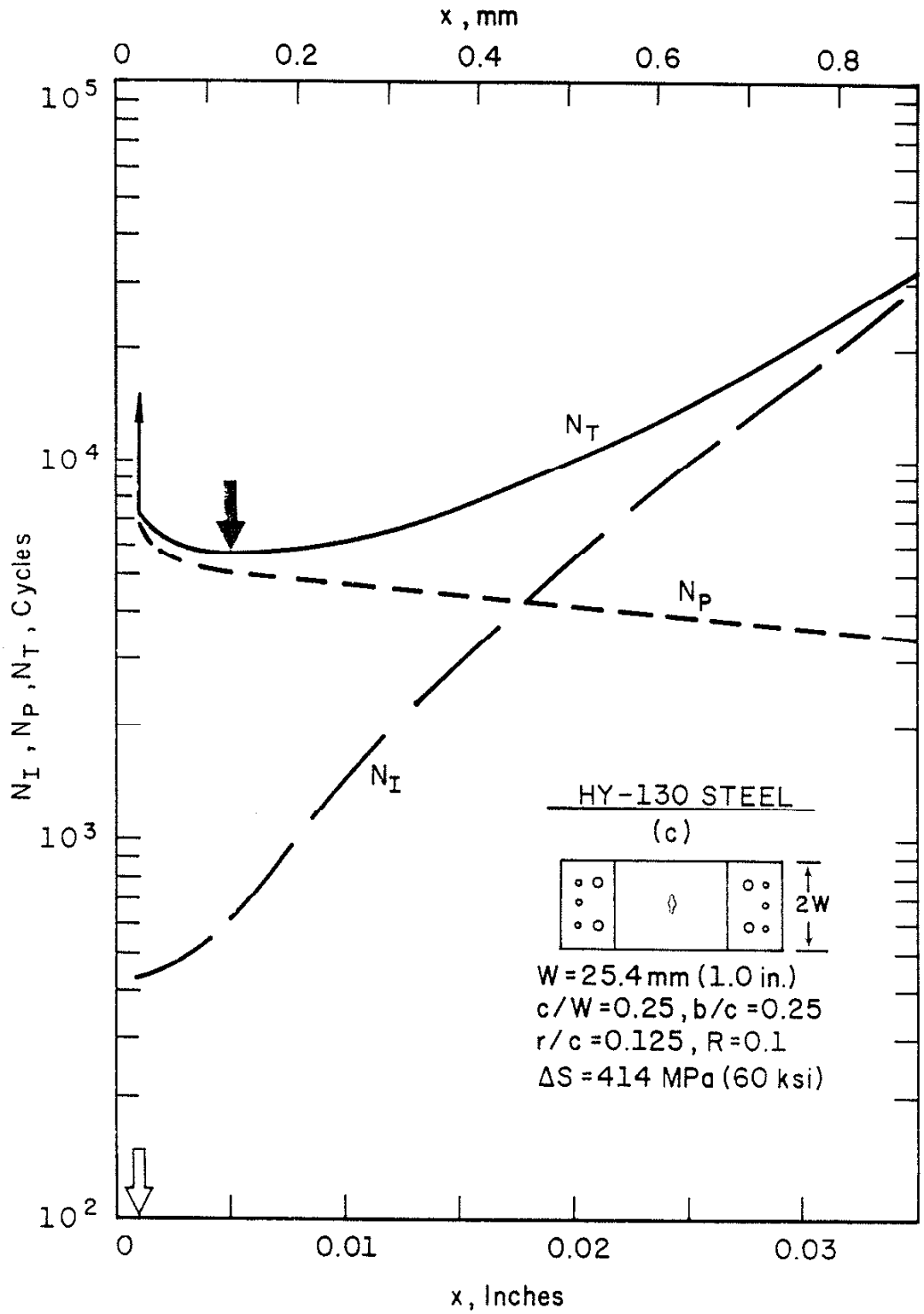

FIGURE A-7. SAMPLE CALCULATION OF N_I, N_P AND N_T